

University of Windsor

Scholarship at UWindor

Electronic Theses and Dissertations

Theses, Dissertations, and Major Papers

2016

Safety Evaluation of Car-Truck Mixed Traffic Flow on Freeways Using Surrogate Safety Measures

Peibo Zhao
University of Windsor

Follow this and additional works at: <https://scholar.uwindsor.ca/etd>

Recommended Citation

Zhao, Peibo, "Safety Evaluation of Car-Truck Mixed Traffic Flow on Freeways Using Surrogate Safety Measures" (2016). *Electronic Theses and Dissertations*. 5923.
<https://scholar.uwindsor.ca/etd/5923>

This online database contains the full-text of PhD dissertations and Masters' theses of University of Windsor students from 1954 forward. These documents are made available for personal study and research purposes only, in accordance with the Canadian Copyright Act and the Creative Commons license—CC BY-NC-ND (Attribution, Non-Commercial, No Derivative Works). Under this license, works must always be attributed to the copyright holder (original author), cannot be used for any commercial purposes, and may not be altered. Any other use would require the permission of the copyright holder. Students may inquire about withdrawing their dissertation and/or thesis from this database. For additional inquiries, please contact the repository administrator via email (scholarship@uwindsor.ca) or by telephone at 519-253-3000ext. 3208.

**SAFETY EVALUATION OF CAR-TRUCK MIXED
TRAFFIC FLOW ON FREEWAYS USING SURROGATE
SAFETY MEASURES**

By

Peibo Zhao

A Thesis

Submitted to the Faculty of Graduate Studies
through the Department of Civil and Environmental Engineering
in Partial Fulfillment of the Requirements for
the Degree of Master of Applied Science
at the University of Windsor

Windsor, Ontario, Canada

2016

© 2016 Peibo Zhao

**SAFETY EVALUATION OF CAR-TRUCK MIXED TRAFFIC FLOW
ON FREEWAYS USING SURROGATE SAFETY MEASURES**

by

Peibo Zhao

APPROVED BY:

Dr. X. Guo,
Odette School of Business

Prof. J. Tofflemire
Department of Civil and Environmental Engineering

Dr. H. Maoh
Department of Civil and Environmental Engineering

Dr. C. Lee, Advisor
Department of Civil and Environmental Engineering

December 7, 2016

DECLARATION OF PREVIOUS PUBLICATION

This thesis includes material from one original paper that has been submitted for publication in a peer reviewed journal, as follows:

Thesis Chapter	Publication title/full citation	Publication status
<i>Chapter 5</i>	<i>Zhao, P., Lee, C., 2016. Analysis and Validation of Surrogate Safety Measures for Rear-End Collision Risk by Types of Lead and Following Vehicles on Freeways. Submitted for presentation at 96th Transportation Research Board Annual Meeting and publication in Transportation Research Record: Journal of the Transportation Research Board.</i>	<i>under review</i>

I certify that I have obtained a written permission from the copyright owner(s) to include the above published material(s) in my thesis. I certify that the above material describes work completed during my registration as a graduate student at the University of Windsor.

I declare that, to the best of my knowledge, my thesis does not infringe upon anyone's copyright nor violate any proprietary rights and that any ideas, techniques, quotations, or any other material from the work of other people included in my thesis, published or otherwise, are fully acknowledged in accordance with the standard referencing practices. Furthermore, to the extent that I have included copyrighted material that surpasses the bounds of fair dealing within the meaning of the Canada Copyright Act, I certify that I have

obtained a written permission from the copyright owner(s) to include such material(s) in my thesis and have included copies of such copyright clearances to my appendix.

I declare that this is a true copy of my thesis, including any final revisions, as approved by my thesis committee and the Graduate Studies office, and that this thesis has not been submitted for a higher degree to any other University or Institution.

ABSTRACT

This study analyzes car-following and lane-change conflicts in car-heavy vehicle mixed traffic flow on freeways using three surrogate safety measures - time-to-collision (TTC), post-encroachment-time (PET) and crash potential index (CPI). The surrogate safety measures were estimated for different types of lead and following vehicles (car or heavy vehicle) using the individual vehicle trajectory data. The data were collected from a segment of the US-101 freeway in Los Angeles, California, U.S.A. For car-following conflicts, the distributions of TTC and PET were significantly different among different types of lead and following vehicles. For lane-change conflicts between the lane-change vehicle and the trailing vehicle in the target lane, CPIs were higher for angle conflicts than rear-end conflicts. It was also found that the CPI was generally higher for a given spacing interval when the following vehicle is a heavy vehicle in both car-following and lane-change conflicts. This indicates that heavy vehicle's lower braking capability significantly increases collision risk. This study also validates the CPI using historical crash data and the loop detector data extracted a few minutes before crash time upstream and downstream of crash locations. The data were obtained from a section of the Gardiner Expressway, Ontario, Canada. The result shows that the values of CPI were consistently higher for the crash case than the non-crash case. This shows that CPI can be used to capture the collision risk during car-following and lane-change maneuver on freeways. The findings suggest that the differences in collision risk among different vehicle pair types should be considered in the assessment of safety of car-heavy vehicle mixed traffic flow.

ACKNOWLEDGEMENTS

My deepest gratitude goes first and foremost to Dr. Chris Lee, my supervisor, for his constant encouragement and help to my study and life. I do appreciate that he gave me the opportunity to acquire my M.A.Sc in transportation engineering. I derived much benefit from his meticulous attitude to knowledge and critical consciousness throughout my graduate studies. I am also grateful to his time and dedication to recommend me for conferences, presentations and scholarships.

I would like to express my sincere acknowledgement to my thesis committee members: Dr. Hanna Maoh, Dr. Xiaolei Guo and Prof. John Tofflemire for the time and effort they dedicated to reading this thesis and providing constructive comments. Also, thank you to Dr. Faouzi Ghib for taking the time to chair my final defense.

Furthermore, I would like to thank Umair Durrani for providing the processed vehicle trajectory data, and his continuous encouragement and supports to me to complete this thesis. I would also like to show my courtesy to my lab mates. It was my pleasure to work along with those talented people.

Additionally, this research was financially supported by Natural Sciences and Engineering Research Council of Canada. I also appreciate my parents' financial support and meticulously care and attention.

Last but not the least, a special appreciation is also extended to the faculty and staff of the Department of Civil and Environmental Engineering, the Faculty of Engineering, the Faculty of Graduate Studies, and the Leddy Library of the University of Windsor.

TABLE OF CONTENTS

DECLARATION OF PREVIOUS PUBLICATION	iii
ABSTRACT	v
ACKNOWLEDGEMENTS	vi
LIST OF TABLES	xi
LIST OF FIGURES	xiii
LIST OF ACRONYMS	xv
CHAPTER 1 INTRODUCTION	1
1.1. Background.....	1
1.2. Objectives	4
1.3. Organization of Thesis.....	4
CHAPTER 2 LITERATURE REVIEW	6
2.1. Surrogate safety measures	6
2.1.1. Time-to-collision (TTC).....	6
2.1.2. Post-encroachment time (PET)	8
2.1.3. Deceleration to avoid crashes (DRAC).....	8
2.1.4. Crash potential index (CPI).....	9

2.1.5.	Aggregated crash index (ACI)	10
2.1.6.	Modified time-to-collision (MTTC).....	10
2.1.7.	Other surrogate safety measures	11
2.2.	Evaluation of safety using surrogate safety measures	12
2.2.1.	Safety evaluation using video data.....	12
2.2.2.	Safety evaluation using microscopic traffic simulation	13
2.2.3.	Safety evaluation using driving simulator.....	14
2.2.4.	Safety evaluation of countermeasures for car-truck mixed traffic	16
CHAPTER 3 DESCRIPTION OF DATA		18
3.1.	Vehicle trajectory data (US-101 freeway).....	18
3.2.	Crash and loop detector data (Gardiner Expressway)	22
CHAPTER 4 METHODS		27
4.1.	Surrogate Safety Measures for Car-following Conflicts	27
4.1.1.	Time-to-collision (TTC) and Post-encroachment-time (PET).....	27
4.1.2.	Crash potential index (CPI).....	31
4.2.	Surrogate Safety Measures for Lane-change Conflicts	36
4.2.1.	Conflicts between LCV and TV	38
4.2.2.	Conflicts between LCV and LV	43
4.3.	Validation of Surrogate Safety Measures	45

4.3.1.	Calibration and validation of VISSIM simulation	46
4.3.2.	Comparison of crash and non-crash conditions	50
CHAPTER 5	RESULTS AND DISCUSSION.....	54
5.1.	Car-following conflicts.....	54
5.1.1.	Distribution of TTC by vehicle pair type	54
5.1.2.	Distribution of PET by vehicle pair type	55
5.1.3.	Comparison between TTC and PET.....	56
5.1.4.	Comparison of CPI for car-following conflicts.....	57
5.2.	Lane-change conflicts.....	62
5.2.1.	CPI for lane-change conflicts between LCV and TV	62
5.2.2.	CPI for lane-change conflicts between LCV and LV	65
5.3.	Validation of CPI.....	68
5.3.1.	Validation of VISSIM simulation	68
5.3.2.	Validation of CPI for car-following conflicts	71
5.3.3.	Validation of CPI for lane-change conflicts.....	80
CHAPTER 6	CONCLUSION AND RECOMMENDATIONS	83
REFERENCES.....		87
Appendix A: Observed Speed Patterns Upstream and Downstream of Crash Location		95

Appendix B: SAS Code for Estimating Reaction Time using Monte Carlo Simulation.....	102
Appendix C: Sample Calculation of CPI.....	103
VITA AUCTORIS	105

LIST OF TABLES

Table 3-1. Number of observations for different types of lead and following vehicles	19
Table 3-2. Discretionary lane-change duration (LCD) of different vehicle pair types.	22
Table 4-1. VISSIM input parameters (Source: PTV AG 2014)	47
Table 4-2. Calibrated driving behaviour parameters for vehicle-following model in VISSIM (Source: Durrani et al. 2016)	48
Table 5-1. Descriptive Statistics of TTC and PET	56
Table 5-2. Mean reaction times from Monte Carlo Simulation.....	58
Table 5-3. Comparison of CPI for car-following conflicts among different vehicle pair types	59
Table 5-4. Average speed, spacing and DRAC for following vehicle in car-following conflicts	62
Table 5-5. Comparison of CPI for lane-change conflicts among different vehicle pair types of LCV and TV.....	63
Table 5-6. Comparison of average speed, average speed difference, spacing and DRAC for TV in lane-change conflicts between LCV and TV	64
Table 5-7. Comparison of CPI for lane-change conflicts among different vehicle pair types of LCV and LV	66
Table 5-8. Comparison of average speed, average speed difference, spacing and DRAC for LCV in lane-change conflicts between LCV and LV	67
Table 5-9. Estimation errors of VISSIM simulation for Gardiner Expressway	71

Table 5-10. Comparison of CPI for car-following conflicts among different vehicle pair types in crash case.....	72
Table 5-11. Average speed, spacing and DRAC for following vehicle in car-following conflicts in crash case	75
Table 5-12. Comparison of CPI for car-following conflicts among different vehicle pair types in non-crash case	76
Table 5-13. Average speed, spacing and DRAC for following vehicle in car-following conflicts in non-crash case.....	79
Table 5-14. Comparison of mean LCD for different vehicle types between observed and simulated data.....	81
Table 5-15. Comparison of CPI for lane-change conflicts between crash and non-crash cases (Car-Car)	82

LIST OF FIGURES

Figure 3-1. Schematic drawing of US-101 freeway	18
Figure 3-2. Determination of lane change duration using vehicle trajectory data.....	21
Figure 3-3. Lane-change vehicle and surrounding vehicles	22
Figure 3-4. Gardiner Expressway, Toronto, Canada	24
Figure 3-5. Number of crashes at different road sections on Gardiner Expressway	25
Figure 3-6. Speed profiles at detectors upstream and downstream of crash location before and after crash occurrence	26
Figure 4-1. Comparison of spacing between two vehicles for different length of lead vehicle	28
Figure 4-2. Comparison of TTC in time-distance diagrams	29
Figure 4-3. Illustration of TTC and PET in time-distance diagram.....	30
Figure 4-4. Estimation of TTC for one vehicle pair	31
Figure 4-5. Comparison of CPI for a given DRAC between car and truck	32
Figure 4-6. Positions of the lead and following vehicles during the following vehicle's braking maneuver to avoid rear-end crash	33
Figure 4-7. Distributions of driver reaction time	35
Figure 4-8. Types of lane-change conflicts	37
Figure 4-9. Lane-change conflicts between LCV and TV (LCV from inner lane to outer lane)	39
Figure 4-10. Lane-change conflicts between LCV and LV (LCV from inner lane to outer lane)	44
Figure 4-11. Calibration and validation of VISSIM simulation	50

Figure 4-12. Temporal variations in speed for crash and non-crash cases	51
Figure 5-1. Distribution of TTC by vehicle pair type	54
Figure 5-2. Distribution of PET by vehicle pair type	55
Figure 5-3. Relationships between spacing and the following vehicle speed.....	57
Figure 5-4. Comparison of CPI for car-following conflicts among vehicle pair types for different spacing intervals	60
Figure 5-5. Comparison of speed and PET between observed and simulation data with default and calibrated driving behavior parameters.....	69
Figure 5-6. Comparison of CPI for car-following conflicts among vehicle pair types in crash case	74
Figure 5-7. Comparison of CPI for car-following conflicts among vehicle pair types in non-crash case	78
Figure 5-8. Comparison of CPI for car-following conflicts between crash and non- crash cases.....	80

LIST OF ACRONYMS

<i>TTC</i>	Time-to-collision
<i>PET</i>	Post-encroachment time
<i>DRAC</i>	Deceleration to avoid crashes
<i>CPI</i>	Crash potential index
<i>MADR</i>	Maximum deceleration rate of the vehicle
<i>ACI</i>	Aggregated crash index
<i>MTTC</i>	Modified time-to-collision
<i>CI</i>	Crash index
<i>ACPM</i>	Aggregated crash propensity metric
<i>HV</i>	Heavy vehicle
<i>LCD</i>	Lane-change duration
<i>LCV</i>	Lane-change vehicle
<i>TV</i>	Trailing vehicle in the target lane
<i>LV</i>	Lead vehicle in the target lane

CHAPTER 1 INTRODUCTION

1.1. Background

According to the World Health Organization (WHO), approximately 1.24 million people died each year on roadways worldwide due to traffic accidents (WHO 2016). Road traffic accidents are the 9th leading causes of death and account for 2.2% of all deaths globally. In particular, young adults between the ages of 15 and 44 account for 59% of road traffic deaths. In order to solve the current road safety issues, dozens of countries around the world carried out the first Global Decade of Action for Road Safety 2011-2020 (WHO 2011). Many countries such as Australia, Indonesia, the United States and Mexico planned to take new steps to improve road safety and save lives on their roads.

Canada has faced similar issues although road safety in Canada has been improved in recent decades. In Canada, nearly two-thirds of fatal crashes occurred on rural undivided two-lane roads (Transport Canada 2014). In the province of Ontario, the crash rate was the highest in the Great Toronto Area (GTA) in 2010–2012 (Ministry of Transportation of Ontario 2014). The age distribution of the people involved in traffic accidents was similar to global trends: young adults with the age of 15-34 account for 40% of fatalities, and 45% of severe injuries (Transport Canada 2014). In 2009, there were 2,209 fatalities and 11,451 serious injuries related to traffic accidents in Canada, which is a 25% drop from 1996 (Transport Canada 2010).

As economy is globalized in recent few decades, demand for freight transportation has dramatically increased. In particular, road transportation is a major mode of freight transportation. According to Transport Canada (2015), the tonnage of goods by heavy

vehicles increased to 251.4 billion tonne-kilometers in Canada in 2013, which is a 4.1% increase from 2012. Similarly, the United States Department of Transportation reported that the tonnage of goods by heavy vehicles (in million tons) increased from 12,778 in 2007 to 13,182 in 2012, and this tonnage will increase to 18,786 by 2040 (U.S. DOT 2014).

Consequently, as more passenger cars and heavy vehicles share the same road, keeping roads safe becomes a big challenge. In Canada, 524 people died and 11,574 were injured in heavy vehicle-involved crashes in 2001 (Mayhew et al. 2004). This accounts for 20% of fatalities and 5% of reported injuries due to crashes on the roads. Also, 87% of fatalities and 74% of injuries in heavy vehicle-involved collisions were the people other than heavy vehicle drivers or occupants. In the U.S., 4,186 large trucks and buses were involved in fatal crashes in 2013, and large truck and bus fatalities per 100 million vehicle miles traveled by all motor vehicles remained steady at 0.142 from 2012 to 2013 (Federal Motor Carrier Safety Administration 2014). Thus, it is essential to analyze the safety of car-truck mixed traffic flow.

Conventionally, the relationships between crash frequency and factors have been analyzed using statistical models and historical crash data. However, this approach has the following limitations. First, safety problems can be identified only after crashes occur. Second, driver behaviour is not generally recorded in details in crash data. Thus, it is difficult to identify how driving behaviour is associated with crash occurrence or collision risk. Third, due to rare occurrence of crashes, it usually takes several years to collect the crash data with sufficient sample size.

To overcome these limitations, surrogate safety measures have been developed to estimate collision risk using vehicle trajectory data. The data provide detailed information

of driving behaviour such as instantaneous speed, acceleration, deceleration and the gap between two successive vehicles. In addition, trajectory data can be collected in a short period of time unlike crash data. The existing surrogate safety measures include the time-to-collision (TTC), post-encroachment-time (PET), deceleration to avoid crashes (DRAC), crash potential index (CPI) (Cunto and Saccomanno 2008), etc. Federal Highway Administration (FHWA) of the U.S. Department of Transportation also introduced the Safety Surrogate Assessment Model (SSAM) software (Gettman et al. 2008). The SSAM identifies the conflicts and evaluates the safety performance using vehicle trajectory data.

Surrogate safety measures reflect the probability of crash risk. For example, lower TTC, lower PET and higher DRAC values represent higher likelihood of crash occurrence. Gettman et al. (2008) validated the output of SSAM and developed the relationship between the number of conflicts predicted by SSAM and the observed number of crashes. It was found that the observed number of crashes was significantly correlated to the predicted number of conflicts at a 95% confidence interval with correlation coefficient (R-square) of 0.41. Similarly, Ariza (2011) evaluated the prediction accuracy of conflict-based crash prediction models for arterial segments using crash records and simulated vehicle trajectory data. The author found that traditional volume-based crash prediction model performs well when predicting conflicts. The author also found that conflict-based crash prediction model works well for intersections, but not for arterials.

However, cars and trucks have not been differentiated in the safety evaluation using surrogate safety measures in the past studies. Thus, fundamental differences in driving behaviour between car and truck drivers were not clearly captured in the safety evaluation. For instance, car driver's vehicle-following behaviour is affected by the size of lead trucks

due to visibility and difference in speed. Also, car and truck drivers' gap acceptance behaviours are different when they change lanes. Moreover, conflicts have not been classified by the type of vehicles although it affects the severity of crashes. For instance, car drivers are more likely to suffer severe injury if they have collisions with a large truck compared to colliding with a car. Thus, it is essential to estimate surrogate safety measures for different types of vehicles separately.

1.2. Objectives

The primary objectives of this study are as follows:

- 1) To develop more elaborate surrogate safety measures for car-following and lane-change conflicts using vehicle trajectory data;
- 2) To compare surrogate safety measures for different vehicle types (cars and trucks) and different car-following and lane-change conditions;
- 3) To validate surrogate safety measures using the observed crash and traffic data.

1.3. Organization of Thesis

This thesis is organized as follows:

Chapter 2 reviews the conventional and modified surrogate safety measures, and different data sources for evaluating road safety. Chapter 3 describes the vehicle trajectory data, crash data, and traffic data from loop detectors for development and validation of surrogate safety measures. Chapter 4 proposes the modified surrogate safety measures for car-following and lane-change conflicts, and the framework of validating the proposed surrogate safety measures. Chapter 5 presents and discusses the results of the surrogate safety measures for car-following and lane-change conflicts. Chapter 6 draws conclusions

based on findings, identifies limitations in this study and recommends the extensions of this research.

CHAPTER 2 LITERATURE REVIEW

2.1. Surrogate safety measures

This section describes various surrogate safety measures that have been developed using vehicle trajectory data in the past.

2.1.1. *Time-to-collision (TTC)*

Time-to-collision (TTC) has been used to classify the rear-end conflict between two vehicles in car-following conditions. TTC was first introduced by Hayward (1972) and further discussed by Hyden (1987). TTC is the minimum time for the following vehicle to reach the position of the lead vehicle with the initial constant velocity at the time instant when the following vehicle begins braking to avoid the collision with the lead vehicle (Gettman and Head 2003).

Many researchers have expressed TTC in different equations. For instance, Gettman & Head (2003) defined TTC in the Surrogate Safety Assessment Model (SSAM) as the time it takes for the following vehicle to reach the position of the lead vehicle if the following vehicle's speed remains the same. TTC is calculated as follows:

$$TTC(t) = \frac{X_L(t) - X_F(t)}{V_F(t)} \quad (2-1)$$

where $TTC(t)$ is the time-to-collision at time t , $X_L(t)$ and $X_F(t)$ are the positions of the lead and following vehicles at time t , respectively, and $V_F(t)$ is the velocity of the following vehicle at time t .

However, Bachmann et al. (2012) criticized that the TTC in [Eq. \(2-1\)](#) does not account for speed of the lead vehicle. Thus, they revised the definition of TTC assuming that both lead and following vehicles continue moving at their present speeds and on the same trajectory. The revised TTC is calculated as follows:

$$TTC(t) = \begin{cases} \frac{X_L(t) - X_F(t)}{V_F(t) - V_L(t)}, & \text{if } V_F(t) \geq V_L(t) \\ \infty, & \text{if } V_F(t) < V_L(t) \end{cases} \quad (2-2)$$

where $V_L(t)$ is the velocity of the lead vehicle at time t . On the other hand, some researchers defined TTC considering both gap and speed difference between two vehicles (Minderhoud & Bovy 2001; Vogel 2003; Astarita et al. 2012). Unlike Gettman & Head (2003) and Bachmann et al. (2012) which assumed the front end of the vehicle as the positions of both lead and following vehicles, this TTC considers the distance between the rear end of the lead vehicle and the front end of the following vehicle as follows:

$$TTC(t) = \frac{X_L(t) - X_F(t) - L_L}{V_F(t) - V_L(t)}, V_F(t) > V_L(t) \quad (2-3)$$

where L_L is the length of the lead vehicle. Thus, this TTC considers the actual spacing between two vehicles. In this equation, TTC can be calculated only if the lead vehicle's speed is lower than the following vehicle speed ($V_L(t) < V_F(t)$).

The threshold of TTC has been used to define the dangerous situation or a conflict. For example, Minderhoud & Bovy (2001) reported that a conflict occurs if TTC is less than 4 s. Gettman & Head (2003) suggested that a conflict occurs when TTC is less than 1.5 s in the SSAM. Vogel (2003) and Habtemichael and Santos (2012) also adapted this threshold.

El-Tantawy et al. (2009) and Bachmann et al. (2012) defined a conflict as the situation when TTC is less than 0.5 s.

2.1.2. Post-encroachment time (PET)

Post-encroachment time (PET) is defined as “the minimum post-encroachment time observed during the conflict” according to Gettman & Head (2003). The post-encroachment time is the difference between the time when the lead vehicle last occupied a position and the time when the following vehicle first reached the same position. Lower PET value represents higher probability of a collision and zero-value indicates a collision.

Unlike TTC, PET is an observed value which considers the speed and acceleration variability of the two vehicles during the conflict. Most drivers of the following vehicles will decelerate to maintain sufficient safety distance when the gap with the lead vehicle decreases. Due to this driver’s speed adjustment, the value of PET is generally longer than that of TTC. Vogel (2003) explored the differences between TTC and PET to evaluate the road safety performance of junctions. The study found that the values of PET were similar in different locations whereas the values of TTC varied among different locations. The study also found that TTC was shorter at the locations further away from the junction, and longer at the locations closer to the junction.

2.1.3. Deceleration to avoid crashes (DRAC)

The deceleration to avoid crashes (DRAC) is defined as the minimum of the deceleration rate of the following vehicle to timely stop behind the lead vehicle. DRAC is calculated using the following equation:

$$\text{DRAC}(t) = \frac{(V_L(t) - V_F(t))^2}{2(X_L(t) - X_F(t) - L_L)}, V_F(t) > V_L(t) \quad (2-4)$$

This equation is only valid when the following vehicle's speed is higher than the lead vehicle's speed. Higher value of DRAC represents higher chance of collision. The value of DRAC longer than a given threshold is recorded as a conflict similar to TTC. For instance, the American Association of State Highway and Transportation Officials suggested that DRAC longer than 3.4 m/s² is a conflict (AASHTO 2004). Archer (2004) and Astarita et al. (2012) reported that conflicts are detected if DRAC is longer than 3.35 m/s² or TTC is shorter than 1.5 seconds. Cunto & Saccomanno (2008) and Cunto et al. (2009) applied DRAC to calibration and validation of the safety performance on freeways and intersections.

2.1.4. Crash potential index (CPI)

Crash potential index (CPI) is defined as the probability that a given vehicle's DRAC exceeds its maximum available deceleration rate (MADR) or braking capacity (Cunto & Saccomanno 2008). The mathematical expression of CPI for a vehicle *i* is as follows:

$$\text{CPI}_i = \frac{\sum_{t=0}^N \Pr(\text{DRAC}_i(t) > \text{MADR}_i(t)) \times \Delta t}{T} \quad (2-5)$$

where DRAC_{*i*}(*t*) and MADR_{*i*}(*t*) are the DRAC and MADR of the vehicle *i* at time *t*, respectively, *N* is the total number of time intervals, Δ*t* is the observation time interval and *T* is the total observation time period (*T* = *N* × Δ*t*). MADR_{*i*}(*t*) varies in different surface conditions of the roadway (wet or dry) and vehicle mechanical characteristics (braking

system). Due to these variations, MADR was assumed to follow the truncated normal distribution (AASHTO 2004; Cunto & Saccomanno 2008; Weng & Meng 2011).

2.1.5. Aggregated crash index (ACI)

Aggregated Crash Index (ACI) was introduced by Kuang et al. (2015). ACI represents the cumulative crash probabilities of all possible conflicts in car-following situations. The authors argued that the conventional surrogate safety measures such as TTC, DRAC, CPI and PSD (proportion of stopping distance) neglect the reaction time of the following vehicle driver. Moreover, these measures cannot be applied when the speed of the following vehicle is lower than the speed of the lead vehicle, which occurs more frequently in congested traffic conditions. To compute ACI, car-following scenarios were classified into different conflict types using tree structures based on the distributions of driver reaction time and braking capability (MADR). Then, probabilities for each conflict type were estimated. It was found that ACI outperforms TTC, PSD and CPI in predicting the number of rear-end crashes. Also, the distributions are likely to vary with different driving behaviours in different regions.

2.1.6. Modified time-to-collision (MTTC)

Ozbay et al. (2008) developed the modified TTC (MTTC) and crash index (CI) which were extended from the TTC. The researchers argued that the conventional TTC ignores the potential conflict when the lead vehicle speed is higher than the following vehicle speed and the accelerations of the lead and following vehicles. Unlike TTC, MTTC is determined based on both relative speed and relative acceleration of two successive vehicles. More specifically, MTTC assumes that vehicle speeds change at constant acceleration during conflicts. However, it is uncertain why this assumption is more valid than the assumption

of TTC that vehicle speeds are constant. CI was also proposed to indicate the severity of a potential crash. The two surrogate safety measures were calculated using the vehicle trajectory data extracted from PARAMICS microscopic traffic simulation model and validated with 10-year historical crash record. The results showed that MTTC and CI were correlated with hourly crash frequency.

2.1.7. Other surrogate safety measures

Jiménez et al. (2013) also proposed an improved approach to calculate TTC for two-vehicle conflicts at the intersections, which was utilized in collision avoidance system. They developed different equations of TTC for 6 types of conflicts which are classified by the point of impact. However, these surrogate safety measures were not validated using the observed crash data. Also, the width and length of vehicles were neglected in determining the point of impact.

Wang and Stamatiadis (2013) introduced the aggregated crash propensity metric (ACPM) for safety evaluation of signalized intersections. Unlike TTC, the ACPM considers driver's reaction time and vehicle's maximum braking rates based on the distributions of reaction time and maximum braking rates. They estimated ACPM for crossing, rear-end and lane-change conflicts using the vehicle trajectories from VISSIM simulation. They found that the ACPM was strongly correlated with actual crash frequency at 12 intersections. However, similar to ACI, the distributions of reaction time and maximum braking rates were not validated for different vehicle types.

Besides the surrogate safety measures discussed above, other surrogate safety measures were proposed in the SSAM (Gettman & Head 2003). MaxS is the maximum speed of the lead and following vehicles throughout the conflict. DeltaS is the difference in speeds

between the lead and following vehicles at the time of minimum TTC. Higher value of MaxS or DeltaS represents higher severity of potential crashes.

2.2. Evaluation of safety using surrogate safety measures

This section reviews the studies that evaluated road safety using the above surrogate safety measures and traffic data from different sources.

2.2.1. Safety evaluation using video data

In recent years, vehicle trajectory data were collected using video to determine the surrogate safety measures. For instance, St-Aubin et al. (2013) estimated TTC using the video data from cameras at the entrance of one highway in Montreal, Canada. Using the data, they evaluated safety of the protected highway on-ramps. This treatment prohibits lane change from inner lanes to outer lanes immediately downstream of on-ramps in the weaving zone. This will help avoid conflicts between exit vehicles to off-ramps and merging vehicles from on-ramps. Based on the cross-sectional comparison of statistics and distribution of TTC, it was found that rear-end conflicts are more likely to occur than lane-change conflicts in the merging area.

Silvano et al. (2016) also collected vehicle and bicycle trajectory data using video to evaluate safety at signalized intersections. Using the data, they estimated the probability of conflicts between a vehicle and a bicycle which approach the intersection. They found that the conflict probability depends on which type of user (driver or bicyclist) arrives the conflict zone first.

2.2.2. Safety evaluation using microscopic traffic simulation

Evaluating safety performance using traffic simulation was first proposed by Cooper & Ferguson (1976). Instead of collecting vehicle trajectory data using video, the data can be generated using traffic simulation. Traffic simulation can replicate complex and dynamic interactions among road geometry, traffic, and drivers. Traffic simulation can also be used to examine the impacts of traffic control strategies and geometric design on performance and safety before actual implementation.

Some researchers evaluated road safety using traffic simulation. For instance, Saccomanno et al. (2009) used the calibrated VISSIM traffic simulation model for safety evaluation of car-truck mixed traffic. However, they assumed the same driving behaviour parameters for both cars and trucks although car and truck driver behaviours are different. In this regard, Zheng et al. (2015) pointed that the conventional car-following models (e.g. Optimal Velocity Model (OVM), Intelligent Driver Model (IDM), Gipp's model, Krauss model and Wiedemann99 model) did not incorporate the parameters related to vehicle types. Thus, the researchers proposed a new model called the Visual Imaging model (VIM) which can model car-following behaviour in the heterogeneous traffic flow with mixed vehicle types. After the validation of the model with vehicle trajectory data for the US-101 freeway in California, it was found that VIM could replicate the observed trajectory for different types of lead and following vehicles.

Habtemichael and Santos (2012) evaluated the effect of different types of aggressive driving behaviours on conflicts using a microscopic traffic simulation model and TTC. They found that TTC was shorter for speeding, following too close and unsafe lane change in a weaving section. They also found that the numbers of conflicts for these three

dangerous behaviours increased by up to 2.36, 6.16, and 7.02 times, respectively, compared to the normal driving behaviour.

Chai and Wong (2015) estimated the occurrence and severity of traffic conflicts at signalized intersections in Singapore using a cellular automata (CA) model. They claimed that CA models are simpler, more computationally efficient and more flexible for modeling individual vehicle movements than commercial simulation packages. They found that the TTC and PET estimated using the CA model predicted the observed conflicts between vehicles and pedestrians more accurately than the TTC and PET estimated using SSAM and VISSIM traffic simulation model.

2.2.3. Safety evaluation using driving simulator

Surrogate safety measures have also been estimated using a driver simulator. A driving simulator becomes a popular research tool for investigating driving behaviour and evaluating safety (Shechtman et al. 2009). Compared to the field experiment, driving simulators have many benefits including control of the environment, efficiency and expense (Classen et al. 2011). As driving simulators eliminate the risk of driver injury during the experiment, they can be used to investigate the effects of aggressive driving behaviour and countermeasures on safety. Furthermore, detailed vehicle trajectory and vehicle dynamics data can be obtained from the driving simulator. Also, demographic characteristics of subjects who drive the simulator can be used to investigate the association of driver characteristics with driving behaviour.

Some studies evaluated safety using a driving simulator. For instance, Levulis et al. (2015) explored the influence of vehicle type and vehicle size on overtaking maneuver on a two-lane highway using a driving simulator. The study showed that the size of oncoming

vehicles in the opposite direction plays more significant role than the type of oncoming vehicles in drivers' overtaking maneuver. This indicates that drivers generally feel unsafe and keep longer gap when a larger oncoming vehicle is approaching in the opposite direction.

Yan et al. (2008) validated surrogate safety measures using a motion-based driving simulator. They observed traffic parameter (speed) and safety parameter (crash history) for a four-leg intersection with the highest crash frequencies in Orlando, Florida. The results showed that the speed was closely related to the number of crashes at different locations at the intersection. The results also showed that the speed followed the normal distribution and mean speeds were similar between the field data and the simulator data. Thus, the results indicate that a driving simulator can be used as a valid tool to investigate safety at intersections.

Yang et al. (2013) explored the influence of the curbs and their interactions with other factors (speed limit, weather and traffic density) on driver behaviour on a four-lane rural highway. They obtained the driving behaviour data (e.g., average speed, speed variability, lateral position and lane position variability) using the DriveSafety DS-600c driving simulator. The results showed that the influences of the factors are complex and interrelated. It was found that drivers are more likely to determine the speed based on the speed limit and the relative speed to other vehicles instead of the road configuration or curbs. However, they found that the presence of curbs and other roadside infrastructures made drivers feel safer in bad weather and visibility conditions.

Wang et al. (2016) investigated driver's collision avoidance behaviour in different car-following situation using a driving simulator. They observed that driver's perception

reception time (PRT) increased as the headway with the lead vehicle increased. They also found that PRT decreased for the latter trials than the first trial.

2.2.4. Safety evaluation of countermeasures for car-truck mixed traffic

Researchers have evaluated the impacts of countermeasures on safety using surrogate safety measures. For instance, Nezamuddin et al. (2011) tested the safety of two active freeway management strategies (ATM), variable speed limit (VSL) and peak-hour shoulder use, based on the number of conflicts as defined in the SSAM. They found that both VSL and peak hour shoulder use decreased the average vehicle delay and the number of conflicts by reducing speed variability.

Some studies specifically focused on safety evaluation of the countermeasures for car-truck mixed traffic. For instance, Saccomanno et al. (2009) examined how limiting the maximum operating speed of heavy vehicles on freeways affects crash risk. A speed limiter installed on heavy vehicles reduces the revolution of the engine and thereby restricts the maximum speed. The study found that a mandated speed limiter set at 105 km/h could significantly enhance the safety in uncongested traffic conditions. However, the effect of speed limiter was not significant as the traffic volume and truck percentage increased.

El-Tantawy et al. (2009) evaluated safety of truck lane restrictions and dedicated truck lanes using the PARAMICS traffic simulation model and the SSAM. The results showed that truck lane restrictions and dedicated truck lanes reduced the number of lane-change conflicts, but increased the numbers of merging and rear-end conflicts. In particular, designating the innermost lane as the dedicated truck lane or restricting trucks in the two innermost lanes significantly reduced the interactions between trucks and passenger cars, and lane-change conflicts.

Some researchers compared safety effects between differential speed limits (DSL) DSL and uniform speed limits (USL). Garber et al. (2000) found that there was no significant difference in mean speed, 85th percentile speed and speed variance between DSL and USL in different states. Thus, speed characteristics were not influenced by the type of speed limit policy on rural Interstate highways. Similarly, there was no significant difference in crashes between DSL and USL. On the other hand, Ghods et al. (2012) found that DSL encourages car drivers to overtake trucks on two-lane highway and has adverse impact on road safety. However, DSL enhances road safety by reducing the rate of cars-overtaking-cars and the interactions between cars.

CHAPTER 3 DESCRIPTION OF DATA

3.1. Vehicle trajectory data (US-101 freeway)

To estimate the surrogate safety measures, the trajectory data were retrieved from the Next Generation Simulation (NGSIM) website. In the NGSIM project, individual vehicle trajectories were obtained from a 640-meter (2100 feet) section of US-101 freeway in Los Angeles, California, U.S.A for the three time periods: 1) 7:50 a.m. - 8:05 a.m.; 2) 8:05 a.m. - 8:20 a.m.; and 3) 8:20 a.m. - 8:35 a.m. The study area consists of five lanes in the mainline freeway (Lanes 1-5) with one auxiliary lane (Lane 6) between the on-ramp and the off-ramp as shown in [Figure 3-1](#). The vehicle trajectory data were collected for every one-tenth second (0.1 s) using 8 digital cameras mounted at the top of an adjacent 36-story building.

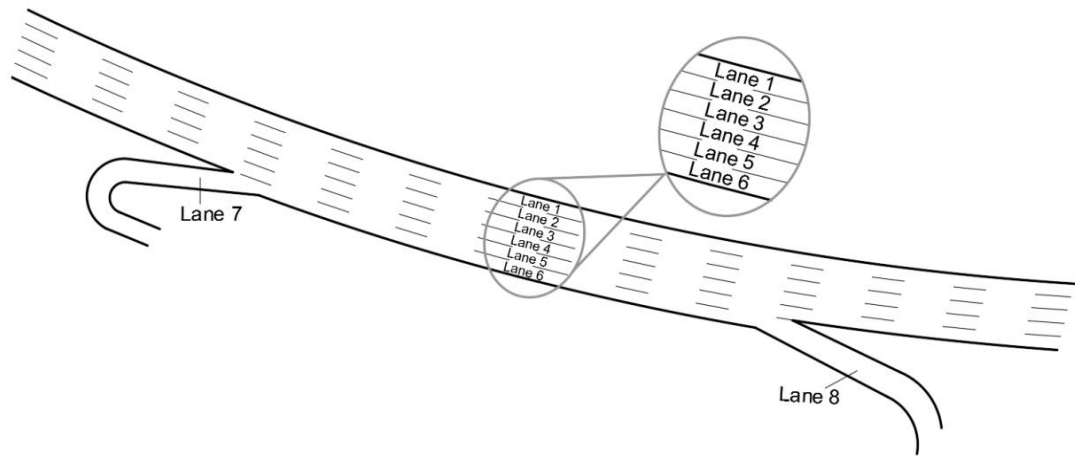


Figure 3-1. Schematic drawing of US-101 freeway

To estimate rear-end conflicts between the lead and following vehicles in the same lane, the trajectories of the vehicles which did not change lanes were only extracted from the data. Also, the trajectories of the vehicles in the three innermost lanes (Lanes 1-3) were

only extracted to minimize the effects of merging and diverging vehicles on the vehicles in the mainline freeway.

Vehicles in the dataset are classified into motorcycles, automobiles (cars) and heavy vehicles (trucks and buses). The numbers of the four vehicle pair types (a car following a car (Car-Car), a car following a heavy vehicle (Car-HV), a heavy vehicle following a car (HV-Car) and a heavy vehicle following a heavy vehicle (HV-HV) in the three time periods are shown in [Table 3-1](#). The table shows that a car followed by a car is the most common vehicle pair type on this freeway segment. However, due to a lack of data, the case of HV-HV could not be analyzed in this study.

Table 3-1. Number of observations for different types of lead and following vehicles

Following vehicle type	Lead vehicle type	Symbol	Number of observations
Car	Car	Car-Car	4440
Car	Heavy Vehicle	Car-HV	63
Heavy Vehicle	Car	HV-Car	94
Heavy Vehicle	Heavy Vehicle	HV-HV	2

It should be noted that the numbers of observations for HV-involved vehicle-following cases are relatively low due to low volume of HV during morning peak period. It is expected that during the time period of higher volume of HV, the number of HV-involved vehicle-following cases will be higher. However, this does not necessarily indicate that the collision risk will also be higher since speed and spacing between vehicles will be lower and car drivers will take more caution to avoid conflicts with HV.

To estimate lane-change conflicts, the trajectories of lane-change vehicles (LCVs) were also extracted from the data. Considering geometric conditions of the study area, changing

the lane from the entrance ramp (Lane 7) to inner lanes (Lanes 1-5) or changing the lane from inner lanes to the auxiliary lane (Lane 6) and then the exit ramp (Lane 8) was considered as mandatory lane changes. All other lane changes were considered as discretionary lane changes. This study only analyzed the discretionary lane changes among different vehicle type pairs. In discretionary lane changes, drivers accept the gap only when they feel safe.

As discussed in many studies, lane changes do not occur instantly because it takes some time for drivers to observe the traffic conditions in the current lane and the target lane, and gradually change the lateral position of their vehicles. (Wei et al. 2000; Moridpour et al. 2010). Some studies also claimed that average lane-change duration (LCD) was different for different vehicle types (Toledo and Zohar 2007; Aghabayk et al. 2011). In these studies, LCD was determined based on the lateral position of the front center of each lane-change vehicle (LCV). However, this approach neglects the width of LCV and it does not objectively determine the start and end times of lane change.

Thus, an objective method of determining LCD based on the width and lateral position of each LCV was developed in this study. For instance, assume that the lateral position of the front center of a LCV changes the lane from Lane 3 to Lane 4 as shown in [Figure 3-2](#). Lane markings are denoted as dashed lines in the figure. The blue and red reference lines in Lane 3 and Lane 4 represent the front center position of LCV where its front-right and front-left touch the lane marking, respectively. The lateral positions of these two lines are different for different width of LCVs. Thus, the start of lane change is defined as the last time frame when the LCV touches the blue line in the current lane and the end of lane

change is the first time frame when the LCV touches the red line in the target lane. LCD is recorded as the difference between the start and end time frames of lane change.

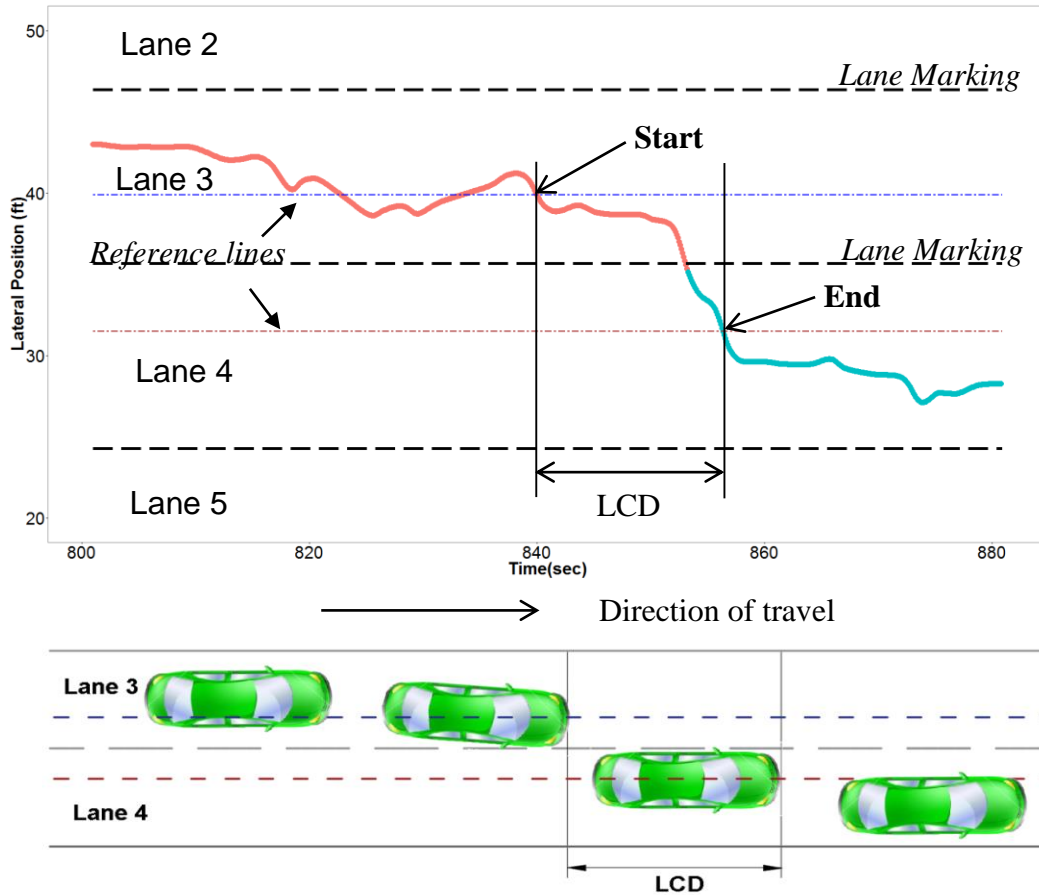


Figure 3-2. Determination of lane change duration using vehicle trajectory data

[Figure 3-3](#) shows the LCV and the surrounding vehicles including the lead vehicle (LV) and the trailing vehicle (TV) in the target lane. [Table 3-2](#) shows the LCD for different types of LCV, LV and TV. It was found that the time it took for cars to change the lane between the lead car and the trailing heavy vehicle was shorter than the time for cars to change the lane between the lead car and the trailing car. Besides, the mean LCD for heavy vehicles was approximately 5 times longer than the mean LCD for cars. This is because the average width of heavy vehicles (8.33 ft) was higher than that of cars (6.31 ft) and the lateral extent

of movement was larger for heavy vehicles than cars during lane changes. This is also because speed and acceleration are lower for heavy vehicles than cars during lane changes.

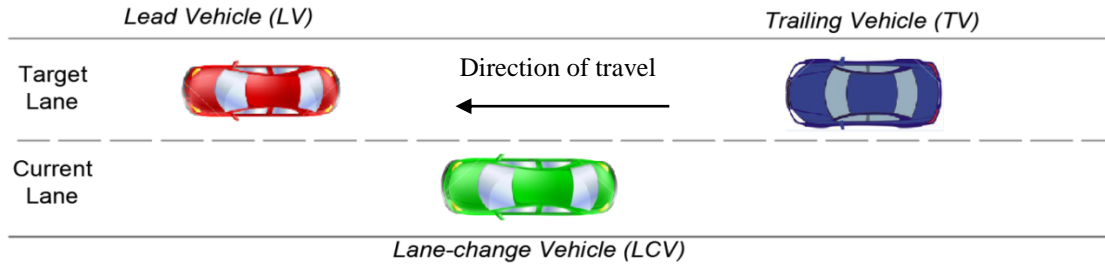


Figure 3-3. Lane-change vehicle and surrounding vehicles

Table 3-2. Discretionary lane-change duration (LCD) of different vehicle pair types

LCV	LV	TV	Min (s)	Mean (s)	Max (s)	SD (s)	Number of observations
Car	Car	Car	1.20	3.46	14.90	1.93	255
		HV	1.50	3.09	7.60	1.40	24
	HV	Car	4.90	4.90	4.90	0	1
HV	Car	Car	4.60	15.08	21.80	6.20	2

3.2. Crash and loop detector data (Gardiner Expressway)

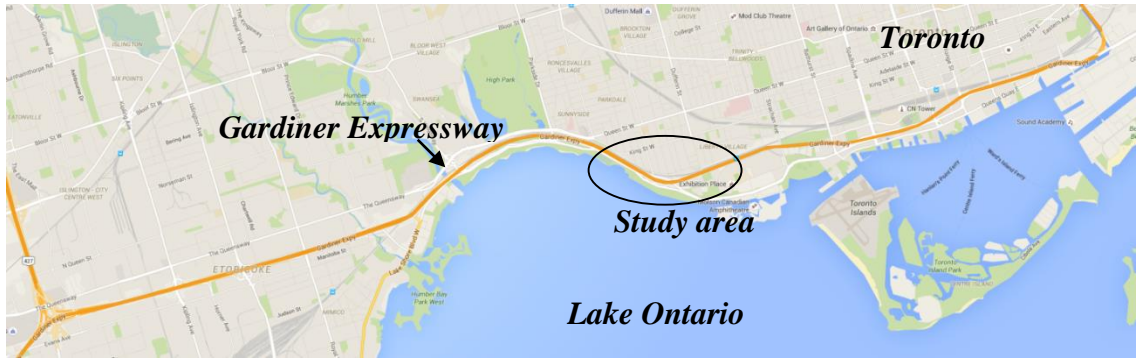
To validate the surrogate safety measures, they have been compared with the observed crash frequency (Shahdah et al. 2015; Essa and Sayed 2015; Ariza 2011). If the values of surrogate safety measures are significantly correlated with crash frequency, the surrogate safety measures reflect risk of crashes (Gettman and Head 2003).

However, since not all the events with high risk of crash lead to a collision, this approach has a limitation in validating surrogate safety measures (Cunto et al. 2009). Thus, Cunto et al. (2009) proposed that surrogate safety measures are estimated for a few minutes before the time of actual crashes. They hypothesized that the value of surrogate safety measures would be higher at the time period closer to the time of crashes. They also hypothesized

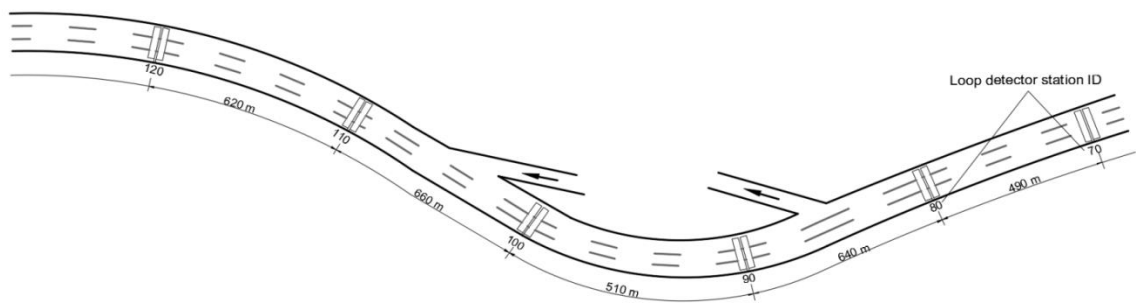
that the value of surrogate safety measures would be higher in the time period immediately before the time of crashes than the time period of normal traffic condition.

However, crashes are rare events and individual vehicle trajectories at the time of crashes are not readily available. Instead, loop detector data can capture aggregated traffic characteristics at the location closer to the crash site at the time of crashes. These traffic data are typically available at fixed locations of loop detector stations for 24 hours a day at short time intervals (20 sec. - 1 min.) on instrumented freeways. Since surrogate safety measures cannot be estimated using the aggregated traffic data, individual vehicle trajectories can be replicated in a microscopic traffic simulation model calibrated using the observed loop detector data (Cunto et al. 2009).

Since crash data were not available for the US-101 freeway, crash and loop detector data were collected from a 2.9-km segment of the westbound Gardiner Expressway in Toronto, Canada as shown in [Figure 3-4](#). Loop detectors installed at six locations along the expressway recorded the average speed, volume and occupancy in every 20 seconds for weekdays over 13 months from the beginning of January 1998 to the end of January 1999. Within the study area, there were three westbound through lanes, one off-ramp and one on-ramp. A vehicular capacity was 1,800 vehicles per lane per hour and a total capacity in one direction was 5,400 vehicles per hour (Livey 2015).



(a) Map (Google Map 2016)



(b) Schematic drawing

Figure 3-4. Gardiner Expressway, Toronto, Canada

During the 13-month period, a total of 108 crashes have occurred on this section of the freeway. The time and location of crashes were reported in the incident logs by the operator at the City of Toronto Traffic Operation Centre. The location of crash was verified using the close circuit cameras and the distance to the closest loop detector station upstream of the crash site was recorded. In this study, the location of crash was identified as the closest loop detector station upstream of the crash site.

[Figure 3-5](#) shows the number of crashes at different locations during the 13-month period. It was found that the number of crashes at the road section between the detector stations 80 and 90 - upstream and downstream of the off-ramp, respectively - was

significantly higher than the other road sections. Thus, the analysis focused on the crashes at the section between the stations 80 and 90.

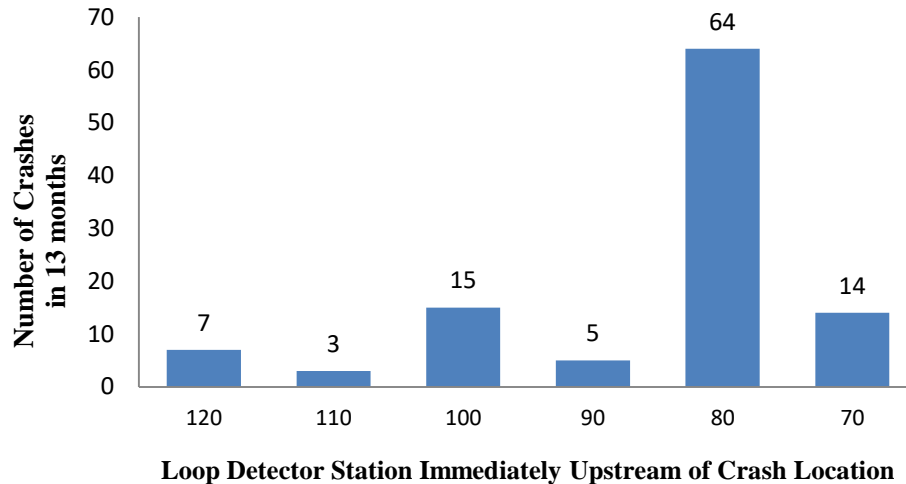


Figure 3-5. Number of crashes at different road sections on Gardiner Expressway

Although the time of crash occurrence was reported in the incident logs, the time may not be actual crash time due to delay in detection and reporting of crashes. Thus, the crash time was estimated using the speed profile at the upstream station during 30 minutes before and after the reported crash time. It was hypothesized that the speed upstream of the crash location abruptly drops immediately after the crash occurs due to lane blockage and capacity reduction. Thus, the time of crash was estimated as the time when the speed at the closest upstream detector abruptly dropped.

[Figure 3-6](#) shows an example of the speed profiles at the detectors stations 80 and 90 which are the stations immediately upstream and downstream of the location of one crash (crash ID 6613) 30 minutes before and after the reported time of crash. Based on a sudden speed drop at the upstream detector, 17:28:00 was estimated as the crash time. The figure shows that the speed at the downstream detector abruptly dropped a few minutes before

the crash time. Similar speed patterns were also observed for the other crashes that occurred between detector stations 80 and 90 as shown in Appendix A.

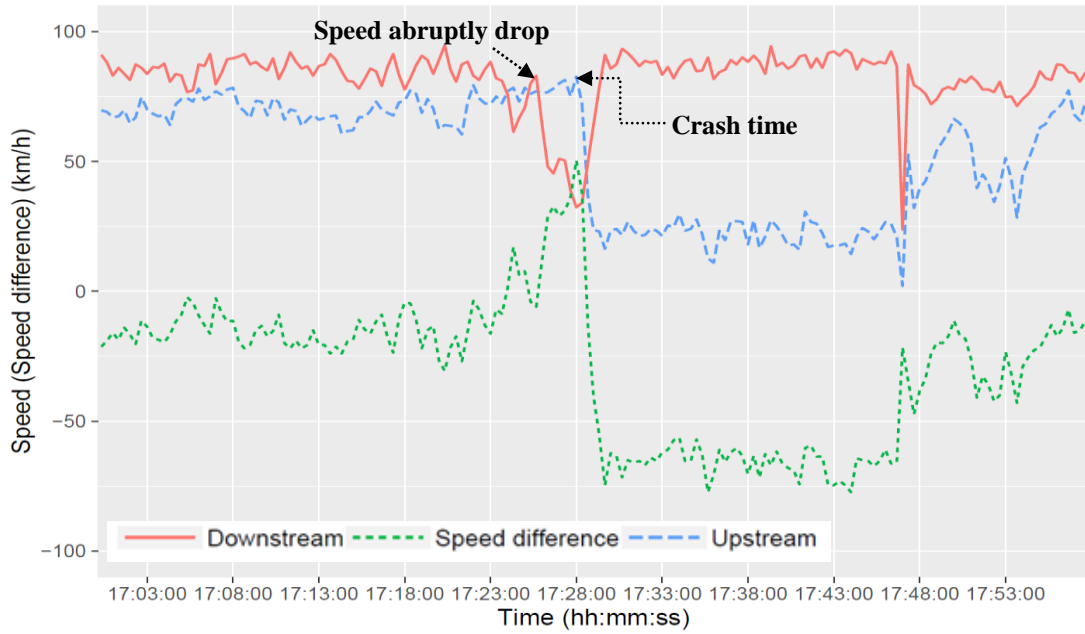


Figure 3-6. Speed profiles at detectors upstream and downstream of crash location before and after crash occurrence

CHAPTER 4 METHODS

This section develops the surrogate safety measures for two types of conflicts – car-following conflicts and lane-change conflicts.

4.1. Surrogate Safety Measures for Car-following Conflicts

“Car-following conflicts” are defined as the conflicts between the lead and following vehicles in the same lane. These conflicts are likely to lead to rear-end collisions. Three surrogate safety measures for car-following conflicts - Time-to-collision (TTC), post-encroachment-time (PET) and crash potential index (CPI) - were estimated in this study.

4.1.1. *Time-to-collision (TTC) and Post-encroachment-time (PET)*

The TTC used in this study was calculated based on the spacing between the rear end of the lead vehicle and the front end of the following vehicle, and the velocity of the following vehicle. This is because a rear-end collision occurs when the front end of the following vehicle hits the rear end of the lead vehicle. Also, actual spacing between the two vehicles better reflects risk of collision than front-to-front spacing since the length of the lead vehicles varies. [Figure 4-1](#) illustrates that although the front-to-front spacing is the same for two vehicle pairs – car following car and car following truck, actual spacing is shorter for car following truck than car following car.

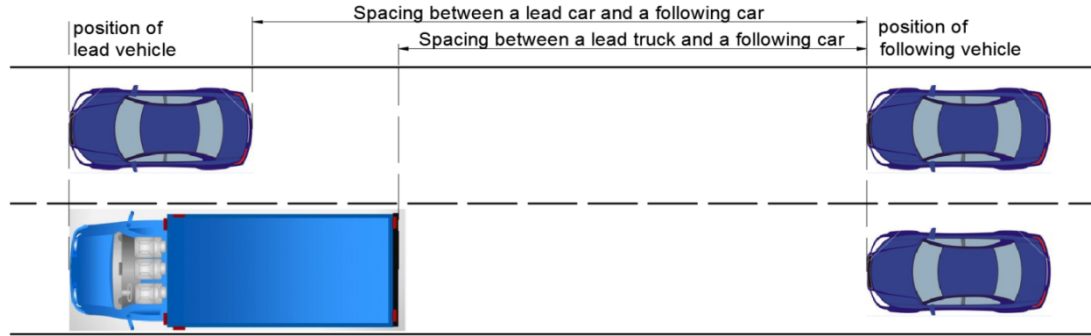


Figure 4-1. Comparison of spacing between two vehicles for different length of lead vehicle

In this study, TTC is calculated using the following equation:

$$TTC_i(t) = \frac{X_L(t) - X_F(t) - L_L}{V_F(t)} \quad (4-1)$$

This equation of TTC was adapted by Kusano and Gabler (2011). This TTC denotes the time it takes for the front-end of the following vehicle to reach the rear-end of the lead vehicle if the lead vehicle suddenly stops at a given time instant and the following vehicle maintains the same speed. This TTC does not consider the speed of the lead vehicle unlike the TTC in [Eq. \(2-3\)](#).

The TTC in [Eq. \(4-1\)](#) is used in this study because of the following limitations of the TTC in [Eq. \(2-3\)](#). First, [Eq. \(2-3\)](#) implicitly assumes that the spacing at a given time instant remains constant until the front-end of the following vehicle reaches the position of rear-end of the lead vehicle. However, the spacing is not constant since the lead vehicle would continue moving (instead of stopping) at the instantaneous speed for a given time instant. [Figure 4-2\(a\)](#) illustrates that the spacing observed at a given time instant is shorter than actual spacing that should have been used to calculate TTC. Second, [Eq. \(2-3\)](#) cannot

be used when the lead vehicle's speed is higher than the following vehicle's speed. Since the lead vehicle's instantaneous speed can significantly fluctuate particularly at very short time frames, the TTC may not be measured in some time frames. This makes difficult to observe general distribution of TTC. The PET is defined as the time headway between the front-end of the following vehicle and the rear-end of the lead vehicle.

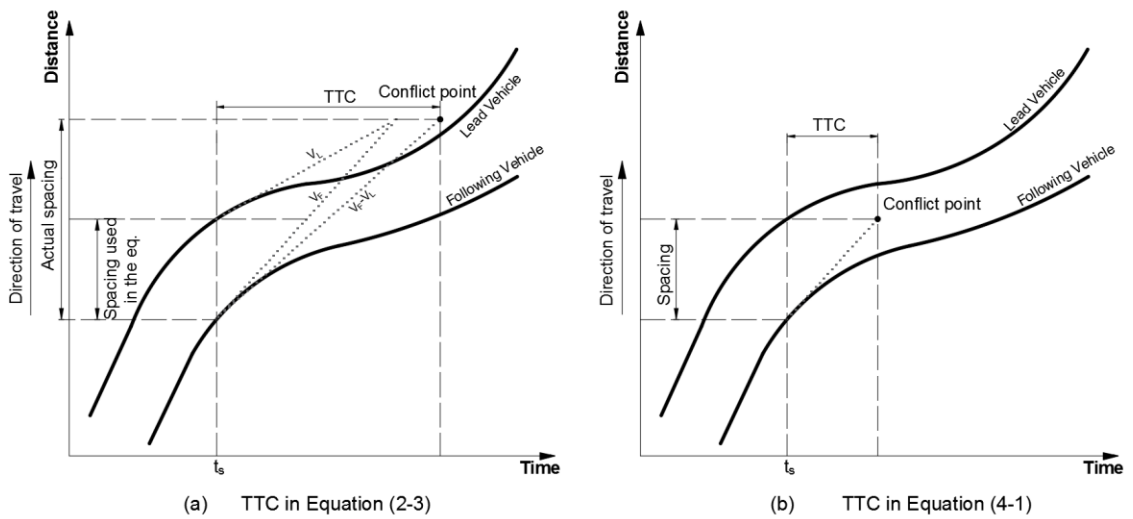


Figure 4-2. Comparison of TTC in time-distance diagrams

[Figure 4-3](#) illustrates how the TTC in [Eq. \(4-1\)](#) and PET can be measured in the time-distance diagram of the lead and following vehicles' trajectory. The horizontal axis of the figure is the time whereas the vertical axis is the positions of the vehicles. Two curves represent the trajectories of the lead and following vehicles.

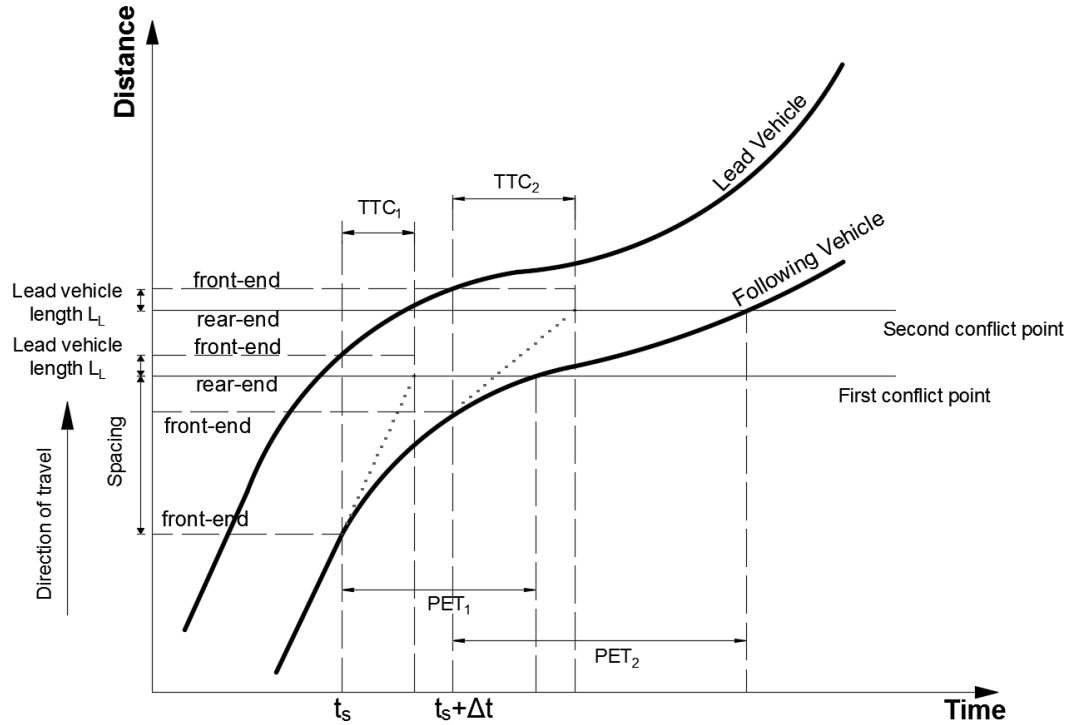


Figure 4-3. Illustration of TTC and PET in time-distance diagram

After $TTC(t)$ is calculated for each time t , a minimum value of TTC during the car-following condition is determined as the TTC for each vehicle pair. For example, [Figure 4-4](#) shows the estimated $TTC(t)$ at each time t in 0.1 s intervals and the minimum TTC (= 0.84 s) for one vehicle pair. Although this TTC does not consider the speed of the lead vehicle, it can capture the following vehicle's responses to the lead vehicle's speed change at every time frame and determines the highest risk of rear-end collision for the vehicle pair. Also, this TTC can be estimated even when the lead vehicle's speed is higher than the following vehicle's speed. The PET is also observed for each time frame and a minimum time headway during the car-following condition is determined as the PET for each vehicle pair. The minimum values represent the most dangerous situation of each vehicle pair.

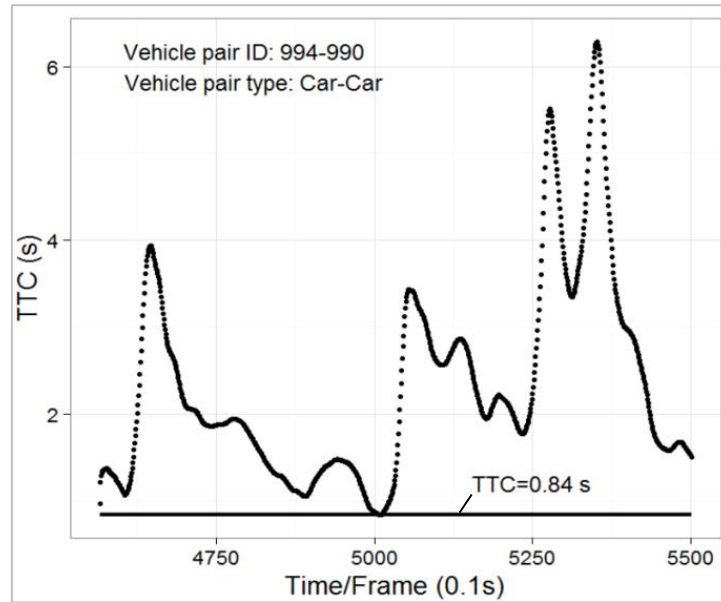


Figure 4-4. Estimation of TTC for one vehicle pair

4.1.2. Crash potential index (CPI)

Although TTC and PET have been widely used as surrogate safety measures, they do not take into account drivers' reaction time and vehicles' deceleration capability. In this regard, crash potential index (CPI) (Cunto & Saccomanno 2008) is more suitable for reflecting collision risk for different vehicle pair types since it considers vehicles' deceleration capability. The CPI represents the probability that a given vehicle's deceleration to avoid crashes (DRAC) exceeds its maximum available deceleration rate (MADR) as shown in [Eq. \(2-5\)](#). Cunto (2008) specified different MADRs for cars and trucks, and suggested that MADR follows a truncated normal distribution with average of 8.45 m/s^2 for cars and 5.01 m/s^2 for trucks with a standard deviation of 1.40 m/s^2 .

[Figure 4-5](#) illustrates the distributions of MADR for cars and trucks and how the CPIs are estimated for a given DRAC using the probability density function (PDF). The area

under the PDF for the range of MADR less than DRAC represents the probability that MADR is less than DRAC, i.e., CPI. The figure shows that even if a car and a heavy vehicle have the same DRAC at a given time instant, the heavy vehicle's CPI (indicated by red shaded area) is higher than the car's CPI (indicated by black shaded area). This is due to the heavy vehicle's lower deceleration capability.

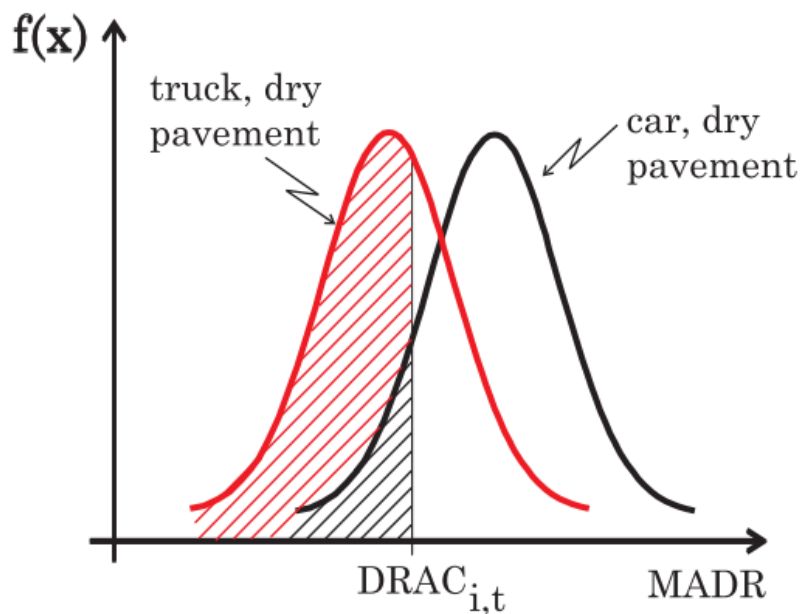


Figure 4-5. Comparison of CPI for a given DRAC between car and truck
(Source: Cunto 2008)

However, the current DRAC does not consider driver's reaction time although it takes some time for drivers to apply brakes to decelerate. Driver's reaction time is particularly a critical factor affecting the risk of collision in emergency situations when drivers do not anticipate immediate changes in traffic condition. Thus, the DRAC in [Eq. \(2-4\)](#) is modified to account for the effect of driver's reaction time on the CPI as follows.

Suppose the following vehicle initially travels at the speed V_F and the lead vehicle travels at the constant speed V_L . If the lead vehicle speed is lower than the following vehicle speed, the following vehicle is required to brake at a uniform deceleration to avoid rear-end crash. After the following vehicle driver's reaction time (t_r), the following vehicle starts braking. Then the following vehicle reduces speed from V_F to V_L and the spacing between the lead and following vehicles becomes zero. This car-following scenario is illustrated in [Figure 4-6](#).

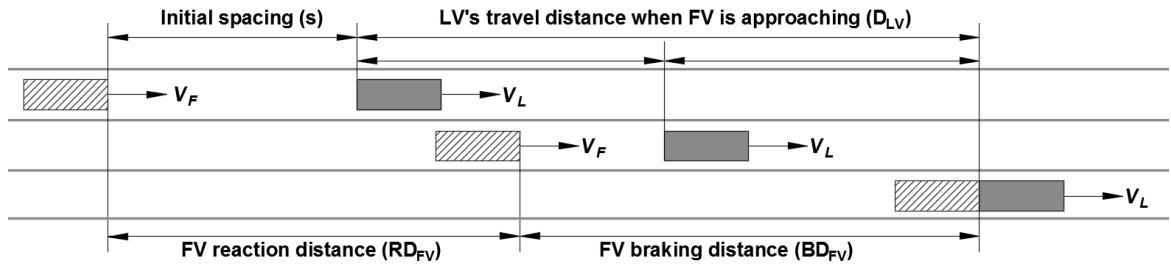


Figure 4-6. Positions of the lead and following vehicles during the following vehicle's braking maneuver to avoid rear-end crash

[Figure 4-6](#) shows that the distance travelled by the following vehicle is equal to the distance travelled by the lead vehicle plus the initial spacing ($s = X_L(t) - X_F(t) - L_L$) when the spacing between the two vehicles is zero. This is expressed in the following equation:

$$X_L(t) - X_F(t) - L_L + D_{LV} = RD_{FV} + BD_{FV} \quad (4-2)$$

where D_{LV} is the lead vehicle's travel distance when the following vehicle is approaching; RD_{FV} is the following vehicle's travel distance during reaction time; and BD_{FV} is the following vehicle's travel distance during the braking maneuver.

If the following vehicle's uniform deceleration rate is DRAC during the braking maneuver, [Eq. \(4-2\)](#) can be re-written as follows:

$$X_L(t) - X_F(t) - L_L + V_L(t)t_r + V_L \times \frac{V_F(t) - V_L(t)}{DRAC(t)} = V_F(t)t_r + \frac{V_F(t)^2 - V_L(t)^2}{2DRAC(t)} \quad (4-3)$$

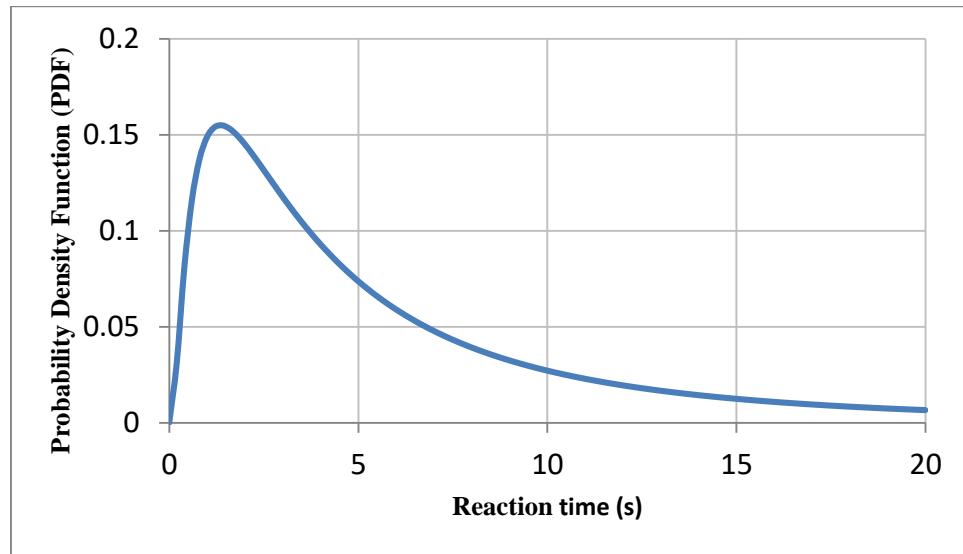
where t_r is the following vehicle driver's reaction time. Then, the modified DRAC is calculated as follows:

$$DRAC_i(t) = \frac{(V_F(t) - V_L(t))^2}{2((X_L(t) - X_F(t) - L_L) - (V_F(t) - V_L(t)) \times t_r)} \quad (4-4)$$

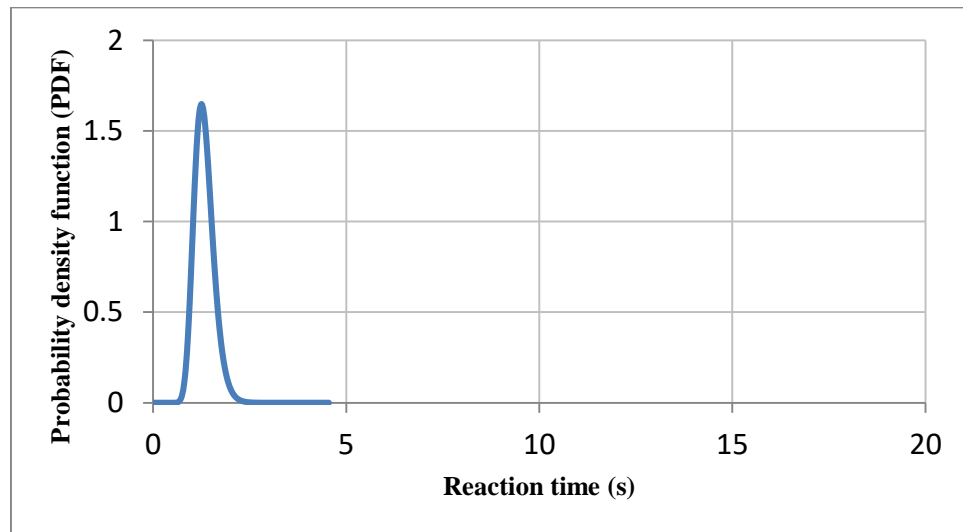
The CPI with the modified DRAC considers not only vehicles' braking capability, but also driver's reaction time, unlike the original CPI proposed by Cunto and Saccomanno (2008).

As shown in [Eq. \(4-4\)](#), driver's reaction time is one of the parameters affecting the DRAC. Driver's reaction time is impacted by multiple factors such as driver's age, gender, visibility, vehicle type, traffic conditions, etc. For example, older driver's reaction time is generally longer than younger driver's reaction time. Some studies assumed that driver's reaction time follows a lognormal distribution with a mean of 0.92 s and a standard deviation of 0.28 s (Wang and Stamatiadis 2013, Kuang et al. 2015). However, these studies did not consider the difference in reaction time between car and truck drivers although their sight distance and driving skill are potentially different. In this regard, Dozza (2013) found that reaction times were different between car and truck drivers - car drivers had longer reaction time with higher variation (mean: 1.45 s and standard deviation: 1.07 s, number of observation: 472) than truck drivers (mean: 0.26 s and standard deviation: 0.19 s, number of observation: 21). Thus, car driver's and truck driver's reaction times are

assumed to follow a lognormal distribution with pre-specified means and variances for car and truck drivers as observed in Dozza (2013). These distributions are shown in [Figure 4-7](#).



(a) Car drivers



(b) HV drivers

Figure 4-7. Distributions of driver reaction time

Since driver reaction time is not a fixed value, random samples are drawn from this population distribution of reaction time and the mean of these sample reaction times is used to calculate DRAC. In this study, log normal distributions for cars and trucks are generated using the mean, standard deviation and number of observations reported in Dozza (2013). Then a total of 30 and 20 samples of reaction times are drawn for cars and heavy vehicles, respectively, from these normal distributions using a Monte Carlo simulation. The same sample size (i.e., 30) for both cars and trucks could not be used since only 21 observations for heavy vehicles were used in Dozza (2013). The Monte Carlo simulation is run 10 times using SAS 9.3 (SAS Institute 2012) as shown in Appendix B. Then the CPI is calculated using [Eq. \(2-5\)](#) with the modified DRAC ([Eq. 4-4](#)). The sample calculation of the CPI for one vehicle at one time instant is shown in Appendix C. To facilitate the calculation for all vehicles with different reaction times, the CPIs are calculated using R as shown in Appendix C.

4.2. Surrogate Safety Measures for Lane-change Conflicts

According to Gettman and Head (2003), lane-change conflicts are defined as “rear-end events where the lead vehicle changes lanes abruptly in front of the following vehicle, requiring the vehicle in the adjacent lane to brake to avoid collision”. In the SSAM, lane-change conflicts occur when the conflict angle is greater than 30° and less than 85° (Gettman et al. 2008). This definition of lane-change conflicts only considers the risk of rear-end collision *after* lane changes.

However, during lane changes, sideswipe and angle collisions between the lane change vehicle (LCV) and the trailing vehicle (TV) or between the LCV and the lead vehicle (LV) can also occur in the target lane as shown in [Figure 4-8](#). Since the equation of DRAC for car-following conflicts ([Eq. 4-4](#)) does not explicitly account for the change in the LCV's lateral position, it cannot estimate the risk of sideswipe or angle collision during lane changes.

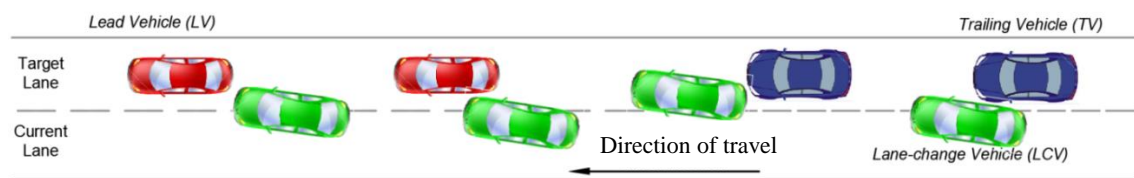


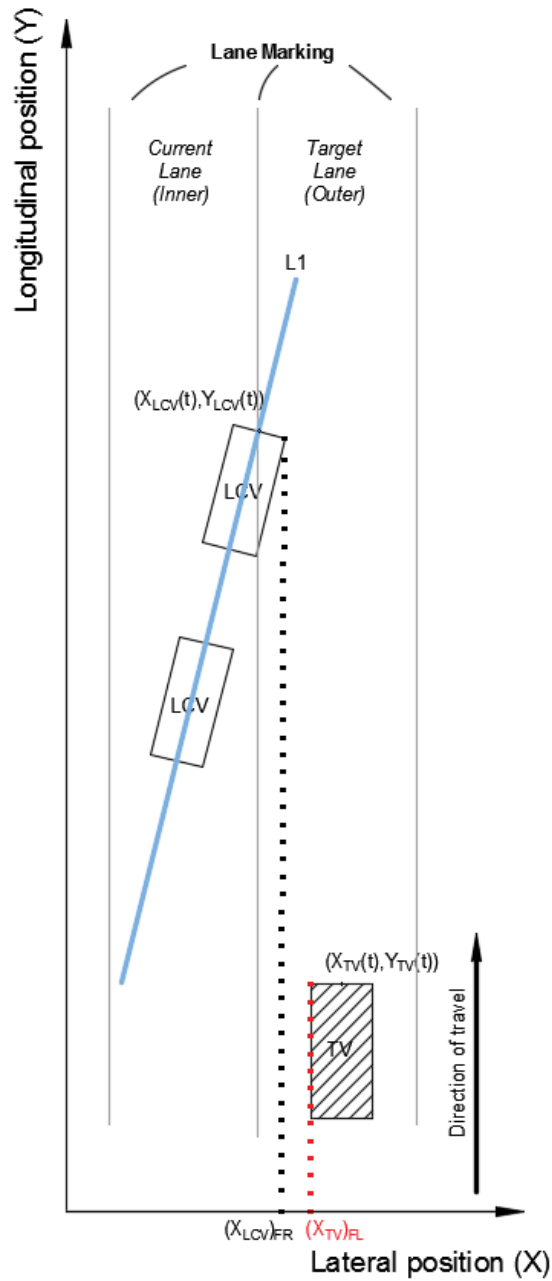
Figure 4-8. Types of lane-change conflicts

In this regard, Wang and Stamatiadis (2013) developed the surrogate safety measure of lane-change conflicts based on conflict angle, reaction time, and maximum braking rate. However, this measure has the following limitations: 1) the computation of the measure is complex as it requires many parameters; and 2) it does not clearly specify the beginning and end of the lane-change maneuver – i.e., it's unclear whether the conflict occurs during lane changes or not.

Due to these limitations, the CPI for lane-change conflicts is developed. Similar to the CPI for car-following conflicts, the CPI for lane-change conflicts is defined as the probability that DRAC is greater than MADR during lane changes. CPIs are separately computed for the following two types of lane-change conflicts – 1) conflicts between the LCV and the TV and 2) conflicts between the LCV and the LV. This is explained in the next subsections.

4.2.1. Conflicts between LCV and TV

Figure 4-9 shows the schematic diagram of lane-change conflicts between LCV and TV. The shape of vehicles was simplified as a rectangle. There are two types of lane-change conflict between LCV and TV: (a) the front-end of the TV hits the rear-end of the LCV ([Figure 4-9 \(c\)](#)); and (b) the front left corner of the TV (if the LCV changes from an inner lane to an outer lane) ([Figure 4-9 \(b\)](#)) or the front right corner of the TV (if a LCV changes from an outer lane to an inner lane) hits the side of the LCV.



(a) Case 1: No potential collision

Figure 4-9. Lane-change conflicts between LCV and TV (LCV from inner lane to outer lane)

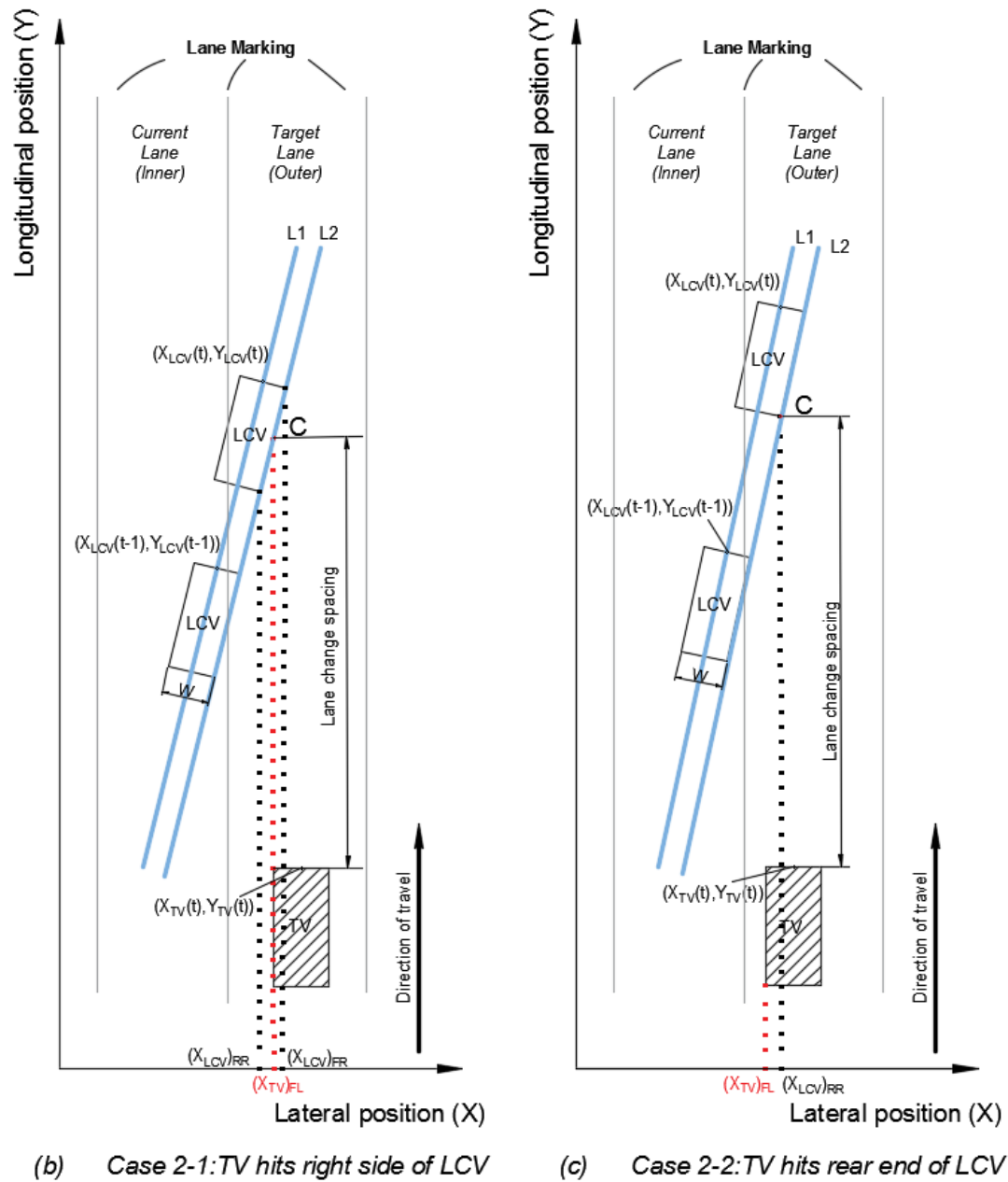


Figure 4-9. Lane-change conflicts between LCV and TV (LCV from inner lane to outer lane) (Continued)

The equation of DRAC(t) is derived as follows: First, the trajectory of the center line of the LCV (i.e., the line L1 in [Figure 4-9](#)) is described in the following linear function:

$$Y = kX + b \quad (4-5)$$

$$k = \frac{Y_{LCV}(t) - Y_{LCV}(t-1)}{X_{LCV}(t) - X_{LCV}(t-1)} \quad (4-6)$$

where $X_{LCV}(t)$ and $Y_{LCV}(t)$ are the lateral and longitudinal coordinates of the front center of the LCV at time t , respectively; and $X_{LCV}(t-1)$ and $Y_{LCV}(t-1)$ are the lateral and longitudinal coordinates of the front center of the LCV at the previous time interval $(t-1)$, respectively; and b is the longitudinal position of the LCV at the start of lane change.

The trajectory of right side of the LCV (i.e., the line L2 in [Figure 4-9](#)) is described in the following linear function:

$$Y = kX + b - k\left(\frac{W}{2}\right) \quad (4-7)$$

where W is the width of the LCV.

The potential point of collision between the LCV and the TV is “C” as shown in [Figure 4-9](#) (b) and (c). The longitudinal position of the point C (Y_C) is determined as follows:

Assume $(X_{LCV})_{FR}$, $(X_{LCV})_{RR}$, and $(X_{TV})_{FL}$ are lateral positions of the front right and rear right corners of the LCV and the front left corner of the TV, respectively. These lateral positions were determined by adding or subtracting $W/2$ from the lateral position of the front center of the LCV or the TV.

For the lane change from an inner lane to an outer lane, two types of events can occur as follows:

Case 1: If $(X_{LCV})_{FR} < (X_{TV})_{FL}$, Y_C cannot be determined (i.e., no potential collision) ([Figure 4-9\(a\)](#)).

Case 2: If $(X_{LCV})_{FR} \geq (X_{TV})_{FL}$,

Case 2-1: If $(X_{LCV})_{RR} \leq (X_{TV})_{FL} \leq (X_{LCV})_{FR}$, Y_C is determined using [Eq. 4-7](#) with $X = (X_{TV})_{FL}$ ([Figure 4-9\(b\)](#)).

Case 2-2: $(X_{TV})_{FL} < (X_{LCV})_{RR}$, Y_C is determined using [Eq. 4-7](#) with $X = (X_{LCV})_{RR}$. ([Figure 4-9\(c\)](#)).

The Y_C can also be determined for the lane change from an outer lane to an inner lane using a similar method. Lane-change spacing (Y_{LCS}) is the distance between the longitudinal position of front end of the TV (Y_{TV}) and the longitudinal position of C (Y_C) as follows:

$$Y_{LCS}(t) = Y_C(t) - Y_{TV}(t) \quad (4-8)$$

The DRAC for the conflicts between LCV and TV is defined as the deceleration rate of the TV to avoid the collision with the LCV as follows:

$$DRAC_{TV}(t) = \frac{(V_{TV}(t) - V_{LCV}(t))^2}{2(Y_{LCS}(t) - (V_{TV}(t) - V_{LCV}(t)) \times t_r)} \quad (4-9)$$

where $V_{TV}(t)$ and $V_{LCV}(t)$ are the speeds of TV and LCV, respectively, at time t , and $Y_{LCS}(t)$ is the lane-change spacing at time t . The CPI for the conflicts between LCV and TV can be calculated during lane changes using [Eq. \(2-5\)](#) with the DRAC in [Eq. \(4-9\)](#). The start and end of lane change maneuver are determined as illustrated in [Figure 3-2](#). Mean driver reaction times are calculated for DRAC using a Monte Carlo simulation.

4.2.2. Conflicts between LCV and LV

[Figure 4-9](#) shows the parameters and the schematic diagram of the lane-change conflicts between LCV and LV. There are two types of conflict between them: (a) the front-end of the LCV hits the side of the LV ([Figure 4-10\(a\)](#)); (b) the front right corner of the LCV (if a LCV changes from an inner lane to an outer lane) or the front left corner of the LCV (if a LCV changes from an outer lane to an inner lane) hits the rear end of the LV ([Figure 4-10\(b\)](#)).

The trajectories of the LCV (lines L1 and L2) and the potential point of collision between the LCV and the LV (point C) can be determined using the method used in Section 4.2.1 as shown in [Figure 4-10](#). The longitudinal position of the point C (Y_C) is determined as follows:

Assume $(X_{LCV})_{FR}$ and $(X_{LV})_{FL}$ are lateral positions of front right and rear right corner of the LCV and front left corner of the LV, respectively. These lateral positions were determined by adding or subtracting $W/2$ from the lateral position of the front center of the LCV or the LV.

For the lane change from an inner lane to an outer lane, two types of events can occur as follows:

Case 1: If $(X_{LCV})_{FR} < (X_{LV})_{FL}$, Y_C is determined using Eq. 4-7 with $X = (X_{LCV})_{FR}$ ([Figure 4-10\(a\)](#))

Case 2: If $(X_{LCV})_{FR} \geq (X_{LV})_{FL}$, Y_C is $(Y_{LV})_{RL}$ ([Figure 4-10\(b\)](#))

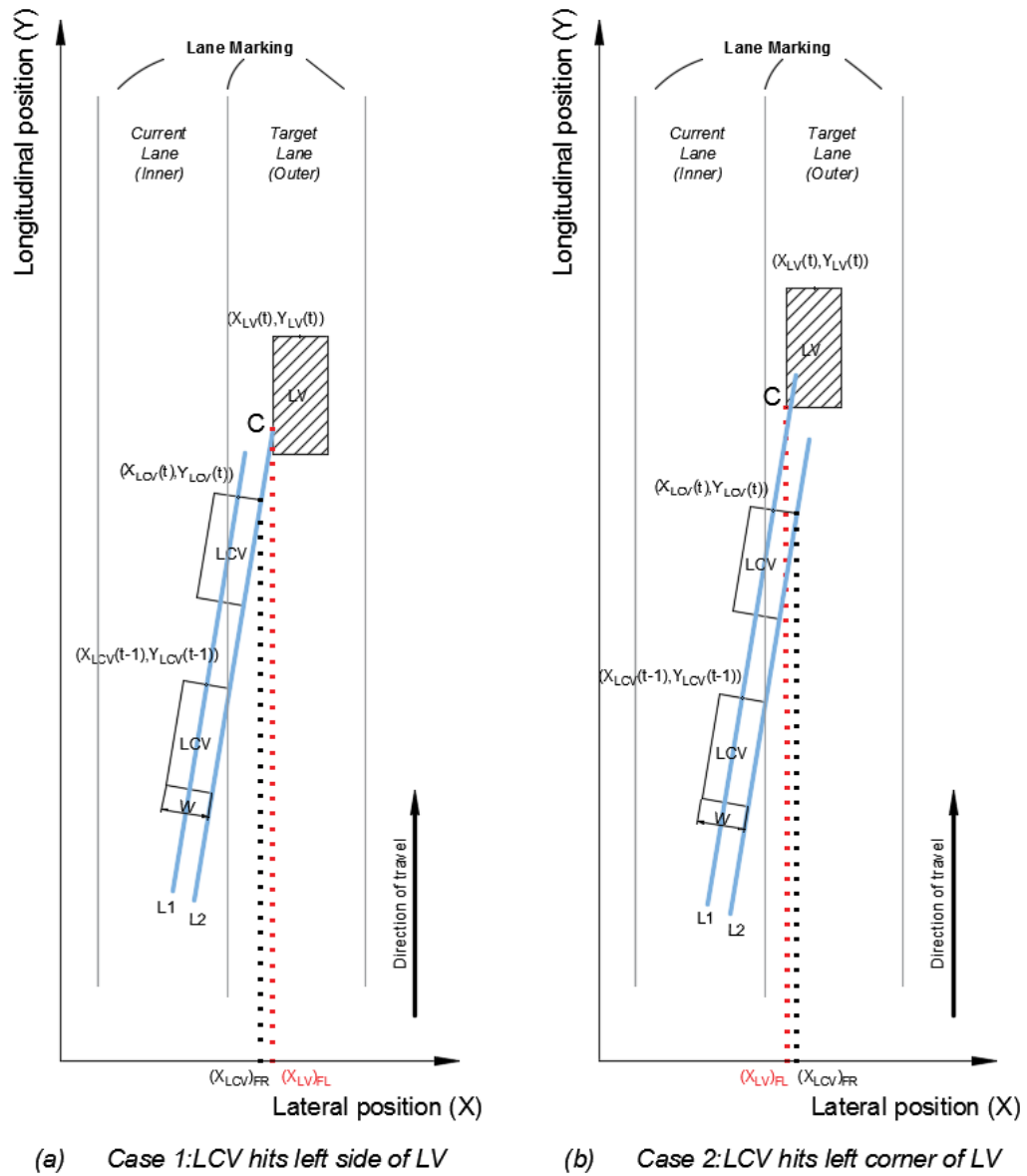


Figure 4-10. Lane-change conflicts between LCV and LV (LCV from inner lane to outer lane)

The Y_C can also be determined for the lane change from an outer lane to an inner lane using a similar method. Lane-change spacing (Y_{LCS}) is the distance between the longitudinal position of front end of the LCV (Y_{LCV}) and the longitudinal position of C (Y_C) as follows:

$$Y_{LCS}(t) = Y_c(t) - Y_{LCV}(t) \quad (4-10)$$

The DRAC for the conflicts between LCV and TV is defined as the deceleration rate of the LCV to avoid the collision with the LV as follows:

$$DRAC_{LCV}(t) = \frac{(V_{LCV}(t) - V_{LV}(t))^2}{2(Y_{LCS}(t) - (V_{LCV}(t) - V_{LV}(t)) \times t_r)} \quad (4-11)$$

where $V_{LV}(t)$ is the speed of the LV at time t . The CPI for the conflicts between LCV and LV is calculated during lane changes using [Eq. \(2-4\)](#) and the DRAC in [Eq. \(4-11\)](#).

4.3. Validation of Surrogate Safety Measures

Surrogate safety measures have been validated using one of the following two approaches. First approach is to compare surrogate safety measures with the observed crash frequencies. However, since not all the events with high risk of crash lead to a collision, this approach has a limitation in validating surrogate safety measures (Cunto et al. 2009). Second approach is to compare surrogate safety measures between crash conditions and non-crash conditions. "Crash conditions" imply the conditions immediately before a crash occurs. If values of surrogate safety measures are significantly different (e.g., higher CPI) between crash and non-crash conditions, surrogate safety measures reflect risk of crashes (Cunto and Saccomanno 2008). In this study, the CPIs for car-following and lane-change conflicts are validated using the second approach because it better reflects actual risk of crashes than the first approach.

4.3.1. Calibration and validation of VISSIM simulation

In the observed vehicle trajectory data for the US-101 freeway, a crash did not occur during the data collection periods. Thus, the proposed surrogate safety measures for car-following and lane-change conflicts could not be validated using the US-101 data. Instead, the surrogate safety measures are validated using the simulated traffic data for the Gardiner Expressway where crashes occurred during the period of collecting loop detector data. The simulation is performed using the VISSIM 7.00 microscopic traffic simulation software (PTV AG 2014). VISSIM simulation can mimic actual traffic conditions before a crash occurs and also generate individual vehicle trajectory which can be used to compute surrogate safety measures. The road network and the detector stations are created in VISSIM as shown in [Figure 3-4](#).

In the VISSIM simulation model, driver behaviors are controlled by the car-following and lane-change models. The input parameters in each model are shown in [Table 4-1](#).

Table 4-1. VISSIM input parameters (Source: PTV AG 2014)

Model	Parameters	Description
Car following	CC0	Standstill Distance The average desired distance between two stopped vehicles.
	CC1	Headway Time The time that the driver wants to keep to the lead vehicles. It has the greatest influence on the capacity. Safety distance, $\Delta X = CC0 + CC1 \times v$.
	CC2	'Following' Variation Restricts the longitudinal oscillation or how much more than the safety distance a driver allows before moving closer to the lead vehicle.
	CC3	Threshold for Entering 'Following' Defines how far before reaching the safety distance the driver starts to decelerate.
	CC4	Negative 'Following' Threshold Controls the negative relative speed (i.e., the lead vehicle's speed is higher than the following vehicle's speed) during the 'Following' state. Smaller values results in more sensitive reactions of drivers, resulting in more tightly coupled vehicles.
	CC5	Positive 'Following' Threshold Controls the positive relative speed (i.e., the following vehicle's speed is higher than the lead vehicle's speed) during the 'Following' state.
	CC6	Speed Dependency of Oscillation Influences distance on speed oscillation while in following process.
	CC7	Oscillation Acceleration Actual acceleration during the oscillation process
	CC8	Standstill Acceleration Desired acceleration when starting from standstill
Lane change	CC9	Acceleration with 80km/h Desired acceleration at 80km/h
	Safety distance reduction factor	Factor applied to the original safety distance during the lane change maneuver. Lane changing driver will reduce its original safety distance during the maneuver.

In order to replicate the observed traffic in the simulation model, the above parameters must be calibrated. In previous studies, traffic simulation models have been calibrated at macroscopic level. For example, Astarita et al. (2012) calibrated the 5 General Motors car-

following model parameters such that the difference between the observed and simulated travel times is minimized. Additionally, average delay times, average number of conflicts, the total length of queues, and the number of completed trips per time interval were main criteria of calibrating the car-following model parameters (CC0, CC1, CC4& CC5) and lane change model parameters (safety distance reduction factor) in VISSIM in the past studies (Essa and Sayed 2015, Park and Qi 2005). Dowling et al. (2004) and Ma and Abdulhai (2002) calibrated mean queue discharge headway at traffic signals and mean headway on the freeway links in PARAMICS simulation model. Recently, Durrani et al. (2016) calibrated the driving behaviour parameter for the car-following (or vehicle-following) model in VISSIM for cars and heavy vehicles separately using the NGSIM vehicle trajectory data from the US-101 freeway during Period 1 (7:50 am – 8:05 am). [Table 4-2](#) shows the calibrated driving behaviour parameters for the vehicle-following model in VISSIM.

Table 4-2. Calibrated driving behaviour parameters for vehicle-following model in VISSIM (Source: Durrani et al. 2016)

Model parameters	Unit	Default	Calibrated	
			Car	Heavy Vehicle
CC0	m	1.5	4.15	4.69
CC1	s	0.9	1.5	2.7
CC2	m	4	11.58	14.02
CC3	s	-8	-4	-4.55
CC4	m/s	-0.35	-1.65	-2.07
CC5	m/s	0.35	1.65	2.07
CC6	m/s	11.44	11.44	11.44
CC7	m/s ²	0.25	0.09	0.1
CC8	m/s ²	3.5	0.49	0.27
CC9	m/s ²	1.5	0.45	0.25

To validate the VISSIM simulation with the calibrated parameters shown in [Table 4-2](#), the distributions of speed and surrogate safety measures are compared between the observed and simulation data for the US-101 freeway during Period 2 (8:05 am – 8:20 am).

After the simulation with the calibrated parameters is validated for the US-101 freeway, the same parameters are applied to the simulation of traffic for the Gardiner Expressway. This is based on the assumption that driver behavior is similar between the US-101 freeway and the Gardiner Expressway. To verify this assumption, the speeds at the detector stations 80 and 90 on the Gardiner Expressway are compared between the observed data and the data from simulation with the aforementioned calibrated parameters. The errors are estimated using the Root-mean-square Percentage Error (RMSPE) test and Mean Percentage Error (MPE) test as suggested by Bham and Benekohal (2004). The RMSPE and MPE are described as follows:

$$\text{RMSPE} = \sqrt{\frac{1}{N} \sum_{n=1}^N \left(\frac{y_s(t) - y_o(t)}{y_o(t)} \right)^2} \quad (4-12)$$

$$\text{MPE} = \frac{1}{N} \sum_{n=1}^N \left(\frac{y_s(t) - y_o(t)}{y_o(t)} \right) \quad (4-13)$$

where N = the number of observations or time periods; $y_s(t)$ = the speed from the simulation with the calibrated parameters at time t; and $y_o(t)$ = the observed speed at time t. If these errors are sufficiently low, the parameters calibrated using the US-101 data are transferrable to the Gardiner Expressway. The procedure of calibration and validation of the VISSIM simulation is summarized as shown in [Figure 4-11](#).

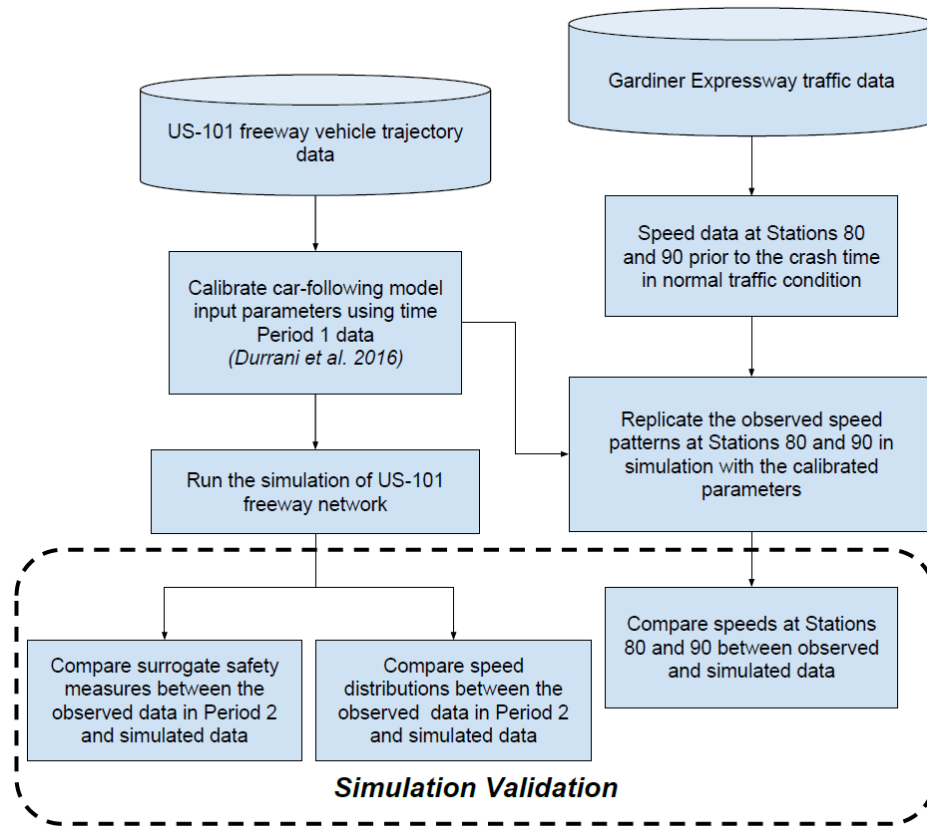


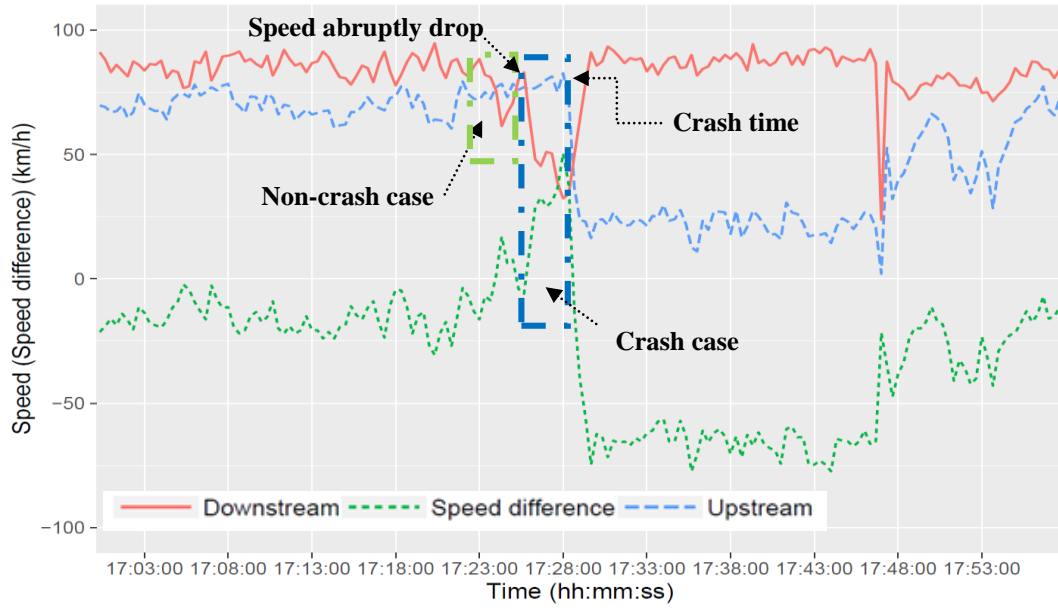
Figure 4-11. Calibration and validation of VISSIM simulation

4.3.2. Comparison of crash and non-crash conditions

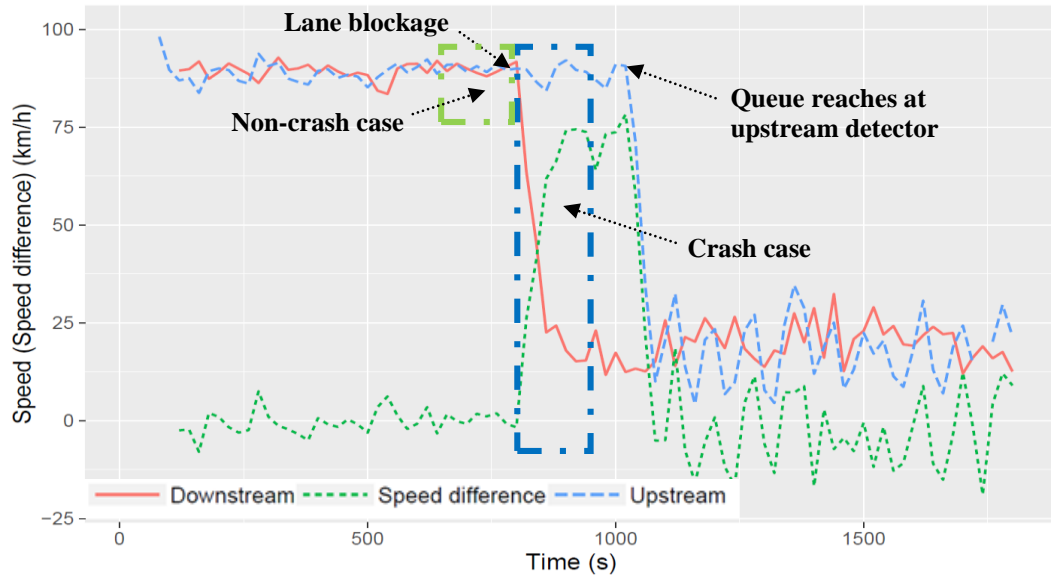
Based on the observed speed patterns upstream and downstream of crash location before crash occurrence on the Gardiner Expressway (refer to [Figure 3-6](#) and Appendix A), the traffic conditions are classified into the “crash case” and the “non-crash case” as follows. The crash case denotes the traffic conditions from the time when speed abruptly dropped at the downstream detector to the estimated crash time. The non-crash case denotes normal traffic condition before speed abruptly dropped at the downstream detector.

An example of determining these two cases in the observed detector data is shown in

[Figure 4-12\(a\).](#)



(a) Observed data



(b) Simulation data

$$*\text{Speed difference} = \text{Speed}_{\text{Upstream}} - \text{Speed}_{\text{Downstream}}$$

Figure 4-12. Temporal variations in speed for crash and non-crash cases

It is hypothesized that the risk of collision is higher for the crash case than non-crash case. In the crash case, temporal variations in speed and the speed difference between upstream and downstream detectors are higher. Thus, the following vehicles are more likely to collide with the lead vehicle in the same lane. In these conditions, the vehicles are also more likely to change lanes to avoid conflicts with the lead vehicle in the same lane. Thus, the lane-change vehicles are more likely to collide with the vehicles in the target lane.

The aforementioned speed patterns for the crash and non-crash cases are replicated in VISSIM simulation as follows. The outermost lane downstream of the station 90 (downstream detector) is blocked to mimic an abrupt drop in downstream speed 800s after the start of the simulation. This lane blockage reduces capacity and a queue grows towards upstream of the traffic flow. Then, the crash time is determined as the time when the end of queue reaches at the station 80 (upstream detector).

It was observed that it took 3-4 minutes for the queue to reach the station 80 after the lane blockage in the simulation. To ensure that only traffic condition before the crash time is selected, the crash case is defined as the traffic condition 2-min. interval after the lane blockage. Similarly, the non-crash case is defined as the traffic condition 2-min. interval before the lane blockage. The same observation period must be used for both crash and non-crash cases because the value of CPI is generally higher for longer observation time period (due to more frequent conflicts). Otherwise, CPIs for the two cases are not comparable. An example of determining these two cases in the simulation data is shown in [Figure 4-12\(b\)](#). The individual vehicle trajectory data extracted from the simulation show that the proportion of lane-change vehicle is generally higher for the crash case than the non-crash case (on average, 23.9% and 14.3% for crash and non-crash cases, respectively).

From the comparison between [Figures 4-12 \(a\) and \(b\)](#), speed patterns before the crash occurrence are similar between the observed and simulation data.

To validate surrogate safety measures, they are estimated for the crash and non-crash cases separately. If the values of surrogate safety measures are higher for the crash case than the non-crash case, it can be concluded that the measures realistically reflect actual risk of collision.

CHAPTER 5 RESULTS AND DISCUSSION

In this section, surrogate safety measures for car-following conflicts (TTC, PET and CPI) and lane-change conflicts (CPI) were estimated and compared between different vehicle pair types using the observed vehicle trajectory data for the US-101 freeway. The CPI for car-following and lane-change conflicts were also validated using the simulated vehicle trajectory data for the Gardiner Expressway.

5.1. Car-following conflicts

5.1.1. Distribution of TTC by vehicle pair type

TTC for car-following conflicts was calculated using the US-101 data. [Figure 5-1](#) shows the distributions of TTC for different vehicle pair types.

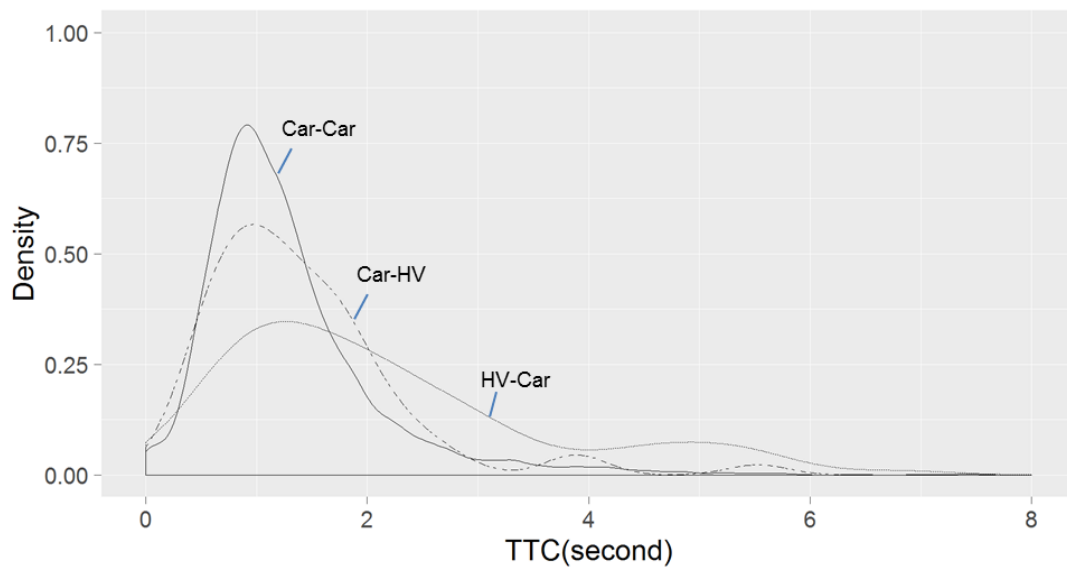


Figure 5-1. Distribution of TTC by vehicle pair type

Non-parametric statistical tests were performed to check if these TTC values are statistically different between two different vehicle pair types. Mann-Whitney U-test

(Zheng et al. 2015) was adapted with the assumption that the distribution of the samples is unknown.

It was found that TTCs are not statistically different between Car-Car and Car-HV (p-value = 0.234) whereas TTCs are statistically different between Car-Car and HV-Car (p-value < 0.001). Thus, although TTC is slightly higher for Car-Car than Car-HV, the difference is not statistically significant. This result also indicates that rear-end collision risk is significantly different between the following car and HV drivers.

5.1.2. Distribution of PET by vehicle pair type

[Figure 5-2](#) shows the distributions of PET for different vehicle pair types.

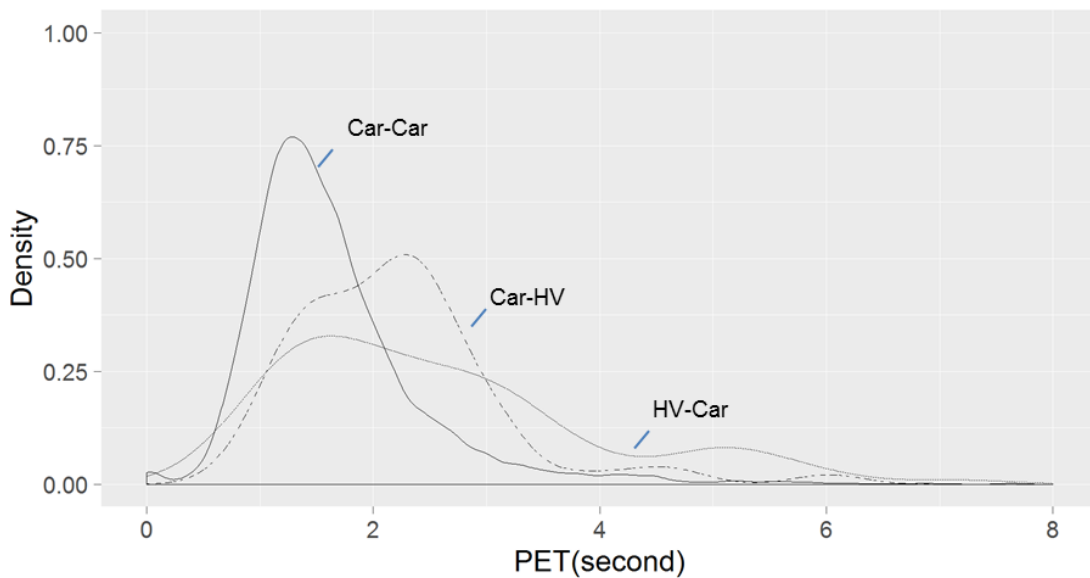


Figure 5-2. Distribution of PET by vehicle pair type

The PETs were also compared among the three different vehicle pair types. The Mann-Whitney U-test result shows that the PET for Car-Car is statistically different from the PETs for Car-HV and HV-Car (p-value < 0.001). This result indicates that the difference

between Car-Car and Car-HV is significant for PET, but not TTC. This indicates that car drivers are more likely to adjust their speeds to avoid collisions when they follow HVs compared to following cars.

5.1.3. Comparison between TTC and PET

PET considers the speed variance of the lead and following vehicles, and the difference in acceleration between the two vehicles during the car-following condition. In general, when the spacing with the lead vehicle is shorter, the following vehicle’s driver is more likely to decelerate to maintain enough safety distance. However, in the definition of TTC, the following vehicle’s driver is assumed to continue traveling at the same speed regardless of the spacing. Therefore, for a given vehicle pair, the value of PET is greater than the value of TTC as shown in [Table 5-1](#).

Table 5-1. Descriptive Statistics of TTC and PET

Vehicle pair type	TTC(s)		PET (s)	
	Mean	SD	Mean	SD
Car-Car	1.2952	0.9031	1.6743	1.1400
Car-HV	1.4123	0.9110	2.2076	0.9116
HV-Car	2.2797	1.6735	2.6989	1.6419

Higher rear-end collision risk for Car-Car than HV-Car may be counter-intuitive since it is more difficult for the following heavy vehicle to avoid collision with the stopped lead car compared to the following car. TTC is longer for HV-Car than Car-Car because a heavy vehicle generally follows a car at lower speed than a car following a car for a given spacing as shown in [Figure 5-3](#). Consequently, it takes longer time for the following heavy vehicle to reach the position of the lead car than the following car. However, TTC does not reflect

difference in braking capability between car and HV. Thus, CPIs were compared between HV-Car than Car-Car in the next section.

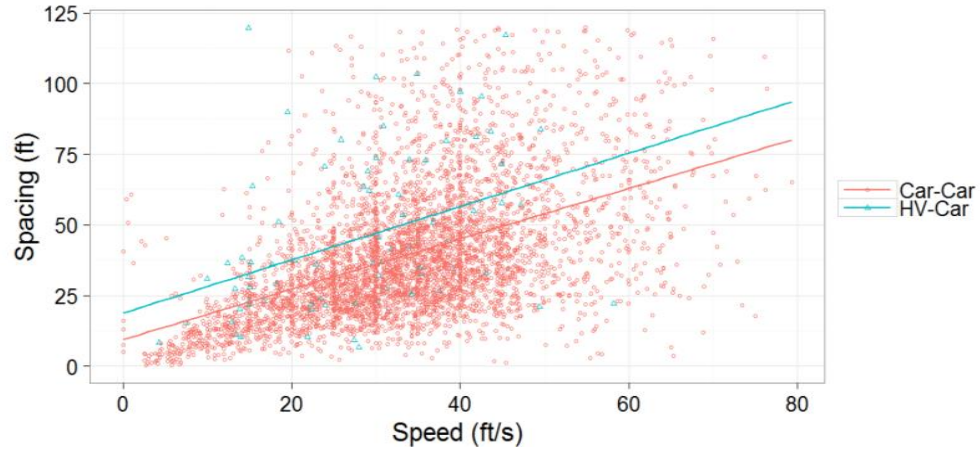


Figure 5-3. Relationships between spacing and the following vehicle speed

5.1.4. Comparison of CPI for car-following conflicts

For the calculation of the CPI with the modified DRAC ([Eq. 4-4](#)), a total of 30 and 20 samples of reaction times were drawn for car and HV, respectively using a Monte Carlo simulation and the simulation was run 10 times. [Table 5-2](#) shows car and HV drivers' reaction times in each simulation run. Since the Monte Carlo simulation is a stochastic process, mean values from the simulation were slightly different from the observed mean reaction times for car and HV drivers.

Table 5-2. Mean reaction times from Monte Carlo Simulation

Run	Reaction time (s)	
	Car	HV
1	1.22	0.24
2	1.96	0.20
3	2.07	0.23
4	1.20	0.24
5	1.70	0.24
6	1.33	0.24
7	1.50	0.23
8	1.43	0.24
9	1.57	0.23
10	1.22	0.24
<i>Ave</i>	<i>1.52</i>	<i>0.23</i>

[Table 5-3](#) and [Figure 5-4](#) compare the mean values and variances of CPI for car-following conflicts among different vehicle pair types using the NGSIM vehicle trajectory data. To eliminate the effect of spacing between the lead and the following vehicles on CPI, CPIs were compared among different vehicle pair types for each of the following five intervals of spacing – 1) 0-20 m, 2) 20-40 m, 3) 40-60 m, 4) 60-80 m, and 5) 80-100 m. It was found that mean CPI for HV-Car was highest, followed by Car-Car and Car-HV for all the spacing intervals except for the spacing interval of 0-20 m. This result indicates that HV has high rear-end collision risk with the lead car for a given spacing. The variances for Car-Car and Car-HV were significantly higher for the spacing interval of 0-20 m than the spacing greater than 20 m. However, the variances for HV-Car were relatively similar for all spacing intervals.

Table 5-3. Comparison of CPI for car-following conflicts among different vehicle pair types

Vehicle Pair Type	Spacing Interval (m)									
	0-20		20-40		40-60		60-80		80-100	
	Mean	SD	Mean	SD	Mean	SD	Mean	SD	Mean	SD
Car-Car ($\times 10^{-9}$)										
1*	348000	5920000	4.11	124	1.23	2.8	1.11	1.93	1.52	2.28
2	706000	6030000	96.3	3310	1.58	6.51	1.22	3.02	1.72	2.95
3	748000	5950000	333	11700	1.69	7.65	1.25	3.26	1.76	3.08
4	364000	6250000	4.05	124	1.22	2.75	1.1	1.91	1.51	2.27
5	588000	6610000	13.3	379	1.41	4.63	1.17	2.54	1.64	2.68
6	430000	6540000	4.63	130	1.26	3.11	1.12	2.04	1.54	2.36
7	522000	7370000	6.32	162	1.32	3.69	1.14	2.25	1.59	2.5
8	478000	6860000	5.42	143	1.29	3.43	1.13	2.16	1.57	2.44
9	559000	7720000	7.73	199	1.35	3.99	1.15	2.35	1.6	2.56
10	348000	5920000	4.11	124	1.23	2.8	1.11	1.93	1.52	2.28
Ave	480000	6520000	47.9	1640	1.36	4.14	1.15	2.34	1.6	2.54
Std. dev.	136000		98.9		0.151		0.0481		0.0817	
No. of obs.	3656		2652		491		107		11	
Car-HV ($\times 10^{-9}$)										
1	61100	437000	0.57	0.305	0.854	0.139	0.851	0.0166	NA	NA
2	218000	913000	0.577	0.308	0.858	0.143	0.852	0.0171	NA	NA
3	127000	501000	0.579	0.309	0.859	0.144	0.852	0.0172	NA	NA
4	112000	799000	0.569	0.304	0.854	0.139	0.851	0.0166	NA	NA
5	158000	831000	0.574	0.307	0.856	0.142	0.851	0.017	NA	NA
6	106000	756000	0.571	0.305	0.854	0.14	0.851	0.0167	NA	NA
7	103000	738000	0.572	0.306	0.855	0.141	0.851	0.0168	NA	NA
8	69100	493000	0.572	0.305	0.855	0.14	0.851	0.0168	NA	NA
9	59700	411000	0.573	0.306	0.856	0.141	0.851	0.0169	NA	NA
10	61100	437000	0.57	0.305	0.854	0.139	0.851	0.0166	NA	NA
Ave	108000	632000	0.573	0.306	0.856	0.141	0.851	0.0168	NA	NA
Std. dev.	48400		0.00318		0.0016		0.000557		NA	
No. of obs.	51		35		11		2		NA	

*The number denotes different sets of reaction time.

Table 5-3. Comparison of CPI for car-following conflicts among different vehicle pair types (Continued)

Vehicle Pair Type	Spacing Interval (m)									
	0-20		20-40		40-60		60-80		80-100	
	Mean	SD	Mean	SD	Mean	SD	Mean	SD	Mean	SD
HV-Car ($\times 10^{-9}$)										
1	170000	126000	138000	80400	163000	62900	190000	36000	176000	3130
2	169000	124000	137000	80100	162000	62800	190000	35900	176000	3130
3	170000	125000	137000	80300	163000	62900	190000	36000	176000	3130
4	170000	126000	138000	80400	163000	62900	190000	36000	176000	3130
5	170000	126000	138000	80400	163000	62900	190000	36000	176000	3130
6	170000	126000	138000	80400	163000	62900	190000	36000	176000	3130
7	170000	125000	137000	80300	163000	62900	190000	36000	176000	3130
8	170000	126000	138000	80400	163000	62900	190000	36000	176000	3130
9	170000	125000	137000	80300	163000	62900	190000	36000	176000	3130
10	170000	126000	138000	80400	163000	62900	190000	36000	176000	3130
Ave	170000	125000	137000	80300	163000	62900	190000	36000	176000	3130
Std. dev.	278		41.9		16.3		16		0.859	
No. of obs.	50		51		17		5		3	

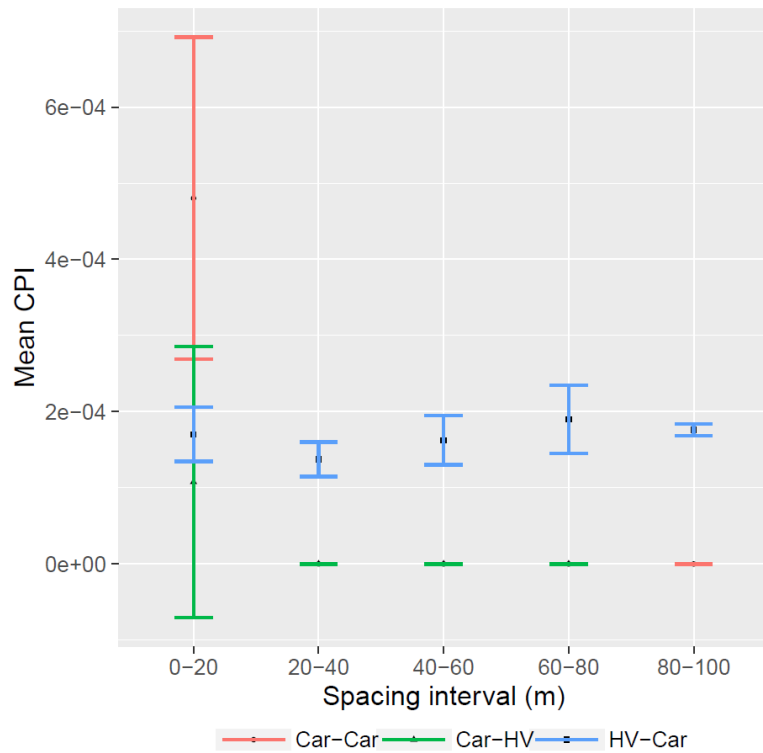


Figure 5-4. Comparison of CPI for car-following conflicts among vehicle pair types for different spacing intervals

In Table 5-3, the values of CPI for Car-Car were significantly higher in Runs 2 and 3 than those in the other runs for the spacing interval of 0-40 m. This is because car drivers' reaction times were longer in these two runs (1.96 s and 2.07 s) as shown in Table 5-2. Since the values of DRAC and CPI are more sensitive to reaction time for a very short spacing interval, these long reaction times drastically increased the values of CPI.

Average speed and spacing for the following vehicle were also compared among different spacing intervals as shown in [Table 5-4](#). It was found that average speeds for different vehicle pair types were similar in spacing interval of 0-20 m. However, as the spacing increased, average speeds were much higher for cars than HVs.

On the other hand, DRAC was significantly higher for Car-Car than HV-Car for the spacing interval of 0-20 m. It should be noted that DRAC is calculated based on the braking distance and driver's reaction time. The braking distance is generally shorter for cars than HVs whereas driver's reaction time is longer for car drivers than HV drivers. It was found that the frequency of shorter spacing was relatively higher for Car-Car than Car-HV and HV-Car for the spacing interval of 0-20 m. Very short spacing with the following car driver's longer reaction time (1.20 s to 2.07 s) resulted in a significantly large average value of DRAC for Car-Car as shown in [Table 5-4](#). Overall, HV-Car has the highest rear-end collision risk among the three vehicle pair types mainly due to HV's low braking capability for the spacing greater than 20 m.

Table 5-4. Average speed, spacing and DRAC for following vehicle in car-following conflicts

Vehicle Pair Type	Spacing Interval (m)				
	0-20	20-40	40-60	60-80	80-100
Average Speed (km/h)					
Car-Car	25.43	39.91	44.56	47.99	53.47
Car-HV	26.58	38.82	44.34	50.90	NA
HV-Car	23.10	30.98	34.88	35.43	37.75
Average Spacing (m)					
Car-Car	11.17	26.37	46.45	66.70	88.64
Car-HV	11.19	27.19	46.66	62.38	NA
HV-Car	12.36	27.54	45.35	67.90	85.19
Average DRAC (m/s ²)					
Car-Car	0.23	0.05	0.05	0.03	0.05
Car-HV	0.05	0.03	0.02	0.02	NA
HV-Car	0.06	0.05	0.02	0.05	0.01

5.2. Lane-change conflicts

5.2.1. CPI for lane-change conflicts between LCV and TV

According to Section 4.2.1, there are two types of lane-change conflict between LCV and TV: (a) case 2-1: front corner of the TV hits the side of the LCV during the lane change, which is termed as “Angle” conflict, and (b) case 2-2: the front-end of the TV hits the rear-end of the LCV during the lane change, which is termed as “Rear-end” conflicts. CPI for the two types of conflicts between LCV and TV was estimated using the method proposed in Section 4.2.1. [Table 5-5](#) summarizes CPIs for different lane change spacing intervals among different vehicle pair types of LCV and TV. The lane-change spacing is defined as the longitudinal distance between the front end of the TV and the potential point of collision between the LCV and the TV.

Table 5-5. Comparison of CPI for lane-change conflicts among different vehicle pair types of LCV and TV

Lane change spacing interval (m)	CPI ($\times 10^{-10}$) -Angle*			CPI ($\times 10^{-10}$) - Rear-end**		
	Mean	SD	No. of ob.	Mean	SD	No. of ob.
Car-Car (LCV-TV)						
0-20	5603.28	192.07	87	121.97	14541.26	100
20-40	29.15	11.55	66	12.92	0.56	40
40-60	11.79	0.22	12	10.08	0.08	7
60-80	13.00	0.21	4	9.19	0.02	3
80-100	8.99	0.02	3	NA	NA	NA
Car-HV (LCV-TV)						
0-20	2209000	3162.28	3	1910000	0.001	3
20-40	2420000	0	1	1770000	0.001	3
HV-Car(LCV-TV)						
20-40	8.222	0.004	1	7.96	0	1

*Angle conflicts occur where the TV is likely to hit the side of the LCV (Case 2-1).

**Rear-end conflicts occur when the TV is likely to hit the rear-end of the LCV (Case 2-2).

It was found that CPIs were consistently higher for angle conflicts than rear-end conflicts. This is potentially because speed difference between the TV and the LCV is higher for angle conflicts. In general, angle conflicts occur at the beginning of lane-change maneuver when the LCV accelerates. On the other hand, rear-end conflicts occur at end of lane-change maneuver when the LCV reaches similar speed as the TV in the target lane. Thus, this results in higher speed difference between the LCV and the TV for angle conflicts than rear-end conflicts as shown in [Table 5-6](#).

Table 5-6. Comparison of average speed, average speed difference, spacing and DRAC for TV in lane-change conflicts between LCV and TV

Vehicle Pair Type (LCV-TV)		Spacing Interval (m)				
		0-20	20-40	40-60	60-80	80-100
Average Speed of TV (km/h)						
Car-Car	Angle	10.32	11.82	13.21	13.85	14.35
	Rear-end	11.35	12.23	13.11	13.00	NA
Car-HV	Angle	9.93	12.17	NA	NA	NA
	Rear-end	8.79	12.87	NA	NA	NA
HV-Car	Angle	NA	9.13	NA	NA	NA
	Rear-end	NA	10.20	NA	NA	NA
Average Speed difference (km/h) (= TV speed minus LCV speed)						
Car-Car	Angle	1.20	1.87	1.81	2.25	2.10
	Rear-end	1.08	1.52	1.10	1.91	NA
Car-HV	Angle	1.39	2.25	NA	NA	NA
	Rear-end	0.78	0.77	NA	NA	NA
HV-Car	Angle	NA	0.59	NA	NA	NA
	Rear-end	NA	0.23	NA	NA	NA
Average Spacing (m)						
Car-Car	Angle	14.39	27.30	46.50	66.60	82.30
	Rear-end	14.01	28.61	48.29	69.60	NA
Car-HV	Angle	15.49	20.39	NA	NA	NA
	Rear-end	12.20	25.52	NA	NA	NA
HV-Car	Angle	NA	28.10	NA	NA	NA
	Rear-end	NA	24.01	NA	NA	NA
Average DRAC (m/s ²)						
Car-Car	Angle	0.11	0.12	0.06	0.06	0.04
	Rear-end	0.10	0.08	0.02	0.03	NA
Car-HV	Angle	0.09	0.12	NA	NA	NA
	Rear-end	0.03	0.01	NA	NA	NA
HV-Car	Angle	NA	0.01	NA	NA	NA
	Rear-end	NA	0.001	NA	NA	NA

It is worth noting that only one HV changed the lane in front of a car in the target lane (HV-Car) in the dataset. Due to the limited sample size of the data, CPIs were compared between Car-Car and Car-HV for the spacing intervals of 0-20 m and 20-40 m only. It was found that the CPI was significantly higher for Car-HV than Car-Car. This is mainly because HVs, as a trailing vehicle in the target lane, have lower deceleration capability than cars.

[Table 5-6](#) also shows that the following vehicle's speed increased and DRAC decreased as the spacing interval increased. Due to a decrease in DRAC with the spacing between the LCV and the TV, mean and variance of CPI also generally decreased as the spacing interval increased as shown in [Table 5-5](#).

5.2.2. CPI for lane-change conflicts between LCV and LV

According to Section 4.2.2, there are two types of lane-change conflict between LCV and LV: (a) case 1: front corner of the LCV hits the side of the LV during the lane change, which is termed as "Angle" conflict, and (b) case 2: the front-end of the LCV hits the rear-end of the LV during the lane change, which is termed as "Rear-end" conflicts. CPI for the two types of conflicts between LCV and LV was estimated using the method proposed in Section 4.2.2. [Table 5-7](#) compares CPIs for lane-change conflicts between the LCV and the LV for different lane change spacing intervals among different vehicle pair types. The lane-change spacing is defined as the longitudinal distance between the front end of the LCV and the potential point of collision between the LCV and the LV.

Table 5-7. Comparison of CPI for lane-change conflicts among different vehicle pair types of LCV and LV

Lane change spacing interval (m)	CPI ($\times 10^{-10}$) - Angle*			CPI ($\times 10^{-10}$) - Rear-end*		
	Mean	SD	No. of	Mean	SD	No. of
Car-Car (LCV-LV)						
0-20	17.55	2.84	16	66.90	111.43	50
20-40	10.60	0.29	3	12.28	0.21	25
40-60	14.25	0	1	14.30	5.32	10
60-80	NA	NA	NA	14.42	0.27	4
Car-HV(LCV-LV)						
0-20	11.12	1.61	4	19.00	0	1
HV-Car(LCV-LV)						
20-40	NA	NA	NA	1760000	0	1

*Angle conflicts occur when the LCV is likely to hit the side of the LV (Case 1).

**Rear-end conflicts occur when the LCV is likely to hit the rear-end of the LV (Case 2).

The table shows that CPIs for LCV-LV conflicts were higher for rear-end conflicts than angle conflicts in Car-Car in all spacing intervals. However, this result is opposite to the result of CPIs for LCV-TV conflict ([Table 5-5](#)) which shows that both speed difference and DRAC are consistently higher for angle conflicts than rear-end conflicts. This is mainly due to higher number of observations for rear-end conflicts than angle conflicts between the LCV and the LV during lane changes. In fact, the values of CPIs are not consistent with DRAC and speed difference as shown in [Table 5-8](#). Thus, CPIs are not comparable between angle and rear-end conflicts for lane-change conflicts between the LCV and the LV.

Table 5-8. Comparison of average speed, average speed difference, spacing and DRAC for LCV in lane-change conflicts between LCV and LV

Vehicle Pair Type (LCV-LV)		Spacing Interval (m)				
		0-20	20-40	40-60	60-80	80-100
Average Speed of LCV (km/h)						
Car-Car	Angle	12.58	13.48	16.80	NA	NA
	Rear-end	11.04	14.02	14.16	16.10	NA
Car-HV	Angle	5.30	NA	NA	NA	NA
	Rear-end	4.30	NA	NA	NA	NA
HV-Car	Angle	NA	NA	NA	NA	NA
	Rear-end	NA	NA	NA	NA	16.31
Average Speed difference (km/h) (= LCV speed minus LV speed)						
Car-Car	Angle	1.08	1.47	3.09	NA	NA
	Rear-end	0.89	1.32	2.00	3.70	NA
Car-HV	Angle	0.91	NA	NA	NA	NA
	Rear-end	0.52	NA	NA	NA	NA
HV-Car	Angle	NA	NA	NA	NA	NA
	Rear-end	NA	NA	NA	NA	1.02
Average Spacing (m)						
Car-Car	Angle	11.51	29.02	40.10	NA	NA
	Rear-end	12.30	28.72	49.78	68.00	NA
Car-HV	Angle	7.66	NA	NA	NA	NA
	Rear-end	1.72	NA	NA	NA	NA
HV-Car	Angle	NA	NA	NA	NA	NA
	Rear-end	NA	NA	NA	NA	98.18
Average DRAC (m/s ²)						
Car-Car	Angle	0.13	0.07	0.13	NA	NA
	Rear-end	0.09	0.06	0.07	0.14	NA
Car-HV	Angle	0.16	NA	NA	NA	NA
	Rear-end	0.17	NA	NA	NA	NA
HV-Car	Angle	NA	NA	NA	NA	NA
	Rear-end	NA	NA	NA	0.01	NA

It was also found that cars rarely changed lanes behind a HV and vice versa (Car-HV and HV-Car). This is potentially because car drivers have little motivation for changing the

lane behind HV in discretionary lane-change maneuvers due to poor visibility. Also, HV drivers are less willing to change the lane due to the size and poor manipulation of HVs.

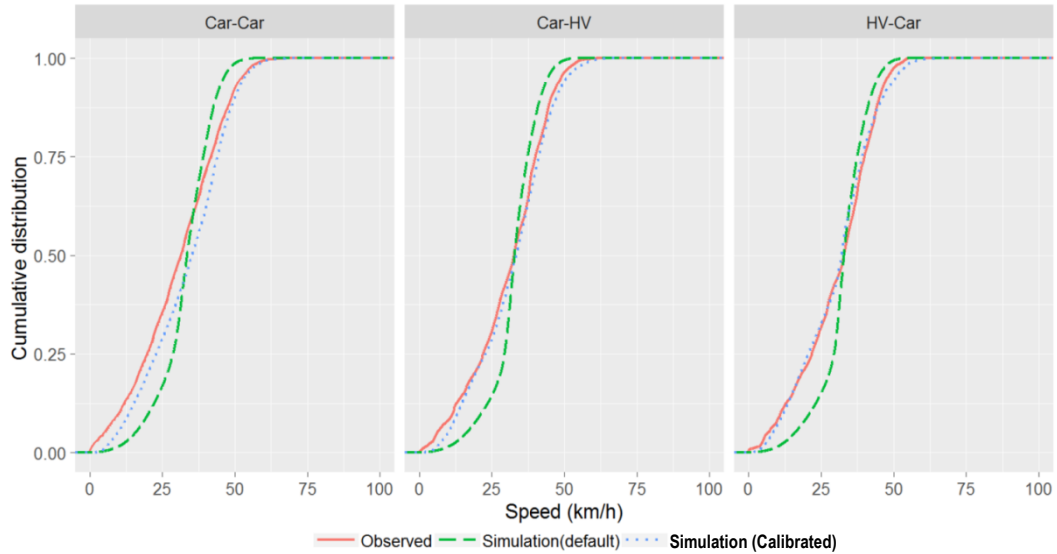
It is worth noting that the CPI for Car-Car was higher for LCV-TV conflicts than LCV-LV conflicts for the spacing intervals of 0-20 m and 20-40 m. This was observed for both angle and rear-end conflicts. This is potentially because LCV drivers usually pay more attention than LV and TV drivers in the target lane during the lane-change maneuver. For instance, TV drivers are less likely to anticipate lane change and cannot promptly adjust their speed to avoid collisions with the LCV.

5.3. Validation of CPI

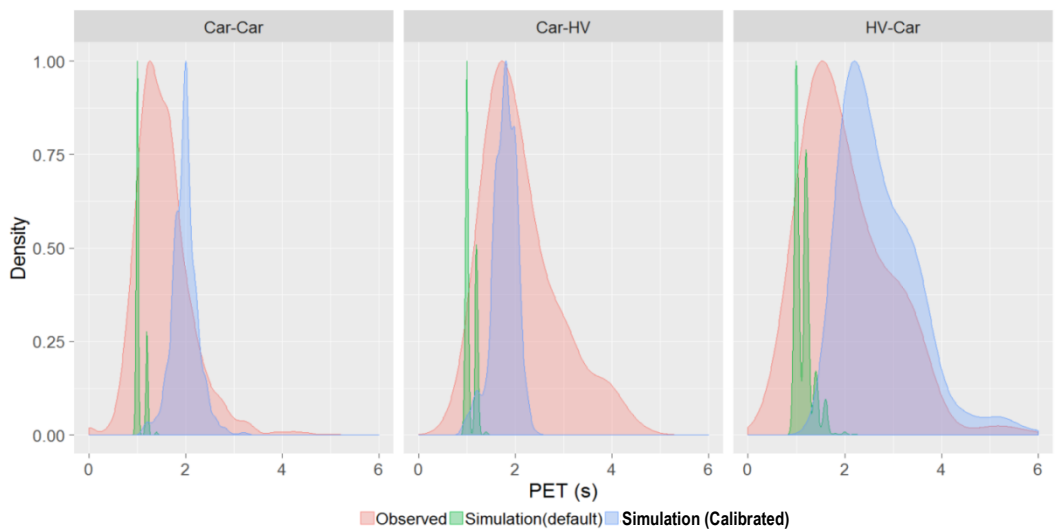
5.3.1. Validation of VISSIM simulation

CPI was validated and compared among different vehicle pair types using simulated vehicle trajectories from VISSIM simulation with the calibrated driving behavior parameters as shown in [Table 4-2](#). To validate the VISSIM simulation, distributions of speed and PET were compared between the observed and simulated data for the US-101 freeway during the time period 2 (8:05 am - 8:20 am).

[Figure 5-5](#) compares the distributions of cumulative speed and PET among the observed data, the simulation data with default parameters (default data) and the simulation data with calibrated parameters (calibrated data) for the three vehicle pair types. It was found that the calibrated data better reflect actual distributions of speed and PET than the default data for all vehicle pair types.



(a) Cumulative speed distribution



(b) Distribution of PET

Figure 5-5. Comparison of speed and PET between observed and simulation data with default and calibrated driving behavior parameters

To apply the same driving behavior parameters to the simulation of traffic on the Gardiner Expressway, the transferability of the parameters must be checked. To check the transferability, 20-second average speeds at the detector stations 80 and 90 during the 500-

s time period (number of observations = 25) prior to the abrupt speed drop at the downstream detector (station 90) were compared between the observed data and the data from simulation with the calibrated parameters. It was found that a majority (90%) of vehicles were in the car-following condition during the 500-s time period. In VISSIM simulation, the car-following condition occurs when the spacing between the subject vehicle and their corresponding lead vehicle is less than 250 m (PTV AG 2014). In the car-following condition, the driving behaviour parameters are critical factors for determining the subject vehicle's behaviour in response to the lead vehicle's behaviour. Thus, if the observed and simulated speeds are similar, this implies that the calibrated driving behaviour parameters realistically reflect actual car-following behaviour of the drivers on the Gardiner Expressway.

[Table 5-9](#) shows the two types of estimation errors - RMSPE and MPE ([Eq. 4-12](#) and [Eq. 4-13](#)) - of the VISSIM simulation for the 8 crashes that occurred on the Gardiner Expressway as shown in Appendix A. The speed in the simulation data is an average of speeds in 10 simulation runs. It was found that mean RMSPE and MPE were 9.52% - 12.98% and 2.59% - 9.85%, respectively, for upstream and downstream detectors. The negative value of MPE represents the simulation underestimates the observed speed. These errors are similar to the errors in the study by Kuang et al. (2015). Thus, the VISSIM simulation with the calibrated driving behaviour parameters reflects the actual traffic conditions on the Gardiner Expressway with a reasonable accuracy.

Table 5-9. Estimation errors of VISSIM simulation for Gardiner Expressway

Crash ID	Upstream detector (Station 80)		Downstream detector (Station 90)	
	RMSPE (%)	MPE (%)	RMSPE (%)	MPE (%)
6631	14.90	12.91	14.58	7.44
1518	15.15	13.54	8.59	4.28
1766	17.72	17.13	10.78	6.25
2142	13.51	11.94	6.85	-0.48
4070	9.46	6.07	6.73	0.54
7588	11.09	9.46	10.60	6.62
7624	9.38	-7.60	10.41	-7.78
8143	12.77	10.94	7.35	1.50
8573	12.88	9.29	9.83	4.93
Average	12.98	9.85	9.52	2.59

5.3.2. Validation of CPI for car-following conflicts

The CPI for car-following conflicts illustrated in Section 4.1.2 was validated using the simulated data for crash and non-crash cases (Section 4.3.2). In order to eliminate the effect of contingency and increase the number of observations, VISSIM simulation was run 10 times with different seed numbers for each set of reaction times.

[Table 5-10](#) and [Figure 5-6](#) compare the mean values and variances of CPI for five different spacing intervals among different vehicle pair types in the crash case. It was found that CPI for Car-Car was higher than Car-HV and HV-Car for all spacing intervals.

Table 5-10. Comparison of CPI for car-following conflicts among different vehicle pair types in crash case

Vehicle Pair Type	Spacing Interval (m)									
	0-20		20-40		40-60		60-80		80-100	
	Mean	SD	Mean	SD	Mean	SD	Mean	SD	Mean	SD
Car-Car ($\times 10^{-3}$)										
1*	3.35	18.10	1.71	13.20	1.88	15.40	1.70	11.10	1.97	11.50
2	17.60	57.00	14.6	58.50	8.22	35.20	8.26	31.40	8.65	34.40
3	21.20	67.50	17.3	67.40	10.2	42.00	9.94	36.10	10.4	40.70
4	3.27	17.90	1.65	12.90	1.84	15.30	1.67	11.00	1.96	11.60
5	9.26	38.60	7.10	37.90	4.35	23.60	4.72	22.30	4.74	21.70
6	3.70	17.70	2.27	15.90	2.72	21.50	1.89	11.50	2.11	11.60
7	4.82	26.00	3.54	24.30	2.74	19.60	2.88	16.00	2.81	14.70
8	4.57	22.50	3.20	20.70	2.61	18.20	2.55	14.80	2.67	14.20
9	5.74	29.70	4.33	28.00	3.09	21.00	3.42	17.80	3.57	18.20
10	1.80	9.610	1.03	7.56	1.19	9.38	1.77	11.70	2.11	12.30
Ave	7.53	30.40	5.67	28.60	3.88	22.10	3.88	18.40	4.10	19.10
Std. dev.	6.27		5.42		2.81		2.79		2.86	
No. of obs.	60		2690		3990		2660		1690	
Car-HV($\times 10^{-3}$)										
1	0.64	1.96	0.43	1.61	0.53	1.79	0.43	1.60	0.49	1.69
2	13.60	24.80	12.90	29.60	11.50	26.60	7.33	19.9	6.35	13.00
3	21.60	36.80	21.20	45.50	17.00	39.70	11.30	30.70	8.53	17.40
4	0.63	1.95	0.43	1.60	0.53	1.78	0.423	1.59	0.48	1.69
5	1.91	4.69	1.43	4.14	1.49	4.19	1.116	3.63	1.49	3.77
6	0.47	1.33	0.32	1.12	0.37	1.17	0.317	1.10	0.29	0.88
7	0.61	1.81	0.44	1.55	0.43	1.51	0.398	1.47	0.32	0.91
8	0.40	1.22	0.29	1.04	0.27	0.99	0.266	0.99	0.16	0.47
9	0.88	2.52	0.64	2.17	0.65	2.16	0.567	2.02	0.63	1.73
10	0.64	1.96	0.43	1.61	0.53	1.79	0.428	1.61	0.49	1.69
Ave	4.14	7.9	3.86	9	3.33	8.17	2.25	6.46	1.92	4.32
Std. dev.	6.99		6.88		5.61		3.64		2.82	
No. of obs.	740		1230		1320		1060		670	

*The number denotes different sets of reaction times. CPI is estimated as a mean of CPIs in 10 different VISSIM simulation runs for each set of reaction times.

Table 5-10. Comparison of CPI for car-following conflicts among different vehicle pair types in crash case (Continued)

Vehicle Pair Type	Spacing Interval (m)									
	0-20		20-40		40-60		60-80		80-100	
	Mean	SD	Mean	SD	Mean	SD	Mean	SD	Mean	SD
HV-Car($\times 10^{-3}$)										
1	1.83	2.99	1.53	2.73	1.87	2.99	1.86	3.17	1.09	1.45
2	1.68	2.72	1.43	2.51	1.75	2.75	1.73	2.92	1.07	1.41
3	1.79	2.92	1.51	2.67	1.84	2.93	1.83	3.11	1.09	1.44
4	1.83	2.99	1.53	2.73	1.87	2.99	1.86	3.17	1.09	1.45
5	1.83	2.99	1.53	2.73	1.87	2.99	1.86	3.17	1.09	1.45
6	1.83	2.99	1.53	2.73	1.87	2.99	1.86	3.17	1.09	1.45
7	1.79	2.92	1.51	2.67	1.84	2.93	1.83	3.11	1.09	1.44
8	1.83	2.99	1.53	2.73	1.87	2.99	1.86	3.17	1.09	1.45
9	1.79	2.92	1.51	2.67	1.84	2.93	1.83	3.11	1.09	1.44
10	1.83	2.99	1.53	2.73	1.87	2.99	1.86	3.17	1.09	1.45
<i>Ave</i>	1.8	2.94	1.52	2.69	1.85	2.95	1.84	3.13	1.09	1.45
<i>Std. dev.</i>	0.0454		0.0302		0.0372		0.0382		0.00662	
<i>No. of obs.</i>	800		890		740		660		550	

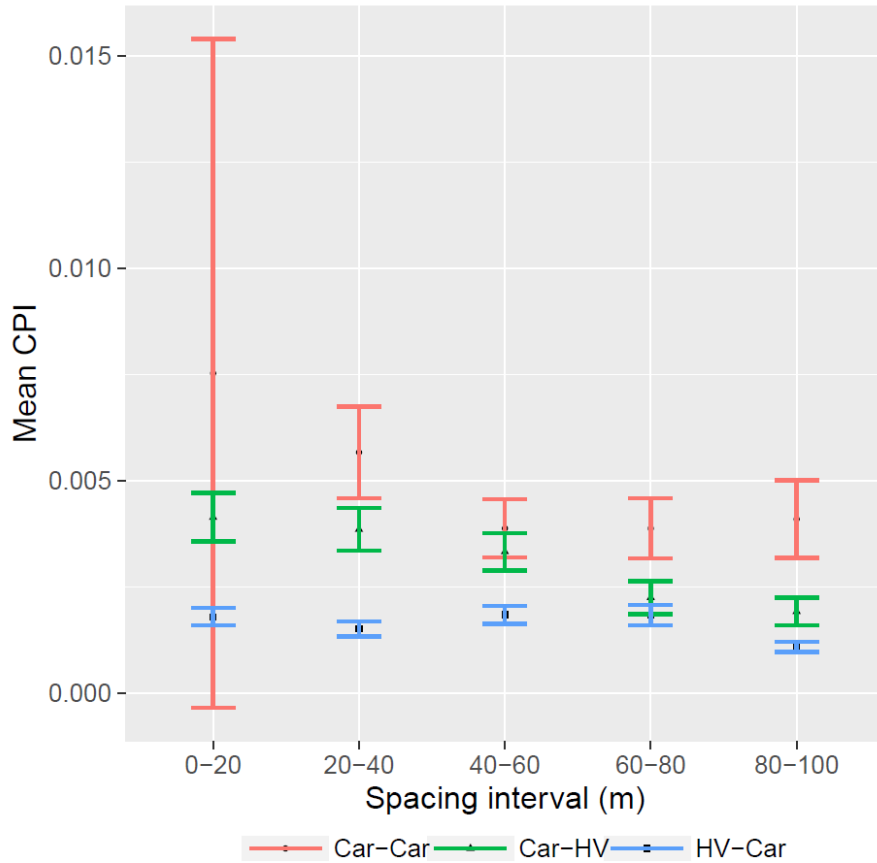


Figure 5-6. Comparison of CPI for car-following conflicts among vehicle pair types in crash case

[Table 5-11](#) compares average speed, spacing and DRAC of the following vehicle for different vehicle pair types among different spacing intervals. It was found that the following vehicle’s average speeds were consistently higher for Car-Car than Car-HV and HV-Car. As the spacing increases, average speeds were much higher for cars than trucks. This reflects that car drivers tend to keep higher speed than HV drivers for a given spacing since car drivers have more confidence in deceleration capabilities than HV drivers. On the other hand, this implies that HV drivers are more cautious (i.e., following at lower speeds)

in crash-prone condition than car drivers. For these reasons, DRAC and CPI were consistently higher for the following car drivers than the following HV drivers.

Table 5-11. Average speed, spacing and DRAC for following vehicle in car-following conflicts in crash case

Vehicle Pair Type	Spacing Interval (m)				
	0-20	20-40	40-60	40-80	80-100
Average Speed (km/h)					
Car-Car	12.17	51.19	80.89	84.38	86.17
Car-HV	7.56	26.85	75.50	84.84	84.87
HV-Car	6.76	15.92	38.62	70.53	75.25
Average Spacing (m)					
Car-Car	14.04	29.74	49.92	67.39	88.66
Car-HV	16.73	27.87	53.05	68.09	88.77
HV-Car	12.91	25.31	52.06	69.63	91.46
Average DRAC (m/s²)					
Car-Car	0.36	0.39	0.40	0.61	0.88
Car-HV	0.30	0.57	0.41	0.61	0.44
HV-Car	0.12	0.17	0.23	0.46	0.48

[Table 5-12](#) and [Figure 5-7](#) compare the mean values and variances of CPI for five different spacing intervals among different vehicle pair types in the non-crash case. There was no observation of Car-HV and HV-Car in the spacing interval of 0-20 m. The CPI was the highest for HV-Car, followed by Car-Car and Car-HV for the spacing greater than 20 m. However, the variance of CPI for Car-Car was still the highest. This is similar to the observed condition in the US-101 freeway.

Table 5-12. Comparison of CPI for car-following conflicts among different vehicle pair types in non-crash case

Vehicle Pair Type	Spacing Interval (m)									
	0-20		20-40		40-60		60-80		80-100	
	Mean	SD	Mean	SD	Mean	SD	Mean	SD	Mean	SD
Car-Car ($\times 10^{-8}$)										
1	0.0813	3270	0.055	265	0.035	215	0.011	355	0.635	254
2	0.0814	166000	33.500	163000	21.500	132000	10.400	356000	14.70	5870
3	0.0814	282000	58.600	279000	36.700	226000	99.100	598000	24.40	9740
4	0.0813	3230	0.048	231	0.031	187	0.012	141	0.590	235
5	0.0814	19200	3.300	16200	2.130	13100	9.250	35400	4.52	1810
6	0.0813	3600	0.124	601	0.079	488	0.297	957	0.967	386
7	0.0813	5480	0.507	2480	0.326	2010	0.892	1210	1.92	766
8	0.0813	4230	0.252	1230	0.162	997	0.144	3560	1.44	575
9	0.0813	7680	0.955	4680	0.616	3800	0.956	3240	2.34	936
10	0.0813	3290	0.061	295	0.039	239	0.032	107	0.705	282
Ave	0.0813	49800	9.740	46800	6.160	38000	12.109	99897	5.221	2090
Std. dev.	0		19.03		11.98		29.24		7.56	
No. of obs.	60		2690		3990		2600		1690	
Car-HV ($\times 10^{-8}$)										
1	NA	NA	0.0888	0.0234	0.126	0.0776	0.138	0.0895	0.177	0.15
2	NA	NA	0.0909	0.0264	0.138	0.103	0.153	0.117	0.203	0.205
3	NA	NA	0.0912	0.027	0.141	0.109	0.156	0.122	0.208	0.216
4	NA	NA	0.0888	0.0234	0.125	0.0772	0.138	0.089	0.177	0.149
5	NA	NA	0.09	0.0253	0.133	0.0928	0.146	0.105	0.192	0.182
6	NA	NA	0.0892	0.0238	0.127	0.0807	0.14	0.0927	0.18	0.156
7	NA	NA	0.0895	0.0245	0.13	0.0858	0.143	0.0981	0.186	0.167
8	NA	NA	0.0893	0.0242	0.129	0.0835	0.141	0.0958	0.183	0.163
9	NA	NA	0.0897	0.0247	0.131	0.0882	0.144	0.101	0.188	0.172
10	NA	NA	0.0888	0.0234	0.126	0.0776	0.138	0.0895	0.177	0.15
Ave	NA	NA	0.0896	0.0246	0.131	0.0876	0.144	0.1	0.187	0.171
Std. dev.	NA		0.000801		0.00502		0.00602		0.0103	
No. of obs.	NA		140		420		450		260	

Table 5-12. Comparison of CPI for car-following conflicts among different vehicle pair types in non-crash case (Continued)

Vehicle Pair Type	Spacing Interval (m)									
	0-20		20-40		40-60		60-80		80-100	
	Mean	SD	Mean	SD	Mean	SD	Mean	SD	Mean	SD
HV-Car($\times 10^8$)										
1	NA	NA	15400	3480	15900	6650	18600	5550	18000	3140
2	NA	NA	15400	3470	15900	6640	18600	5540	18000	3130
3	NA	NA	15400	3480	15900	6640	18600	5540	18000	3140
4	NA	NA	15400	3480	15900	6650	18600	5550	18000	3140
5	NA	NA	15400	3480	15900	6650	18600	5550	18000	3140
6	NA	NA	15400	3480	15900	6650	18600	5550	18000	3140
7	NA	NA	15400	3480	15900	6640	18600	5540	18000	3140
8	NA	NA	15400	3480	15900	6650	18600	5550	18000	3140
9	NA	NA	15400	3480	15900	6640	18600	5540	18000	3140
10	NA	NA	15400	3480	15900	6650	18600	5550	18000	3140
<i>Ave</i>	<i>NA</i>	<i>NA</i>	<i>15400</i>	<i>3470</i>	<i>15900</i>	<i>6640</i>	<i>18600</i>	<i>5550</i>	<i>18000</i>	<i>3140</i>
<i>Std. dev.</i>	<i>NA</i>		<i>0.872</i>		<i>0.235</i>		<i>0.446</i>		<i>0.0803</i>	
<i>No. of obs.</i>	<i>NA</i>		<i>90</i>		<i>150</i>		<i>150</i>		<i>120</i>	

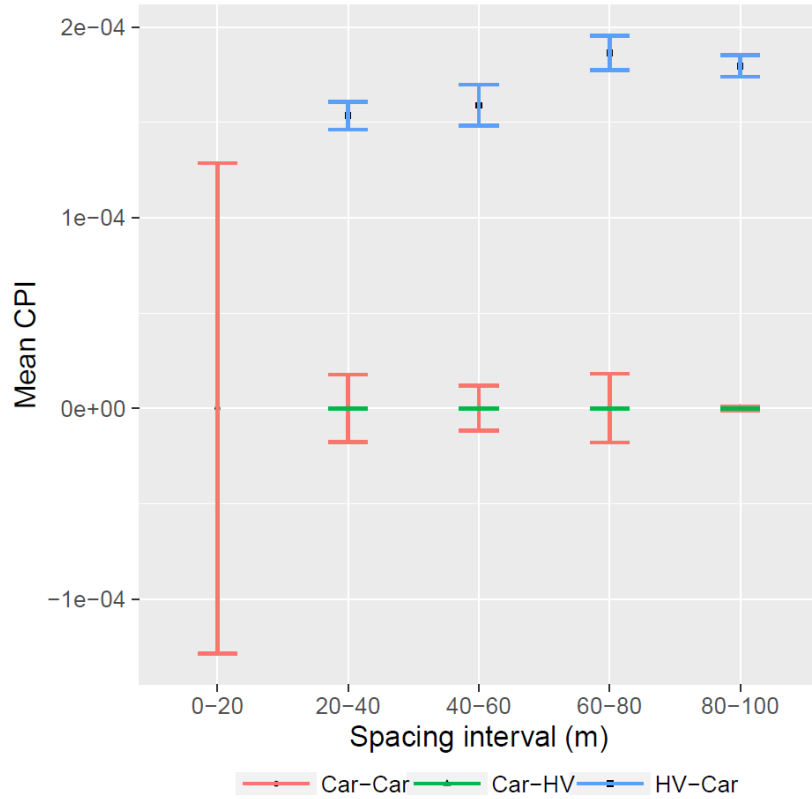


Figure 5-7. Comparison of CPI for car-following conflicts among vehicle pair types in non-crash case

[Table 5-13](#) shows that average speeds were relatively similar among different vehicle-pair types in the non-crash case compared to the crash case. Also, DRAC was significantly lower for HV-Car than Car-Car and Car-HV. This is because driver’s reaction time is shorter for HV drivers than car drivers whereas spacing and following vehicle speed are similar. However, due to HV’s lower braking capability, CPI was highest for the following HV.

Table 5-13. Average speed, spacing and DRAC for following vehicle in car-following conflicts in non-crash case

Vehicle Pair Type	Spacing Interval (m)				
	0-20	20-40	40-60	40-80	80-100
Average Speed (km/h)					
Car-Car	84.86	89.50	93.32	94.74	94.45
Car-HV	NA	89.06	89.04	92.92	92.37
HV-Car	NA	79.70	91.90	93.57	93.23
Average Spacing (m)					
Car-Car	18.97	32.95	50.41	68.14	90.13
Car-HV	NA	35.84	49.03	70.98	90.63
HV-Car	NA	37.38	43.14	63.78	92.66
Average DRAC (m/s ²)					
Car-Car	0.02	0.02	0.03	0.04	0.05
Car-HV	NA	0.01	0.05	0.14	0.06
HV-Car	NA	0.001	0.003	0.063	0.005

[Figure 5-8](#) compares the average CPI among different vehicle pair types for different spacing intervals between crash and non-crash cases. The CPI was consistently higher for the crash case than the non-crash case. This is because an abrupt speed drop at the downstream detector increased the difference in speed between the upstream and downstream detectors, resulting in higher risk of rear-end collisions in the crash case.

However, the difference in CPI between crash and non-crash cases varies among different vehicle pair types. Among the three vehicle pair types, the difference was the highest for Car-Car, followed by Car-HV and HV-Car. It is worth noting that the difference was consistently lower for HV-Car than Car-Car. This is potentially because HV drivers are normally well-trained professional drivers and they are more cautious especially in congested or unstable traffic conditions. In fact, some empirical studies reported that HV drivers showed safer driving behaviour. For example, Blower (1998) pointed that truck

drivers made fewer errors than car drivers when they shared the road with passenger cars. He explained that this was potentially due to stricter laws and higher penalty for truck drivers if they are involved in the passenger car-truck collisions. Rosenbloom et al. (2009) also claimed that truck drivers are usually well-trained to avoid dangerous situations because they have more experience of driving in complex traffic conditions than passenger car drivers and they also have responsibility for their companies and customers.

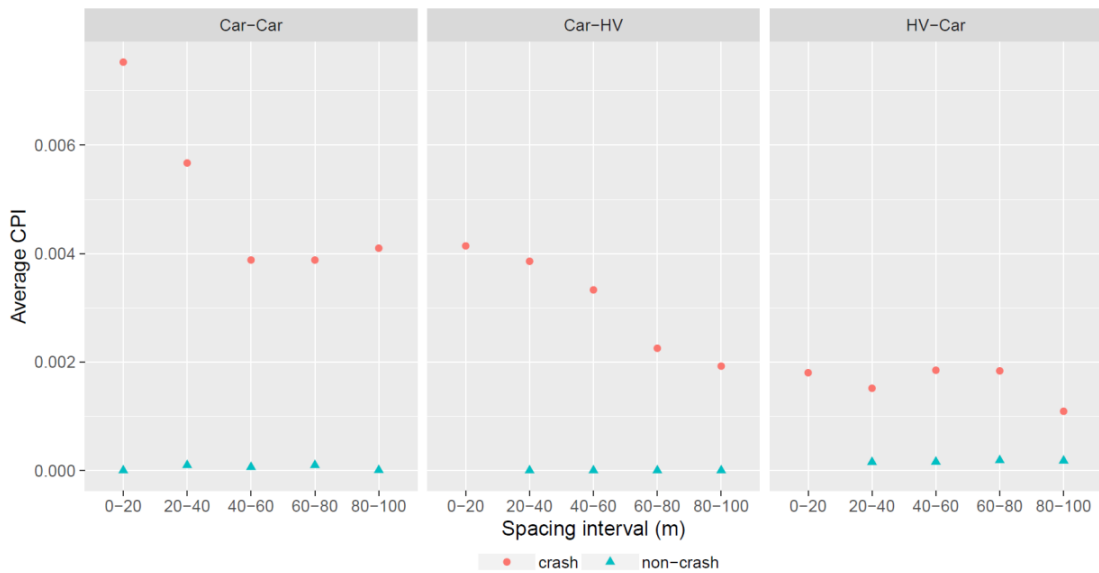


Figure 5-8. Comparison of CPI for car-following conflicts between crash and non-crash cases

5.3.3. Validation of CPI for lane-change conflicts

Since VISSIM only provided the trajectories of the subject vehicle (LCV) and the corresponding lead vehicle (LV), the CPI for lane-change conflicts between the LCV and the TV could not be estimated. In VISSIM simulation, the lane change duration (LCD) is defined as the time it takes for the front center of the LCV to move from the center of the current lane to the middle of the target lane. This LCD is pre-specified as 3 seconds for all

vehicles but this could not be modified. In fact, the definition of LCD in VISSIM is not consistent with the LCD illustrated in Section 3.1. Thus, the LCD in VISSIM simulation was re-estimated using the definition in Section 3.1. It was found that the LCD in VISSIM simulation was 1.41s, which is relatively shorter than the observed LCD from the NGSIM data.

[Table 5-14](#) compares mean LCD for different vehicle types between the observed and simulated data. In particular, the difference in LCD between the observed and simulated data was significantly higher for HVs than cars. Due to unrealistically short LCD for HVs in VISSIM simulation, the CPI was compared between the crash and non-crash cases only for Car-Car.

Table 5-14. Comparison of mean LCD for different vehicle types between observed and simulated data

	Car	HV
Observed	4.86 s	16.04 s
Simulated	1.39 s	1.74 s

The CPI for lane-change conflicts illustrated in Section 4.2.2 was compared between the crash and non-crash cases for the lane change spacing interval of 60 - 80 m due to limited sample size as shown in [Table 5-15](#). For this spacing interval, the CPI was higher for the crash case than the non-crash case for angle conflicts (71.12×10^{-10} VS. 7.52×10^{-10}) and rear-end conflicts (121.90×10^{-10} VS. 8.74×10^{-10}). Thus, the CPI for lane-change conflicts reflects the risk of angle and rear-end collision during lane changes.

Table 5-15. Comparison of CPI for lane-change conflicts between crash and non-crash cases (Car-Car)

Lane-change spacing interval (m)	CPI ($\times 10^{-10}$) -Angle*			CPI ($\times 10^{-10}$) - Rear-end*		
	Mean	SD	No. of ob.	Mean	SD	No. of ob.
Crash case						
0-20	NA	NA	NA	13.47	0.320	20
20-40	20.11	1.46	20	NA	NA	NA
40-60	8.03	0.001	10	121.90	20.2	40
60-80	71.12	0.01	10	71.76	0.01	10
80-100	NA	NA	NA	NA	NA	NA
Non-rash case						
0-20	NA	NA	NA	NA	NA	NA
20-40	NA	NA	NA	NA	NA	NA
40-60	NA	NA	NA	NA	NA	NA
60-80	7.52	0.001	90	8.74	0.001	40
80-100	6.61	0.001	50	NA	NA	NA

In summary, the CPI with the modified DRAC is a proper surrogate safety measure for estimating collision risk in car-following and lane-change conflicts. The CPI considers the following vehicle driver's reaction time and the vehicle's deceleration capability. The CPI also accounts for the difference in reaction time and deceleration capability between cars and HVs, and reflects the variation in collision risk among different vehicle pair types. It was verified that for a given spacing between the two vehicles, the CPIs were consistently higher for the crash case than the non-crash case in both car-following and lane-change conflicts.

CHAPTER 6 CONCLUSION AND RECOMMENDATIONS

This study analyzed collision risk for car-following and lane-change conflicts on freeways using surrogate safety measures by types of lead and following vehicles (vehicle pair types). Three surrogate safety measures for car-following and lane-change conflicts, time-to-collision (TTC), post-encroachment-time (PET) and crash potential index (CPI), were calculated for cars and heavy vehicles separately using individual vehicle trajectories for the US-101 freeway in Los Angeles, U.S.A. The CPIs were calculated for a car following a car (Car-Car), a car following a heavy vehicle (Car-HV), and a heavy vehicle following a car (HV-Car) for both conflicts, but TTC and PET were only estimated for car-following conflicts. This study also validated the CPI using the traffic data collected a few minutes before the time of crashes that occurred on a segment of the Gardiner Expressway in Toronto, Canada. To calculate the CPI, vehicle trajectory data were generated using the calibrated VISSIM traffic simulation model. This validation method can capture the association of the surrogate safety measures with high risk events that may not lead to crashes. Thus, the method is more advantageous over the conventional validation method which uses crash frequency data only.

The main methodological contributions of this thesis are as follows:

1. Modifies the CPI considering driver's reaction time in addition to the following vehicle's deceleration capability;
2. Develops a new surrogate safety measure for lane-change conflicts with more objective definition of lane-change duration and classification of lane-change conflict types based on the vehicles' lateral positions;

3. Evaluates collision risk for car-following and lane-change conflicts among different vehicle pair types (car and heavy vehicle) based on the CPI;
4. Validates the CPI for car-following and lane-change conflicts using common speed patterns in crash-prone conditions replicated in a microscopic traffic simulation.

There are two noteworthy findings in this study. First, CPIs were significantly different among different vehicle pair types in car-following and lane-change conflicts. In car-following conflicts, CPIs were generally higher for the following heavy vehicle than the following car for a given spacing interval greater than 20 m. In lane-change conflicts between the lane-change vehicle (LCV) and the trailing vehicle (TV) in the target lane, CPIs were consistently higher for angle conflicts than rear-end conflicts. CPIs for lane change conflicts were higher when a heavy vehicle follows the LCV or the lead vehicle in the target lane (LV). This indicates that heavy vehicle's lower braking capability significantly increases collision risk.

Second, CPIs for car-following and lane-change conflicts were higher for the crash case than the non-crash case for all vehicle pair types. These results demonstrate that the CPI is a valid surrogate safety measure for both types of conflicts. However, values of CPI vary across different vehicle pair types. The CPI was higher for Car-Car than HV-Car in the crash case whereas the CPI was higher for HV-Car than Car-Car in the non-crash case. This indicates that although HV drivers take more time to decelerate in normal traffic conditions, they generally take more caution in complex and unstable traffic conditions than car drivers.

In summary, the findings in this study demonstrate that collision risks are different among different vehicle pair types due to difference in behavior between car and heavy

vehicle drivers in car-following and lane-change conflicts. TTC, PET and CPI for different vehicle pair types can be used to predict and evaluate the safety of different road geometry improvements and traffic control strategies for car-heavy vehicle mixed traffic flow. Furthermore, these surrogate safety measures can also be applied to prediction of severity of collision risk considering the difference in size and weight between the two vehicles. In practice, the surrogate safety measures can be applied to the development of the advanced driver assistance systems to reduce collision risk and improve driver safety. For instance, drivers are alarmed with a warning message whenever high collision risk is detected based on the vehicle movement data collected from vehicle sensors (e.g., speed, spacing). During lane-change conflicts, vehicle sensors in the side mirrors monitor the movement of vehicles in the target lane and drivers are advised to reduce speed if the risk of angle collision is high.

However, there are some limitations in this study. First, collision risk was estimated solely based on the vehicles' speed, spacing and deceleration capability, and driver's reaction time. However, other variables such as driver condition, visibility, weight of vehicle, condition of pavement, weather conditions, and road geometry are also likely to affect collision risk. For example, wet pavement and rainy weather condition decrease the drivers' visibility and friction between tires and pavement, and thereby increase the collision risk. However, these variables could not be considered in this study due to a lack of the data. Second, actual individual vehicle trajectories at the crash time were not available and thus the calculated CPI could not be validated using real crash data. This study defined common speed patterns prior to the crash time as crash-prone conditions but more work is needed to investigate how such speed patterns lead to actual crashes using

individual trajectory data. Lastly, the sample size of lane-change conflicts was insufficient due to the limited number of heavy vehicles and low frequency of discretionary lane-changes in the study area. Thus, the CPIs for lane-change conflicts were not comparable among different vehicle pair types.

In future studies, it is recommended that car and heavy vehicle driver's car-following and lane-change behaviour be more closely observed in various road geometric, traffic and environmental conditions. From this observation, the difference in collision risk among different vehicle pair types can be more extensively investigated. It is also recommended that the traffic simulation model be calibrated to better replicate the difference in car-following and lane-changing behaviors between cars and heavy vehicles. This behavioral difference in the simulation will help develop the surrogate safety measures to better reflect the risk of collision between cars and heavy vehicles. The simulation and surrogate safety measures will also help develop traffic control strategies to reduce car-heavy vehicle conflicts.

REFERENCES

- Aghabayk, K., Moridpour, S., Young, W., Sarvi, M., and Wang, Y.-B. (2011). “Comparing heavy vehicle and passenger car lane-changing maneuvers on arterial roads and freeways.” *Transportation Research Record: Journal of the Transportation Research Board*, 2260, 94–101.
- American Association of State Highway and Transportation Officials. (2004). *A Policy on Geometric Design of Highways and Streets*. American Association of State Highway and Transportation Officials, Washington D.C.
- Archer, J. (2004). “Methods for the Assessment and Prediction of Traffic Safety at Urban Intersections and their Application in Micro-simulation Modelling.” Division of Transport and Logistics, Royal Institute of Technology, Stockholm, Sweden.
- Ariza, A. (2011). “Validation of Road Safety Surrogate Measures as a Predictor of Crash Frequency Rates on a Large-Scale Microsimulation Network.” Department of Civil Engineering, University of Toronto, Toronto, Ontario.
- Astarita, V., Giofré, V., Guido, G., and Vitale, A. (2012). “Calibration of a new microsimulation package for the evaluation of traffic safety performances.” *Procedia - Social and Behavioral Sciences*, 54, 1019–1026.
- Bachmann, C., Roorda, M. J., and Abdulhai, B. (2012). “Improved time-to-collision definition for simulating traffic conflicts on truck-only infrastructure.” *Transportation Research Record: Journal of the Transportation Research Board*, 2237, 31–40.

- Bham, G. H., and Benekohal, R. F. (2004). "A high fidelity traffic simulation model based on cellular automata and car-following concepts." *Transportation Research Part C*, 12, 1–32.
- Blower, D. (1998). *The Relative Contribution of Truck Drivers and Passenger Vehicle Drivers to Truck-Passenger Vehicle Traffic Crashes*. Ann Arbor, MI.
- Classen, S., Bewernitz, M., and Shechtman, O. (2011). "Driving simulator sickness: An evidence-based review of the literature." *American Journal of Occupational Therapy*, 65(2), 179–188.
- Cooper, D. F., and Ferguson, N. (1976). "Traffic studies at T-Junctions. 2. A conflict simulation Record." *Traffic Engineering & Control*, 17(7), 306-309.
- Cunto, C. (2008). "Assessing Safety Performance of Transportation Systems using Microscopic Simulation." Ph.D. Thesis. Department of Civil and Environmental Engineering, University of Waterloo, Waterloo, Ontario.
- Cunto, F., Duong, D., and Saccomanno, F. F. (2009). "Comparison of simulated freeway safety performance with observed crashes." *Transportation Research Record: Journal of the Transportation Research Board*, 2103, 88–97.
- Cunto, F., and Saccomanno, F. F. (2008). "Calibration and validation of simulated vehicle safety performance at signalized intersections." *Accident Analysis & Prevention*, 40(3), 1171–1179.
- Dowling, R., Skabardonis, A., Halkias, J., McHale, G., and Zammit, G. (2004). "Guidelines for calibration of microsimulation models: Framework and applications."

- Transportation Research Record: Journal of the Transportation Research Board*, 1876, 1–9.
- Dozza, M. (2013). “What factors influence drivers’ response time for evasive maneuvers in real traffic?” *Accident Analysis & Prevention*, 58, 299–308.
- Durrani, U., Lee, C., and Maoh, H. (2016). “Calibrating the Wiedemann’s vehicle-following model using mixed vehicle-pair interactions.” *Transportation Research Part C: Emerging Technologies*, 67, 227–242.
- El-Tantawy, S., Djavadian, S., Roorda, M., and Abdulhai, B. (2009). “Safety evaluation of truck lane restriction strategies using microsimulation modeling.” *Transportation Research Record: Journal of the Transportation Research Board*, 2099, 123–131.
- Essa, M., and Sayed, T. (2015). “Transferability of calibrated microsimulation model parameters for safety assessment using simulated conflicts.” *Accident Analysis & Prevention*, 84, 41–53.
- Federal Motor Carrier Safety Administration. (2014). *LARGE TRUCK AND BUS CRASH FACTS 2013*. Washington, D.C.
- Garber, N. J., Miller, J. S., Yuan, B., and Sun, X. (2000). “Safety effects of differential speed limits on rural Interstate highways.” *Transportation Research Record*, 183, 56–62.
- Gettman, D., and Head, L. (2003). *Surrogate Safety Measures from Traffic Simulation Models*. Final Report. U.S. Department of Transportation, Federal Highway Administration Research, Development, and Technology Office of Safety Research

and Development Turner-Fairbank Highway Research Center. McLean, Virginia.

Gettman, D., Pu, L., Sayed, T., and Shelby, S. G. (2008). *Surrogate Safety Assessment Model and Validation: Final Report*. Washington, D.C.

Ghods, A. H., Saccomanno, F., and Guido, G. (2012). “Truck differential speed limits on two-lane highways safety operation using microscopic simulation.” *Procedia - Social and Behavioral Sciences*, 53, 833–840.

Habtemichael, F. G., and Santos, L. (2012). “Safety evaluations of aggressive driving on motorways through microscopic traffic simulation and surrogate measures.” Presented at the 91st Transportation Research Board Annual Meeting, Washington D.C.

Hayward, J. C. (1972). “Near-miss Determination Through Use of a Scale of Danger.” *Highway Research Record*, 384, 24-34.

Hyden, C. (1987). “Development of a Method for Traffic Safety Evaluation: The Swedish Traffic Conflicts Technique.” Lund Institute of Technology.

Jiménez, F., Naranjo, J. E., and García, F. (2013). “An improved method to calculate the time-to-collision of two vehicles.” *International Journal of Intelligent Transportation Systems Research*, 11(1), 34–42.

Kuang, Y., Qu, X., and Wang, S. (2015). “A tree-structured crash surrogate measure for freeways.” *Accident Analysis & Prevention*, 77, 137–148.

Kusano, K. D., and Gabler, H. (2011). “Method for estimating time to collision at braking in real-world, lead vehicle stopped rear-end crashes for use in pre-crash system

- design.” *SAE Int. J. Passeng. Cars – Mech. Syst.*, 4(1), 435–443.
- Levulis, S. J., DeLucia, P. R., and Jupe, J. (2015). “Effects of oncoming vehicle size on overtaking judgments.” *Accident Analysis & Prevention*, Elsevier Ltd, 82, 163–170.
- Livey, J. (2015). *Gardiner Expressway and Lake Shore Boulevard East Reconfiguration Environmental Assessment (EA) and Integrated Urban Design Study – Updated Evaluation of Alternatives*. Toronto, ON.
- Ma, T., and Abdulhai, B. (2002). “Genetic algorithm-based optimization approach and generic tTool for calibrating traffic microscopic simulation parameters.” *Transportation Research Record*, 1800, 6–15.
- Mayhew, D. R., Simpson, H. M., and Beirness, D. J. (2004). *Heavy Trucks and Road Crashes*. Ottawa, Ontario.
- Minderhoud, M. M., and Bovy, P. H. L. (2001). “Extended time-to-collision measures for road traffic safety assessment.” *Accident Analysis & Prevention*, 33(1), 89–97.
- Ministry of Transportation of Ontario. (2014). *Ontario Road Safety Report 2012*. Toronto, ON, Canada.
- Moridpour, S., Sarvi, M., and Rose, G. (2010). “Modeling the lane-changing execution of multiclass vehicles under heavy traffic conditions.” *Transportation Research Record: Journal of the Transportation Research Board*, 2161, 11–19.
- Nezamuddin, N., Jiang, N., Ma, J., Zhang, T., and Waller, S. T. (2011). “Active traffic management strategies: Implications for freeway operations and traffic safety.” Presented at the 90th Transportation Research Board Annual Meeting.

- Ozbay, K., Yang, H., Bartin, B., and Mudigonda, S. (2008). "Derivation and validation of new simulation-based surrogate safety measure." *Transportation Research Record: Journal of the Transportation Research Board*, 2083, 105–113.
- Park, B., and Qi, H. (2005). "Development and evaluation of a procedure for the calibration of simulation models." *Transportation Research Record: Journal of the Transportation Research Board*, 1934, 208–217.
- PTV AG. (2014). *PTV VISSIM 7 User Manual*. Karlsruhe, Germany.
- Rosenbloom, T., Eldror, E., and Shahar, A. (2009). "Approaches of truck drivers and non-truck drivers toward reckless on-road behavior." *Accident Analysis & Prevention*, 41(4), 723–728.
- Saccommanno, F. F., Duong, D., Cunto, F., Hellinga, B., Philp, C., and Thiffault, P. (2009). "Safety implications of mandated truck speed limiters on freeways." *Transportation Research Record: Journal of the Transportation Research Board*, 2096, 65–75.
- SAS Institute. (2012). *SAS 9.3*. Cary, NC, U.S.A.
- Shahdah, U., Saccommanno, F., and Persaud, B. (2015). "Application of traffic microsimulation for evaluating safety performance of urban signalized intersections." *Transportation Research Part C: Emerging Technologies*, 60, 96–104.
- Shechtman, O., Classen, S., Awadzi, K., and Mann, W. (2009). "Comparison of driving errors between on-the-road and simulated driving assessment: a validation study." *Traffic injury prevention*, 10(4), 379–85.
- Silvano, A. P., Koutsopoulos, H. N., and Ma, X. (2016). "Analysis of vehicle-bicycle

- interactions at unsignalized crossings: A probabilistic approach and application.” *Accident Analysis & Prevention*, 97, 38–48.
- St-Aubin, P., Miranda-Moreno, L., and Saunier, N. (2013). “An automated surrogate safety analysis at protected highway ramps using cross-sectional and before–after video data.” *Transportation Research Part C: Emerging Technologies*, 36, 284–295.
- Toledo, T., and Zohar, D. (2007). “Modeling duration of lane changes.” *Transportation Research Record: Journal of the Transportation Research Board*, 1999, 71–78.
- Transport Canada. (2010). *2008 Canadian Motor Vehicle Collision Statistics*. Ottawa, Canada.
- Transport Canada. (2014). *2012 Canadian Motor Vehicle Collision Statistics*. Ottawa, Canada.
- Vogel, K. (2003). “A comparison of headway and time to collision as safety indicators.” *Accident Analysis & Prevention*, 35(3), 427–433.
- Wang, C., and Stamatiadis, N. (2013). “Surrogate safety measure for simulation-based conflict study.” *Transportation Research Record: Journal of the Transportation Research Board*, 2386, 72–80.
- Wang, X., Zhu, M., Chen, M., and Tremont, P. (2016). “Drivers’ rear end collision avoidance behaviors under different levels of situational urgency.” *Transportation Research Part C: Emerging Technologies*, 71, 419–433.
- Wei, H., Meyer, E., Lee, J., and Feng, C. (2000). “Characterizing and modeling observed lane-changing behavior: Lane-vehicle-based microscopic simulation on urban street

- network.” *Transportation Research Record: Journal of the Transportation Research Board*, 1710, 104–113.
- Weng, J., and Meng, Q. (2011). “Analysis of driver casualty risk for different work zone types.” *Accident Analysis & Prevention*, 43(5), 1811–1817.
- World Health Organization. (2016). “Road Safety.” http://www.who.int/gho/road_safety/en/. Accessed Mar. 17, 2016.
- World Health Organization. (2011). Decade of Action for Road Safety 2011–2020 Saving millions of lives.
- Yan, X., Abdel-Aty, M., Radwan, E., Wang, X., and Chilakapati, P. (2008). “Validating a driving simulator using surrogate safety measures.” *Accident Analysis & Prevention*, 40(1), 274–288.
- Yang, Q., Overton, R., Han, L. D., Yan, X., and Richards, S. H. (2013). “The influence of curbs on driver behaviors in four-lane rural highways: A driving simulator based study.” *Accident Analysis & Prevention*, 50, 1289–1297.
- Zheng, L., Jin, P. J., Huang, H., and Gao, M. (2015). “A vehicle type-dependent visual imaging model for analysing the heterogeneous car-following dynamics.” *Transportmetrica B : Transport Dynamics*, 4, 68–85.

Appendix A: Observed Speed Patterns Upstream and Downstream of Crash Location

[Figures A-1](#) to [A-8](#) show the observed speed patterns upstream and downstream of eight crashes (upstream detector station = 80, downstream detector station = 90) that have occurred on the Gardiner Expressway. These speed patterns were used to validate the simulation of traffic on the Gardiner Expressway. The traffic conditions prior to the abrupt drop in downstream speed were considered typical normal or “non-crash” traffic conditions where the speeds are generally constant and the speed difference between the upstream and downstream detector stations is small. Thus, it is reasonable to assume that these 8 crashes occurred mainly due to the abrupt speed drop.

However, these speed patterns were not observed in the other crashes. For instance, [Figures A-9](#) to [A-11](#) show that speeds significantly fluctuated and the speed difference between upstream and downstream detector stations were high even before the abrupt drop in downstream speed. These conditions are not considered typical normal traffic conditions and it is hard to claim that the abrupt drop in downstream speed caused the crashes. Thus, these cases were not used to validate the simulation.

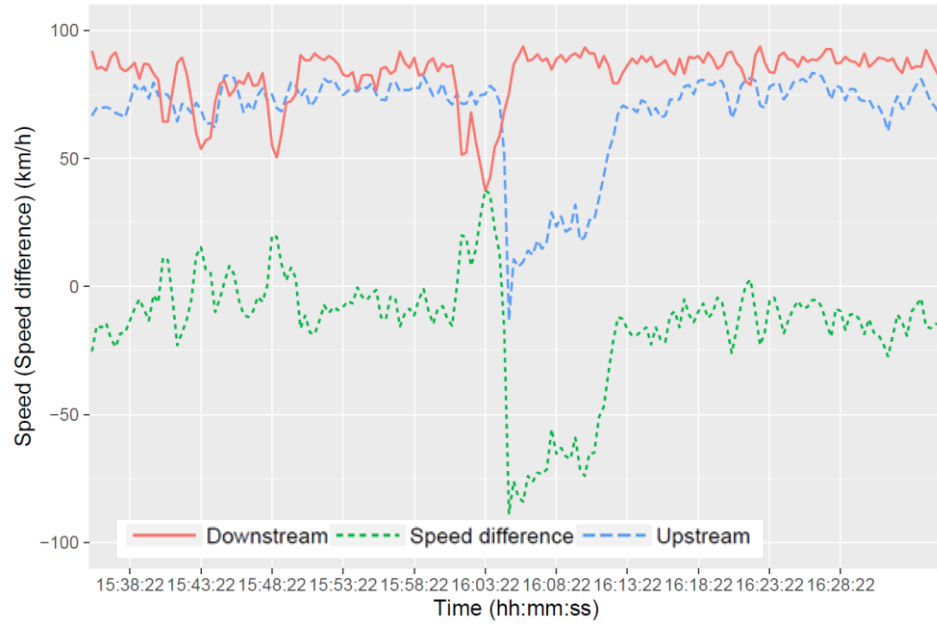


Figure A-1. Upstream and downstream speed pattern of crash 1518

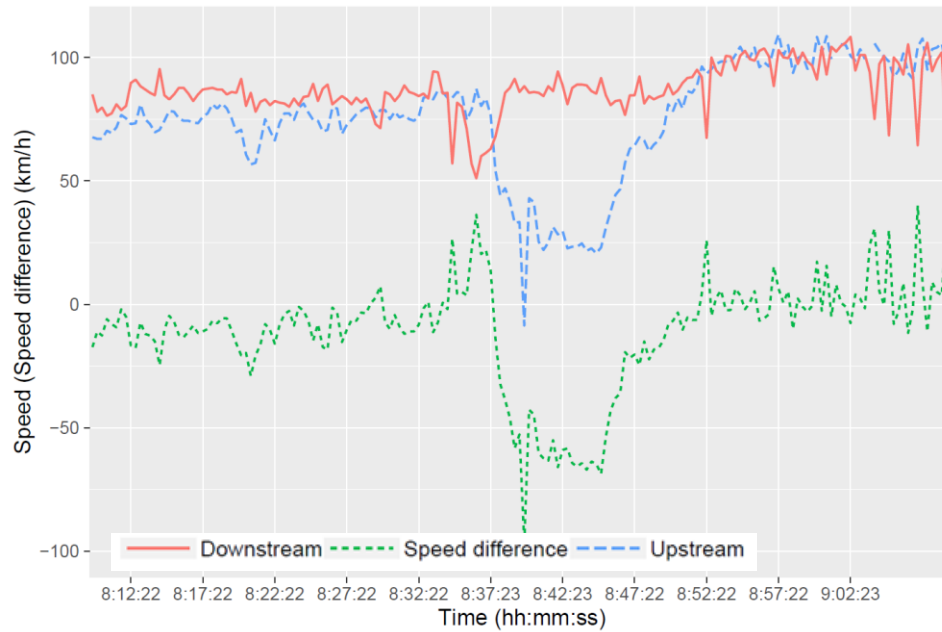


Figure A-2. Upstream and downstream speed pattern of crash 1766

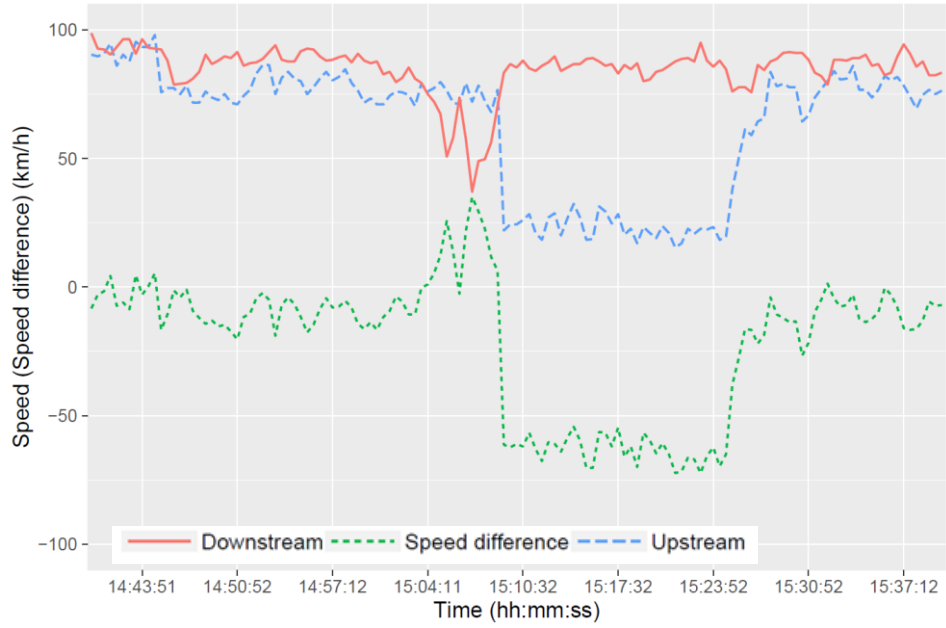


Figure A-3. Upstream and downstream speed pattern of crash 2142

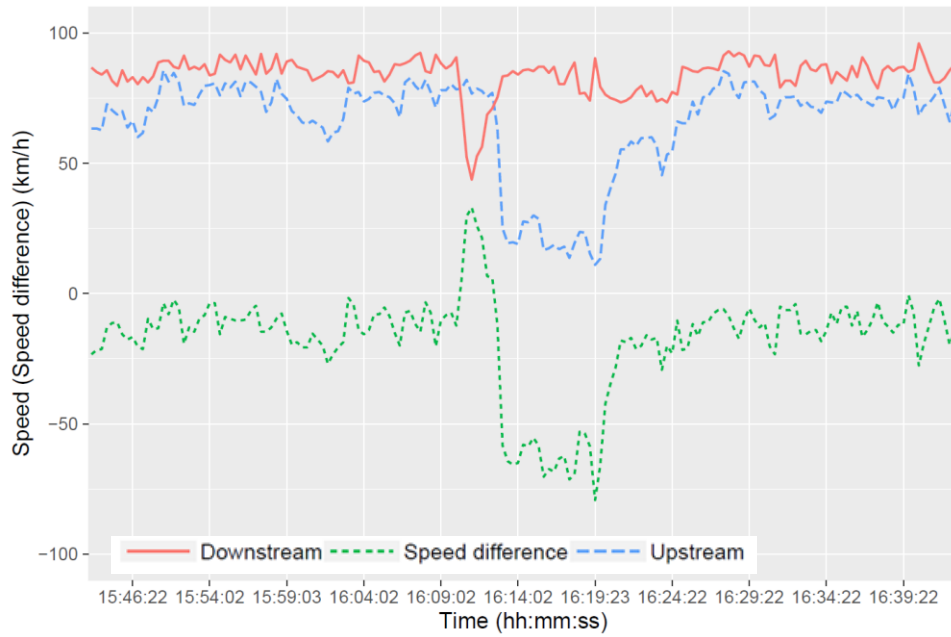


Figure A-4. Upstream and downstream speed pattern of crash 4070

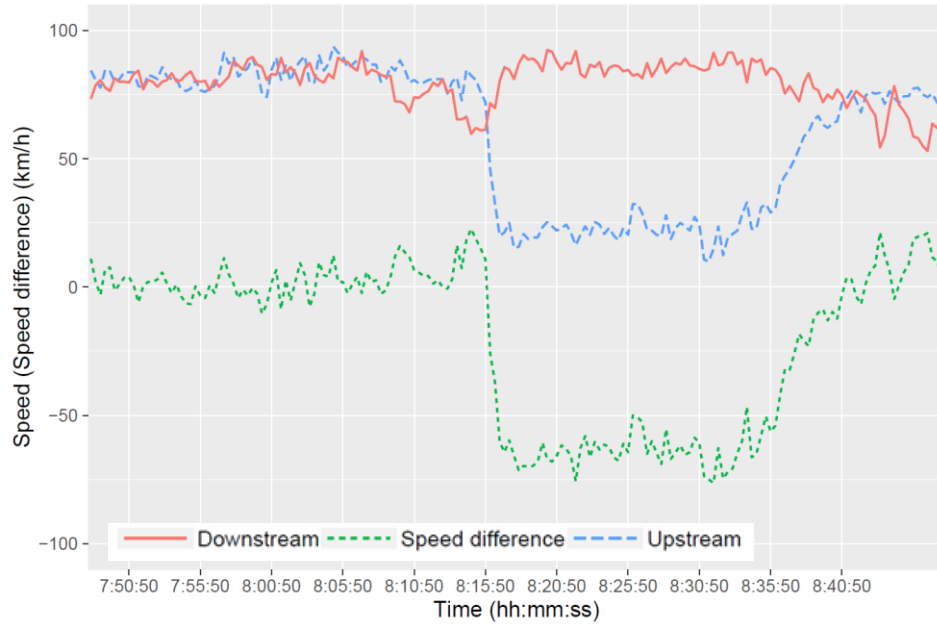


Figure A-5. Upstream and downstream speed pattern of crash 7588

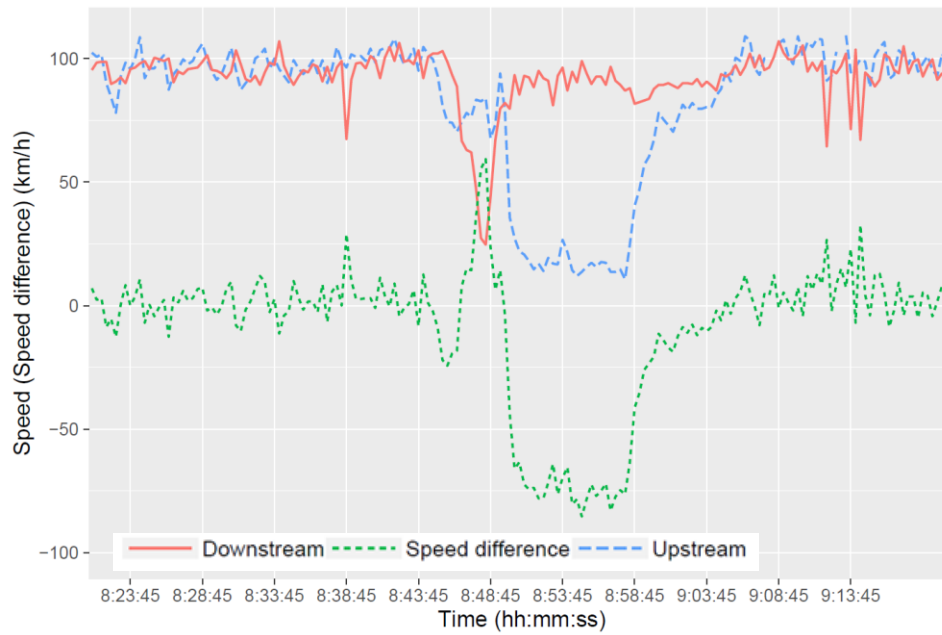


Figure A-6. Upstream and downstream speed pattern of crash 7624

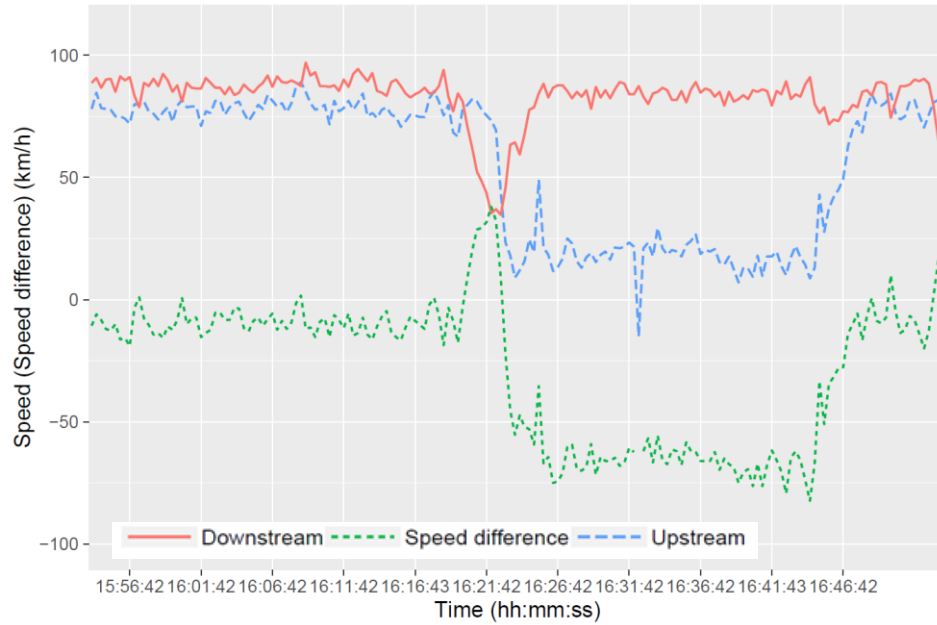


Figure A-7. Upstream and downstream speed pattern of crash 8143

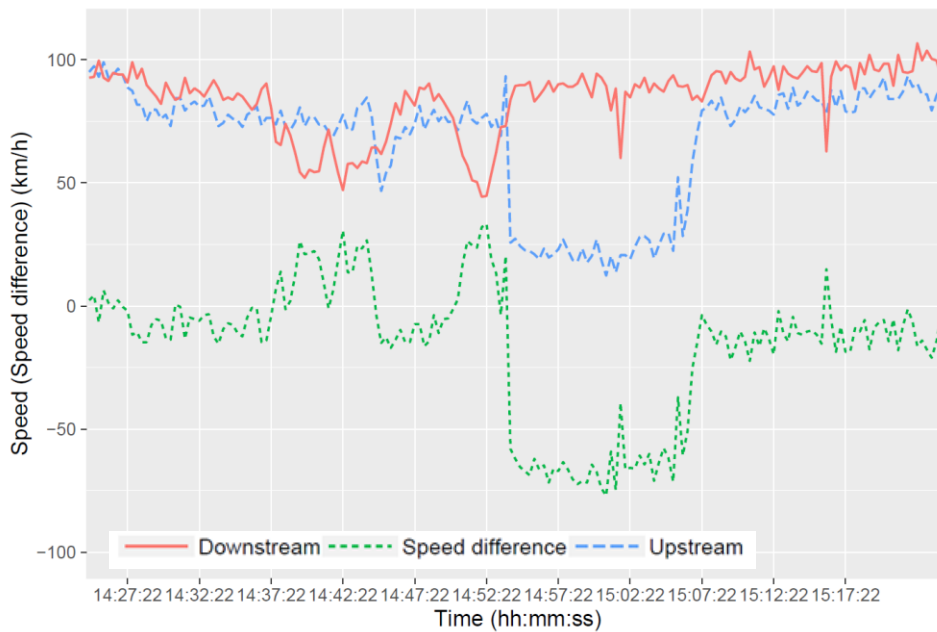


Figure A-8. Upstream and downstream speed pattern of crash 8573

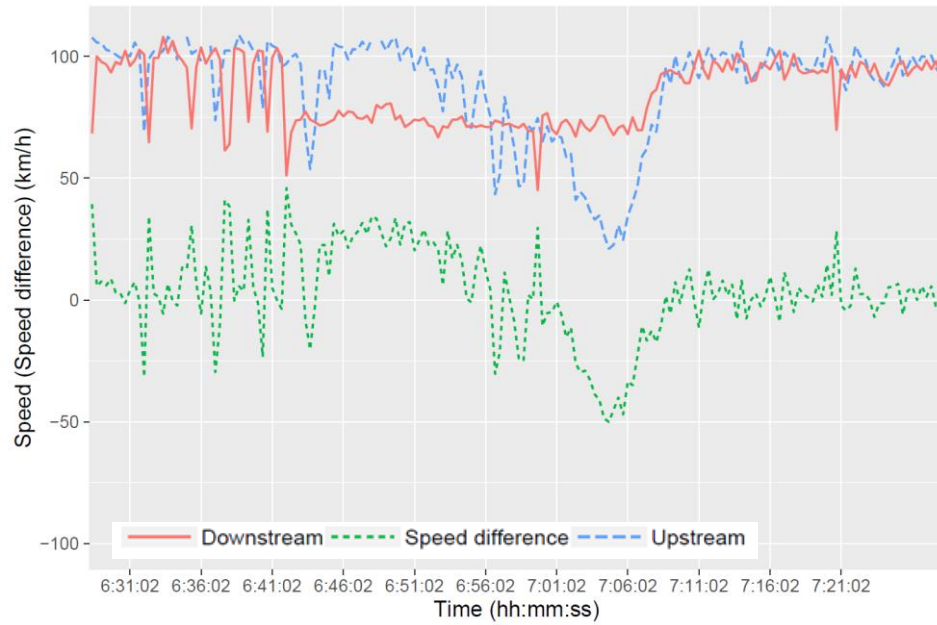


Figure A-9. Upstream and downstream speed pattern of crash 0420

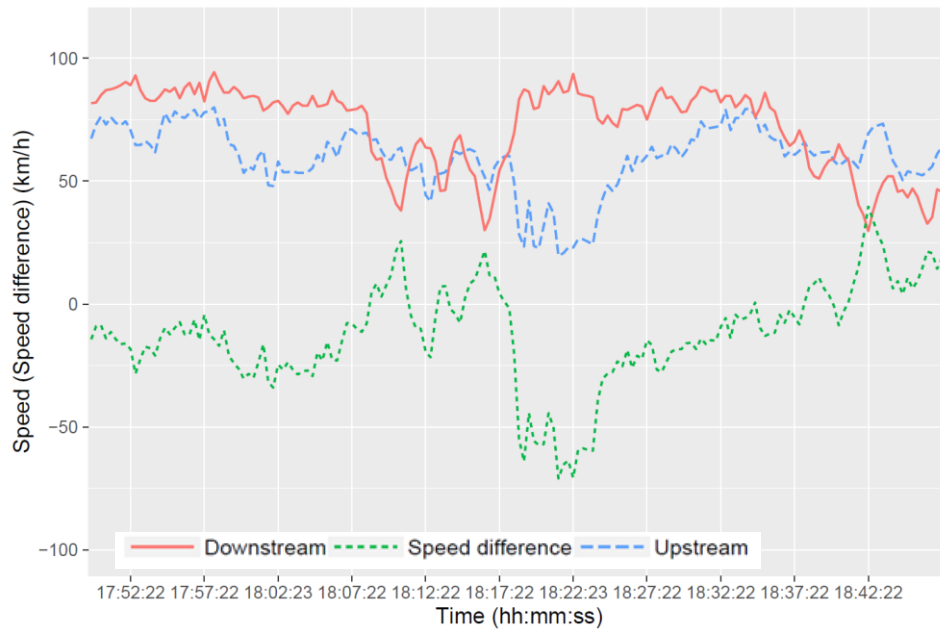


Figure A-10. Upstream and downstream speed pattern of crash 5538

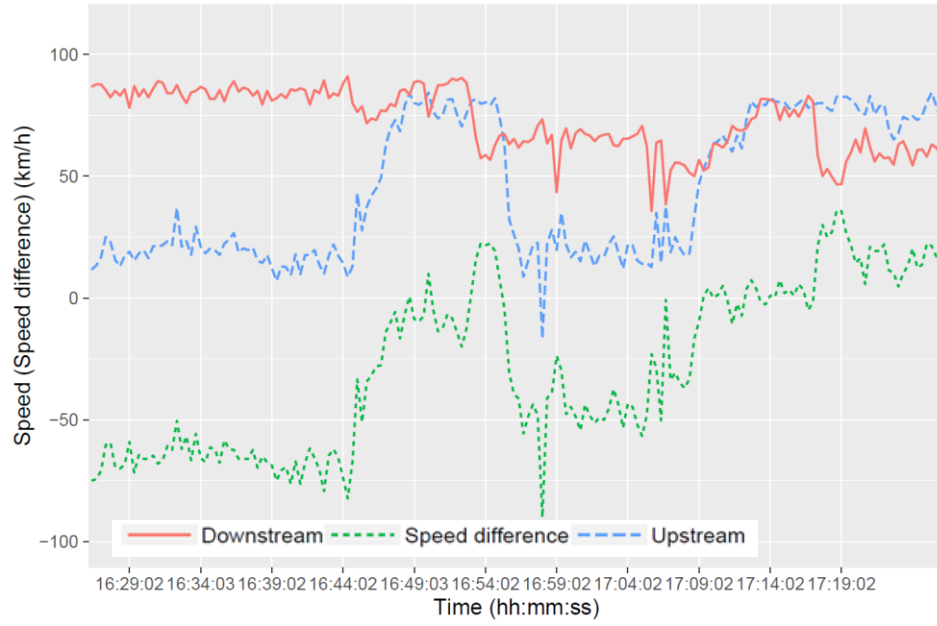


Figure A-11. Upstream and downstream speed pattern of crash 8143

Appendix B: SAS Code for Estimating Reaction Time using Monte Carlo Simulation

The following SAS code generates a lognormal distribution of reaction time with a mean of 0.92 s and a standard deviation of 0.28 s (variance = 0.0784). The code also randomly selects 30 sample reaction times from this distribution for each of 10 data sets and calculates a mean of 30 reaction times for each data set.

```
data lognormal; /* generate lognormal distribution of reaction
time */
m = 0.92; v = 0.0784; /* specify mean and variance of
reaction time */
phi = sqrt(v + m**2);
mu = log(m**2/phi);
sigma = sqrt(log(phi**2/m**2));
do i=1 to 175;
    x = rand('Normal',mu,sigma);
    y = exp(x);
    output;
end;
run;

proc univariate =lognormal; /* plot the lognormal distribution */
var y;
histogram y / lognormal(zeta=EST sigma=EST);
run;

proc surveyselect =lognormal out=outcome method=srs samplesize=30
rep=10; /* generate 10 random sample data sets using a Monte
Carlo simulation */
run;

proc means =outcome noprint; /* calculate the mean reaction time
for each random sample data set */
var y;
by replicate;
output out=results mean= ;
run;
```

Appendix C: Sample Calculation of CPI

The following example illustrates how the CPI is calculated for one following vehicle. Assume that a vehicle ID #10 ($i = 10$) follows the lead vehicle at one time frame ($t = 290$) in the following conditions:

Vehicle.ID	Time frame	V_F (m/s)	V_L (m/s)	S (m)	L (m)
10	290	15.95	10.90	31.79	4.42

where V_F = the speed of vehicle ID #10 (i.e., the following vehicle), V_L = the speed of the lead vehicle, S = the spacing between the lead and following vehicles, and L = length of the lead vehicle.

Since the following vehicle is a car, the driver reaction time (t_r) is assumed to be 1.22 s as shown in Table 5-2. DRAC is calculated using Eq. 4-6 as follows:

$$DRAC_i(t) = \frac{(V_F(t) - V_L(t))^2}{2((S(t) - L_L) - (V_F(t) - V_L(t)) \times t_r)}$$

where,

$DRAC_i(t)$ = DRAC for the following vehicle i at time t ;

$S(t)$ = spacing between the lead and the following vehicle at time t ;

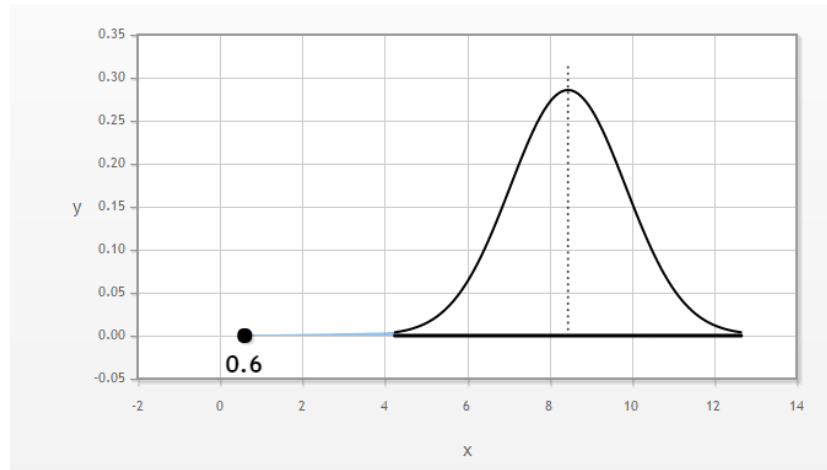
$V_F(t)$ = the velocity of the following vehicle at time t ;

$V_L(t)$ = the velocity of the lead vehicle at time t ;

t_r = the following vehicle driver's reaction time.

$$DRAC_{10}(290) = \frac{(15.95 - 10.90)^2}{2((31.79 - 4.42) - (15.95 - 10.90) \times 1.22)} = 0.60 \text{ m/s}^2$$

MADR for cars follows a truncated normal distribution with average of 8.45 m/s² with a standard deviation of 1.40 m/s², The distribution of $X \sim N(8.45, 1.40)$ is shown as follows:



$$CPI_{10}(290) = \Pr(\text{DRAC}_{10}(290) > \text{MADR}_{10}) = \Pr(0.6 > X)$$

Since $Z = \frac{X - \mu}{\sigma} = \frac{0.6 - 8.45}{1.40} = -5.61$, then

$$CPI_{10}(290) = \Pr(X < 0.6) = \Pr(Z < -5.61) = 1.03 \times 10^{-8}$$

Thus, the CPI for vehicle ID #10 at $t = 290$ is 1.03×10^{-8} . The CPI can also be calculated using the following R code:

```
TRC<- c(1.22,1.96,2.07,1.20,1.70,1.33,1.50,1.43,1.57,1.22) # car drivers' reaction time
TRT<- c(0.24,0.20,0.23,0.24,0.24,0.24,0.23,0.24,0.23,0.24) # truck drivers' reaction time
myobserved<-myobserved %>%
  filter(VF >=VL) %>% # filter out those cases following vehicle's speed is smaller
  mutate(tr=ifelse(Vehicle.Type=="Car",TRC,TRV), #choose drivers' reaction time
         DRAC=((VF-VL)^2)/(2*((gapspacing-PrecVehLength)+(VF-VL)*tr)),
         CPIt=ifelse(VehiclePairType=="Car-Car",pnorm(DRAC,8.45,1.40),
                    ifelse(VehiclePairType=="Car-HV",pnorm(DRAC,8.45,1.40),
                            ifelse(VehiclePairType=="HV-Car",pnorm(DRAC,5.01,1.40),-9999))))
```


VITA AUCTORIS

NAME: Peibo Zhao

PLACE OF BIRTH: Dalian, China

YEAR OF BIRTH: 1992

EDUCATION: Chongqing Jiaotong University, Chongqing, China
2010 - 2014 B.A.Sc. in Civil Engineering

University of Windsor, Windsor, ON
2014 - 2016 M.A.Sc in Civil Engineering